*"**Our passion for learning is our tool for survival**"*

Carl Sagan

To
Amma, Nanna and Thammudu

Molecular correlates of spinal motor neuron functional specification and plasticity

Dissertation

In partial fulfilment of the requirements for the degree

"Doctor of Philosophy (PhD)"

in the Neuroscience Program

at the Georg August University Göttingen,

Faculty of Biology

submitted by

Pitchaiah Cherukuri

born in

Guntupalli, India

Göttingen, September 10, 2012

Members of the Thesis Committee:

Dr. Till Marquardt, Reviewer

Developmental Neurobiology

European Neuroscience Institute, Göttingen

Prof. Klaus-Armin Nave, PhD, Reviewer

Department of Neurogenetics

Max Planck Institute of Experimental Medicine, Göttingen

Prof. Dr. Ernst. A. Wimmer

Department of Developmental Biology

Georg-August-University Göttingen, Johann-Friedrich-Blumenbach-Institute

of Zoology and Anthropology

GZMB- Göttingen Center for Molecular Biosciences, Göttingen

Date of the oral examination: 18th October, 2012

Affidavit

I hereby, declare that this PhD thesis "Molecular correlates of spinal motor neuron functional specification and plasticity" has been written independently with no other aids or sources than quoted.

Pitchaiah Cherukuri

September, 2012

Göttingen, Germany

Table of contents

Acknowledgements

The 'experience dependent plasticity' induced during the graduate training changed my outlook towards research and in this regard, I would like to sincerely thank my supervisor Dr. Till Marquardt for his valuable support and trust, in my abilities. The lively scientific discussions we had, together with his strong penchant for encouraging independent ideas were important in shaping my career as a researcher. Thanks for the patience you had with me. It was nice and inspiring to work with you.

I would also like to express my sincere thanks to my thesis committee members Prof. Klaus-Armin Nave and Prof. Dr. Ernst. A. Wimmer for their valuable remarks and suggestions which shaped my project.

I am grateful to Prof. Dr. Michael Hörner, Sandra Drube and the IMPRS Neuroscience Program for their continuous support, right from the day of my arrival to Göttingen. Thanks a lot. Your support is commendable, without which life would have been impossible in Göttingen.

I have to thank all members of the Developmental Neurobiology Laboratory, ENI-Göttingen- Liang Wang, Lukas Cyganek (Lucy), Lee, Tsung-I (Veltine), Chor Hoon Poh (Anne), Camille Lancelin, Alexandra Klusowski (Alex), Daniel A. Müller, David Herholz and Eva Ling for making the working atmosphere vibrant and wonderful. A warm greeting by Alex in the mornings 'kick-starts' the day. Thanks Alex. Liang and Veltine deserve a special mention for the enormous support they extended during my stay in the lab. Thanks Veltine, for being with me through hard times and remember-*plastics work.*

I sincerely acknowledge the support of our collaborators Dr. Oliver Schlüter, from whom I learnt the "art of patch clamp"; Dr. Lars Wittler and Dr. Phillip Grote, MPI – Berlin, for their help with microarray profiling and data analysis. I would like to thank Frank Kötting, for all the engineering help he extended to realize my project.

I thank all my friends in Göttingen for creating a homely atmosphere. Without you life wouldn't have been easy. There are 'endless' names to quote here, and I extend my

thanks to each and every one to of them. My special thanks to Aniket, Mayur and Soniadi and Chechi. You mean a lot to me. I would also like to thank my friends, Raushan and Tiwariji, a part of the family.

And most importantly, I am indebted to my parents and brother, to whom I owe my life. They complete my existence. Thanks for the faith you have in me. I will cherish your love forever and ever!

List of abbreviations

5ht1d	5-hydroxytryptamine (serotonin) receptor 1D
Actn3	Actinin alpha 3
AHP	Afterhyperpolarization
AIS	Axon initial segment
ALS	Amyotrophic lateral sclerosis
AMPK	5' adenosine monophosphate-activated protein kinase
Angptl4	Angiopoietin-like 4
ATPase	Adenosine triphosphatase
BDNF	Brain-derived neurotrophic factor
C/EBPbeta	CCAAT/enhancer binding protein beta
Calca	Calcitonin/calcitonin-related polypeptide, alpha
Cart	Cocaine- and amphetamine-regulated transcript protein
Chat	Choline acetyltransferase
Chodl	Chondrolectin
CNS	Central nervous system
CTXB	Cholera toxin subunit B
DAVID	Database for Annotation, Visualization and Integrated Discovery
DEPC	Diethylpyrocarbonate
DNA	Deoxyribonucleic acid
Err3	Estrogen-related receptor gamma
Fabp3	Fatty acid binding protein 3
Fig.	Figure
Figs.	Figures
FMNT	Functional motor neuron subtype
FMNTs	Functional motor neuron subtypes
Gapdh	Glyceraldehyde-3-phosphate dehydrogenase
Gfap	Glial fibrillary acidic protein
Gfra1	Glial cell line derived neurotrophic factor family receptor alpha 1
Hprt1	Hypoxanthine phosphoribosyltransferase 1
HS	Hindlimb suspension
KEGG	Kyoto Encyclopedia of Genes and Genomes

m/min	meter/minute
MAPK	Mitogen-activated protein kinase
MEF2	Myocyte enhancer factor 2
MG	Medial gastrocnemius
MHC	Myosin heavy chain
MN	Motor neuron
MNs	Motor neurons
mRNA	Messenger ribonucleic acid
Myh1	Myosin, heavy polypeptide 1, skeletal muscle
Myh2	Myosin, heavy polypeptide 2, skeletal muscle
Myh4	Myosin, heavy polypeptide 4, skeletal muscle
Myh7	Myosin, heavy polypeptide 7, skeletal muscle
NeuN	Neuronal nuclear antigen
NFAT	Nuclear factor of activated T-cells
ng/ml	Nanogram per milliliter
NMDs	Neuromuscular diseases
NMJs	Neuromuscular junctions
OPN	Osteopontin
PKA	Protein kinase A
PKC	Protein kinase C
PPAR	Peroxisome proliferator-activated receptor
Pvalb	Parvalbumin
qPCR	Quantitative polymerase chain reaction
Rcan1	Regulator of calcineurin 1
RNA	Ribonucleic acid
SDH	Succinate dehydrogenase
SOD1	Superoxide dismutase 1
Sv2a	Synaptic vesicle glycoprotein 2a
TA	Tibialis anterior
TrkB	Neurotrophic tyrosine kinase, receptor, type 2
Tuba1b	tubulin, alpha 1b
vAChT	Vesicular acetylcholine transporter
áFF	alpha fast-twitch, fatigable
áFint/FI	alpha fast-twitch, fatigue intermediate

áFR	alpha fast-twitch, fatigue-resistant
áS	alpha slow-twitch, fatigue-resistant
ìm	Micrometer

Lab designated genes

Cabuf	Calcium buffering gene
Calchas1	Calcium channel alpha subunit 1
Calchs1	Calcium channnlel subunit 1
Catch1	Cation channel 1
Cdkx	Cyclin dependent kinase x
Eaarip	Excitatory amino acid receptor interacting protein 1
Grep	Growth response gene 1
Ifx.1	Translation initiation factor 1
KlfX	Kruppel like factor X
Nplx	Neuropeptide ligand x
Potch1	Potassium channel 1
Prkcx	Protein kinase c x
Sodchas1	Sodium channel alpha subunit 1
Svap	Synaptic vesicle associted protein
Syap2	Synaptic vesicle associted protein 2
Tamnec1	Tibialis anterior motor neuron enriched collagenase 1
Tapxe	T-cell activating protein x- e
Tfp2	Transcription factor 2
Lp1	low density lipoprotein receptor related protein 1

I Abstract

The precision with which motor neurons connect to functionally matched muscle fibers ultimately determines the accuracy of behavioural outputs. Motor neurons are functionally diverse and can be subdivided into distinct functional motor neuronal subtypes (FMNTs). Furthermore, the motor neuron-muscle fiber units display a high degree of adaptive plasticity in response to chronically altered activity patterns, thus assuring flexible adjustment of neuromuscular output to habitual changes. While early events in motor neuron development are well understood, much less is known regarding molecular markers or mechanisms underlying FMNT specification or function. Furthermore, while the molecular events underlying muscle fiber plasticity are well documented, neither the functional significance nor the underlying molecular mechanisms contributing to the plasticity of motor neurons are known. Using type-specific gene profiling, I identified novel markers and putative gene signatures of FMNTs in addition to determining gene signatures associated with adaptive motor neuron plasticity. Motor neuron type status appears to be inherently linked to their respective vulnerability (or resistance) towards neuromuscular diseases (NMDs). The ability to alter motor neuron type status, by targeting molecular pathways driving motor neuron plasticity, may eventually provide novel therapeutic intervention strategies aiming at ameliorating motor neuron loss in NMDs.

II Introduction

Animals differ from plants in their ability to move. We humans, standing at the frontier of evolution in animal kingdom, master our environment, by our ability to move and manipulate things around us in an unprecedented fashion. As mentioned by Sir Charles Sherrington, a pioneer in neurophysiology, "all we can do is to move things". The execution phase of locomotion is dependent on the final common pathway: all central and peripheral pathways converge on the motor neurons (MNs) which ultimately elicit contraction of the innervated skeletal muscle fibers (Sherrington, 1904). The final common pathway thus underlies our ability to move and manipulate things.

"The terminal path may, to distinguish it from internuncial common paths, be called the final common path. The motor nerve to a muscle is a collection of such final common paths."

— Sir Charles Scott Sherrington

The spinal MNs receive and integrate inputs (supraspinal, intraspinal and sensory) to control the contraction of muscles and thus enable locomotion. A single MN and all the muscle fibers it innervate is termed a motor unit (Buchthal and Schmalbruch, 1980), which is the most basic and fundamental unit by which the central nervous system (CNS) controls locomotion. A muscle consists of several such units (is a multi-unit interface) and the selective recruitment of these units is what enables a muscle to respond in the most suitable manner to meet functional demands. This arrangement enables CNS to grade force by two mechanisms: rate gradation and recruitment gradation, meaning that the muscle force can be regulated by either altering the firing pattern of the motor unit or by recruiting additional motor units (Kernell, 2003). At another level of organization, all MNs innervating a single muscle cluster within stereotypic coordinates in lamina IX of the spinal cord, thus, forming a discrete nucleus, termed motor pool (McHanwell and Biscoe, 1981). Coordination between different motor pools is a prerequisite for patterned contraction of several muscles, which is critical for eliciting accurate movements. The instigation and coordination of motor pool activities driving synergistic or antagonistic muscle

groups during locomotion is driven by distinct classes of spinal premotor interneurons (Goulding, 2009). The synapse between MN and muscle fiber is called neuromuscular junction (NMJ), a specialized synapse which ensures reliable transmission, ensuring neuromuscular function under a multitude of conditions ranging from breathing to sprinting (Wood and Slater, 2001). Mammalian skeletal muscle fibers are highly heterogeneous in nature, based on contractile, metabolic as well as other properties, and this heterogeneity is the base of the flexibility that enables the same muscle to be used in a wide variety of tasks (Schiaffino and Reggiani, 1996; Serratrice et al., 1976). This flexibility is critically assured by the exquisite match in the functional properties of MNs and the muscle fibers they innervate within motor units (Kernell, 2006). At the most basic level, the spinal MNs can be broadly divided into three types: alpha, beta and gamma-MNs (Kanning et al., 2010; Manuel and Zytnicki, 2011). Alpha-MNs innervate and control the contraction of extrafusal muscle fibers, whereas gamma-MNs innervate and control the contraction of intrafusal muscle fibers (Kuffler and Hunt, 1952). Beta-MNs innervate both extra and intrafusal muscle fibers and are not well characterized (Bessou et al., 1965). Alpha-MNs can be further classified into several functional types (functional motor neuron subtypes-FMNTs), namely alpha-slow (S), alpha-fast fatigue resistant (FR), alpha-fast fatigue intermediate (FI) and alpha-fast fatigable (FF), depending on the type of muscle fibers they innervate (type I, IIa, IIx/d and IIb, respectively) (Kernell, 2006; (Kanning et al., 2010). This diversity and functional coupling of MNs and the respective muscle fibers (motor units) enables the neuromuscular system to perform a wide variety of astonishing tasks. The motor unit is by no means static; it is plastic, in the sense that, it can be modified by chronically elevated physical activity or lack thereof (Edstrom and Grimby, 1986). This dynamic nature of the motor unit enables it to adapt to habitually altered activity levels (such as exercise, etc.). The function of the motor unit is compromised in several disorders affecting the neuromuscular system such as amyotrophic lateral sclerosis (ALS) and spinal muscular atrophy (Wang et al., 2002). Thus, a proper understating of the motor unit, its plasticity could be critical to understand these disorders and to contribute to the development of therapeutic intervention strategies.

2.1 Motor unit types

Motor unit consists of a single MN and all the muscle fibers it innervate. All the muscle fibers of a motor unit are collectively termed as a muscle unit. The motor unit represents the smallest unit that can be activated by the CNS. The concept of the motor unit was introduced by Lidell and Sherrington (Lidell and Sherrington, 1925). Pioneering work by Edstorm and Kugelberg, using single motor axon stimulations in rat revealed that the motor units are homogenous in fiber type composition (Edstrom and Kugelberg, 1968). Further, they also established a correlation between resistance to fatigue and oxidative enzyme activity. Further studies by Burke et al., have established a thorough physiological-histochemical correlation in motor units (Burke et al., 1973; Burke et al., 1971). These studies (performed in the cat) confirmed the existence of 3 different motor units – FF (fast contracting/twitch, fast fatigue), FR (fast contracting/twitch, fatigue resistant), and S (slow contracting/twitch, fatigue resistant) units. Further, they showed that FR and S units can be distinguished by using sag (a decline in force, present in FR units and absent in S units) as a criterion (Burke et al., 1973). However, studies in rat models have shown that there is no consistency between sag behaviour and twitch speed (Bakels and Kernell, 1993). A fourth type of unit was discovered later with intermediate sensitivity to fatigue and was called Fint/FI (fast twitch, intermediate fatigue) (McDonagh et al., 1980). Various methods (innervation ratio, glycogen depletion, etc.) have been applied, to study the number of muscle fibers in a motor unit (Buchthal and Schmalbruch, 1980; Edstrom and Kugelberg, 1968). For example, it has been shown that in rat soleus (a predominantly slow-twitch fiber-containing muscle) there are 50-120 muscle fibers per individual motor unit (Kugelberg, 1976). Further, experiments studying the match between MN and muscle fiber properties have shown that MNs of slow-twitch muscle units have on average a significantly slower time course of AHP compared to the MNs of fast-twitch units that is directly proportional to the duration of unfused (sub-tetanic) motor unit-twitch elicited by these MNs (Bakels and Kernell, 1993). The type S unit MNs also have a low rheobase (minimum amount of current required to elicit an action potential) and a higher input resistance and are therefore more easily excitable (Bakels and Kernell, 1993; Gardiner, 1993). The motor units differ in terms of their recruitment pattern. Motor units are recruited in the following order S<FR<FF (Zajac and Faden, 1985). In other words, the weakest units are

recruited first and the strongest units are recruited later. The fast units are not used frequently and are reserved for high intensity tasks such as jumping. The motor units differ in their biochemical (oxidative enzyme repertoire, energy generation mechanism of the muscle fibers) and physiological properties (contraction time, resistance to fatigue, maximum tetanic force of the muscle fibers, conduction velocity along the motor axon, etc.) (Buchthal and Schmalbruch, 1980; Burke et al., 1974). Studies of the motor unit, thus, greatly advanced our understanding of locomotion. The components of a motor unit are described below.

2.2 Skeletal muscles

Skeletal muscles, as the name indicates are muscles which are attached to the skeletal system of the body. They are of paramount importance in generating forces required for various actions including those required for movement, as well as for maintenance of body posture against gravity. Muscle fibers can be broadly divided into two types – extrafusal and intrafusal muscle fibers. The extrafusal muscle fibers are important for force generation and are innervated by alpha-MNs, whereas the intrafusal muscle fibers are innervated by gamma-MNs and are crucial in maintaining muscle tone, by controlling the discharges of spindle afferent (sensory) fibers (Kernell, 2006). Skeletal muscles contract and generate force, when activated by their innervating MNs and they generate force in the shortening direction. The contractile cells of the muscles are called myofibers. The neurotransmitter acetylcholine released by the MN synaptic terminals acts on the nicotinic acetylcholine receptors located on the myofiber membrane (sarcolemma) and initiates a series of events which eventually lead to contraction of the myofiber (Kernell, 2006; (Berchtold et al., 2000). Skeletal muscle contractions can be isometric, eccentric or concentric (Gardiner, 2001). The contractile elements, thick and thin filaments (myosin and actin), are responsible for force generation in skeletal muscle fibers. The skeletal muscles of mammals are not uniform, they are heterogeneous. The muscle fibers differ from each other in a variety of properties. This complex heterogeneity endows the flexibility, in that the same muscle can be used for a multitude (diverse variety) of actions (Pette, 1985; Schiaffino and Reggiani, 2011). Precursors of skeletal muscles are derived from the paraxial

mesoderm. Somites are formed from the paraxial mesoderm and are divided into dorsal dermomyotome and ventral sclerotome. Skeletal muscles are derived from dermomyotome by the action of various transcription factors (Pax3, Myf5, Mrf4, etc) (Braun and Gautel, 2011; Molkentin and Olson, 1996). Historical studies classified skeletal muscles as white (phasic, glycolytic and fast) and slow (tonic, oxidative, slow, rich in myoglobin, mitochondria and blood supply) (Pette, 2001; Pette and Staron, 1990). Myosin heavy chain immunohistochemistry is the reliable current method of choice for identifying different types of muscle fibers. Based upon their myosin heavy chain repertoire, extrafusal muscle fibers can be broadly divided into 4 different types. They are type I, type IIa/2a, type IIb/2b and type IIx/d (2x/d) muscle fibers. These fibers also differ in their biochemical profile. Type I fibers are slow and oxidative, whereas type IIa fibers are fast and oxidative-glycolytic. On the other hand, type IIb muscle fibers are glycolytic (Pette, 1985; Pette and Spamer, 1986). These different types of muscle fibers exhibit differences in various physiological/mechanical parameters like peak power (slow<fast), fatigue resistance (slow>fast, correlated with mitochondrial content), maximum unloaded shortening velocity (slow<fast, highly correlated with myosin ATPase activity) and twitch contraction time (slow>fast) (Schiaffino and Reggiani, 2011; Schiaffino and Salviati, 1997). The different muscle fibers also differ in their diameter. The mean diameter of slow fibers is usually less than that of fast muscle fibers (Delp and Duan, 1996). Further, various studies carried on single fibers demonstrated that based on MHC profile, fibers can be either pure or hybrid (coexpress different MHC isoforms- I, I/IIa; IIa, IIa/IIx; IIx, IIx/IIb; IIb) (Staron and Pette, 1993). Myosin profile based fiber typing has tremendously advanced our understanding of muscle fiber diversity and dynamic nature (Schiaffino and Reggiani, 1994; Schiaffino and Reggiani, 1996; Scott et al., 2001). The muscle fiber types also differ with respect to their calcium handling/buffering capabilities. For example, parvalbumin is highly expressed in fast fibers, whereas it is expressed at very low levels in slow fibers (Campbell et al., 2001; Celio and Heizmann, 1982). Calmodulin also shows a similar trend (Schiaffino and Reggiani, 2011). The relative proportion of different fibers (fast, slow) may vary according to species. For example, relative percentage of type1 (slow) fibers in common laboratory species is as follows, mouse<rat<cat and rabbit<human (Kernell, 2006). Further, there is a difference with respect to the anatomical site and for instance, muscles involved in postural functions tend to have a higher proportion of slow fibers. In many species, fast fibers (type II)

are more numerous in the forelimbs, as compared to the hind limbs (McComas and Thomas, 1968; Schiaffino and Reggiani, 2011). Further, there are certain muscles with specialized myosins, like the inner ear , extraocular muscles (Rossi et al., 2010). The genetic factors responsible for maintaining "specific fiber type" are recently elucidated. For example, Errγ (estrogen related receptor gamma, an orphan nuclear receptor) is responsible for maintaining inherent slow phenotype in type I skeletal muscle and Sox6 (SRY-box containing gene 6) has been recently implicated in suppression of slow phenotype in fast fibers (Narkar et al., 2011; Quiat et al., 2011).

The muscle fibers are plastic and the myosin profile of the muscles can be altered by physical activity/electrical stimulation and also by hormones (Pette and Staron, 2001). For example, chronic low frequency stimulation can cause fiber type shift from fast to slow (myosin transitions in the order IIb-IIx/d-IIa-I) and thyroid hormone for example, can exert a great effect on muscle fiber phenotypes (hypothyroidism can cause fast to slow transitions, whereas hyperthyroidism can cause slow to fast transitions) (Canepari et al., 1998; Fitts et al., 1980).

2.3 Spinal motor neurons

Spinal MNs, which directly control the contraction of skeletal muscle fibers, are located in Rexed lamina IX in the ventral horn of spinal cord (Rexed, 1952). From here, they send their axons out of the CNS in peripheral nerves to innervate the skeletal muscle fibers. Due to their relative accessibility, historically, spinal MNs were used as 'model neurons' and provided important insights into general neuronal physiology (Kernell, 2006). Pioneering work by Sir Charles Sherrington, Sir John Eccles, Ragnar Granit, Daniel Kernell, Lord Edgar Adrian, Woodbury, Harry Patton, Brock and others yielded key insights into the function of these neurons (Brownstone, 2006) . Further, spinal MNs are among the first central neurons to be extensively studied using intracellular electrodes (Brock et al., 1952). MNs are unique in that, their function is precisely known: to drive muscle contraction. MN cell bodies are larger than most spinal neurons. Vertebrate MNs are multipolar neurons with extensive dendritic profiles (Kernell, 2006). The heterogeneity of MNs regarding their innervation of distinctive muscle fiber types is reflected by systematic differences in their intrinsic electrical properties and in their susceptibility to degeneration in

neurodegenerative conditions, including ALS and ageing (Bakels and Kernell, 1993; Pun et al., 2006; Saxena and Caroni, 2011).

Spinal MNs can be broadly divided into 3 major classes: alpha, beta and gamma-MNs (Kernell, 2006). These classes can be further subdivided into several different subtypes. Alpha-MNs innervate the force generating extrafusal muscle fibers and can be further classified into FMNTs namely, FF, FR, Fint (FI) and S MNs, based on the motor units they form with the distinct muscle fiber types (Fig. 1). This diversity is essential for orderly and reproducible recruitment of motor units that underlies the gradual build-up (development) of muscle force during movements (Kernell, 2003) (Fig. 1). The discharge properties of MNs are matched to the properties of the muscle fibers they synapse with (Bakels and Kernell, 1993). Knowing the electrophysiological properties of MNs, the type of motor unit it forms and the muscle fiber types it innervates can be predicted with high accuracy (Gardiner, 1993; Zengel et al., 1985). Further, it has been shown that motor nerve activity can profoundly impact muscle fiber phenotype during adult life (Buller et al., 1960; Gordon et al., 1997). Gamma (fusimotor)-MNs innervate intrafusal muscle fibers and are important in maintaining muscle tone (Manuel and Zytnicki, 2011). They can be further subdivided into dynamic and static types based on the type of discharge they elicit at the spindle sensory endings (Bessou et al., 1962a; Bessou et al., 1962b). The beta-MNs are not well characterized and understood, and are thought to innervate both extra and intrafusal muscle fibers and can share characteristics with either FF or S alpha MNs. (Kernell, 2006). MNs can be also classified as extensor and flexor MNs, depending on whether they innervate extensor or flexor muscles. It has been shown that extensor and flexor MNs display different firing profiles, maturation patterns and seem to be incorporated into distinct premotor circuits (Cotel et al., 2009; Tripodi et al., 2011; Vinay et al., 2000).

Spinal MNs have been studied extensively using electrophysiological recordings (Kernell, 2006). The effects of neuromodulatory factors on MN properties are well appreciated (Han et al., 2007; Heckman et al., 2009; Hultborn and Kiehn, 1992; Muramoto et al., 1996). Further, the initial events of MN development have been extensively studied. For example, molecular pathways involved in the motor neurogenesis, their arrangement into motor columns supplying distinct muscle

groups and their organization into motor pools have been well characterized (Bonanomi and Pfaff, 2010; Briscoe et al., 2000; Jessell, 2000; Jurata et al., 2000; Lee and Pfaff, 2001; Shirasaki and Pfaff, 2002). The processes were further shown to be inherently linked to the establishment of accurate MN-muscle connectivity patterns. However, molecular mechanisms that underlie the functional properties of the distinct MN types (gamma versus alpha or fast versus slow) or those that drive their specification in the first place, remain elusive. Some studies indicate that fast-slow distinction exists in MNs before muscle innervation, but the mechanisms governing the acquisition of these distinctions remain unknown (Rafuse et al., 1996). Similarly, while maturation of MN presynaptic terminals and possibly some MN type-dependent properties, depend on signals provided by muscle (Chakkalakal et al., 2010; Fox et al., 2007), whether this is also involved in the acquisition of bona fide MN functional type status remains unknown.
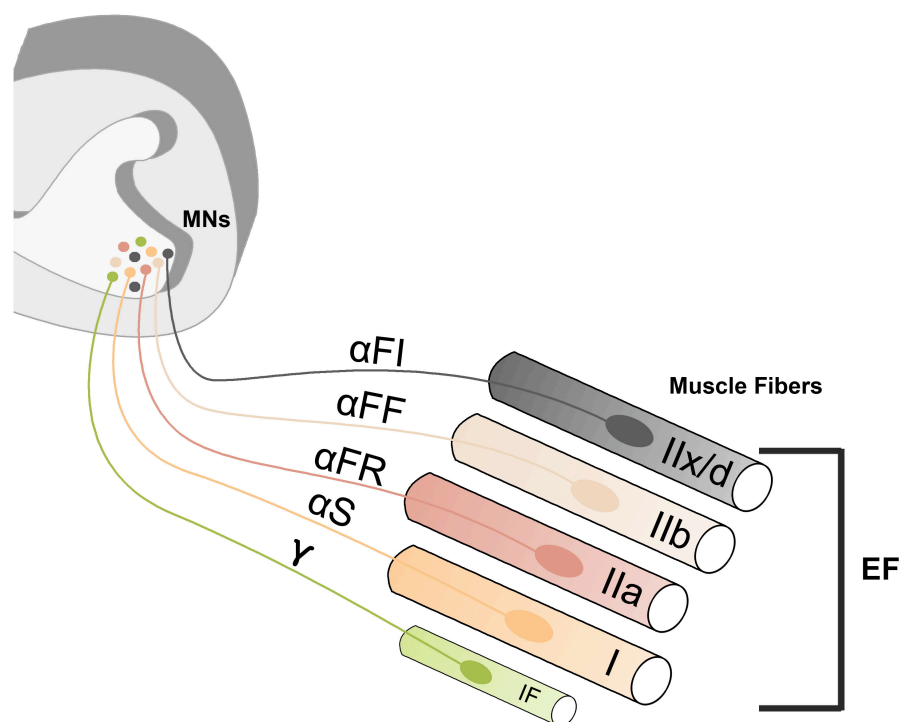
Figure 1: Motor neurons and their associated muscle fibers. Spinal MNs are located in the ventral horn of the spinal cord. From here, they send their axons in peripheral nerves to innervate muscle fibers. Spinal MNs can be broadly divided into alpha, beta and gamma types. Alpha-MNs innervate extrafusal muscle fibers (EF) and can be further subdivided into functional MN types (FMNTs)- namely, αFF, αFI, αFR and αS. These FMNTs innervate type IIb, IIx/d, IIa and type I muscle fibers, respectively. Gamma-MNs innervate intrafusal muscle fibers (IF).

Fast and slow MNs can be reliably identified by using electrophysiological recordings. For instance, membrane electrical properties can be used to predict the motor unit type (Gardiner, 1993; Zengel et al., 1985). In general, fast MNs have a higher rheobase, lower input resistance and shorter AHP half decay time when compared to slow MNs (Zwaagstra and Kernell, 1980) with AHP half decay times being the best predictors of fast versus slow MN type status (Zengel et al., 1985). Further, differences in terms of dendritic branching (dendritic bundles in prominent in slow MNs (Gramsbergen et al., 1996; Westerga and Gramsbergen, 1992)), firing behaviour (phasic versus tonic), bistable behaviour (low versus high, plateau potentials above spike threshold in fast versus plateau potentials at or below spike threshold in slow MNs (Lee and Heckman, 1998a; Lee and Heckman, 1998b)), late adaptation (more prominent in fast when compared to slow MNs (Kernell and Monster, 1982)) and NMJ morphology (more complex in fast versus less complex in slow MNs (Kanning et al., 2010)) exist between fast and slow MNs. Further, the fast and slow motor nerve terminals also differ in synaptic vesicle dynamics (Reid et al., 1999). Recent studies have begun to identify putative molecular markers for fast, slow and gamma-MNs: Calca (calcitonin gene-related peptide), Chodl (chondrolectin) for fast MNs, SV2a (synaptic vesicle glycoprotein 2 a) for slow MNs, Err3, Gfra1 (glial cell line derived neurotrophic factor family receptor alpha 1), 5ht1d (5-hydroxytryptamine (serotonin) receptor 1d) and Wnt7a (wingless-related MMTV integration site 7A) for gamma-MNs (Ashrafi et al., 2012; Chakkalakal et al., 2010; Enjin et al., 2012; Enjin et al., 2010; Friese et al., 2009). Markers like osteopontin and NeuN (neuronal-nuclear antigen) can be used for distinguishing alpha versus gamma-MNs (Misawa et al., 2012). However, particularly markers for fast/slow MNs remain to be verified, and whether any of these play a role in determining fast versus slow, alpha versus gamma-MN properties or type status remains to be addressed. A detailed study of gene signatures specific to fast and slow MNs is currently unavailable. Such a study is interesting in the context of different physiological behaviour of fast and slow MNs and their well-established differential susceptibility towards degeneration in neurodegenerative conditions (Hegedus et al., 2008). Thus, there exists a significant gap in our knowledge regarding FMNTs.

2.4 Exercise and skeletal muscle adaptations

"Lack of activity destroys the good condition of every human being, while movement and methodical physical exercise save it and preserve it."

-Plato

The benefits of physical activity on general health, including prevention of hypertension, type II diabetes, cardiovascular health, among others, are well established. In the past few decades, the beneficial effects of exercise on the brain's health (improved cognitive function, lower risks of cognitive impairment, etc) are well appreciated (Cotman and Berchtold, 2002; Cotman and Engesser-Cesar, 2002). Further, exercise has been shown to have neuroprotective effects in mouse models of ALS. Exercise or lack thereof, has been shown to profoundly impact skeletal muscle fiber type. "Defined ultimately in terms of skeletal muscle contraction, exercise involves every organ system in coordinated response to increased muscular demands" (Harris and Martin, 2003 – Medical Physiology, Rhoades 2003).

Skeletal muscle is a highly plastic tissue. It shows structural and functional adaptations towards altered motor nerve activity patterns (or artificial electrical stimulation), inactivity (or neural activity blockade), endurance or resistance exercise, microgravity, hormonal modifications, etc. (Pette, 1998; Pette, 2002; Pette and Staron, 1997; Pette and Staron, 2001). Pioneering cross-innervation experiments conducted by Buller et al., have shown that slow muscle can acquire 'fast' properties when reinnervated by a fast nerve and vice-versa (Buller et al., 1960). These experiments illustrate the importance of nerve activity in regulating fiber phenotype. Further, nerve stimulation experiments (corroborate with cross innervation experiments) have shown that mimicking fast MN firing (phasic, high frequency stimulation) can promote slow to fast conversion (I-IIa-IIx-IIb), whereas mimicking slow MN firing (tonic, low frequency stimulation) can drive fiber type conversion from fast to slow (IIb-IIx-IIa-I). For example, chronic stimulation of the medial gastrocnemius (MG) muscle by cuff electrodes placed on the MG nerve resulted in increased endurance and reduced, weakened force output of the muscle (Gordon et al., 1997). Moreover, chronic low frequency stimulation (10Hz) leads to an increase in the oxidative enzyme levels in fast muscles. However, the range of these modifications (i.e. the fiber type transformations) is limited by the intrinsic differences

between the muscles and fibers types (Schiaffino et al., 2007; Talmadge et al., 2004). FIT (frequency, intensity and time) principle is important in determining the final output in terms of endurance and strength (Baar, 2009). The combinations of these factors decide the response of the muscle towards various "exercise types" – endurance versus strength training. The adaptive response of the muscle is specific to a given stimulus. For example, different types of exercise evoke different responses, including the degree of fiber type transformation. Highly repetitive, low load exercises (endurance exercise) drive the adaptation towards fatigue resistance type, whereas paradigms which impose high load (strength/resistance training) on the muscle result in fiber hypertrophy (Marini and Veicsteinas, 2010). Type I fibers, as mentioned earlier, are designed for continuous activity and for fatigue resistance (they have high mitochondrial content and rely on oxidative metabolism). On the other hand, type IIb fibers are designed for intense but short activities and accordingly possess low mitochondrial content, high fatigue-sensitivity and rely on glycolytic metabolism. In general, endurance exercise promotes the conversion of fast-twitch fibers to slow-twitch fibers (fatigue sensitive to fatigue resistant) (Pette and Staron, 1997; Thayer et al., 2000; Yan et al., 2011). For example, elite marathon runners typically have 80-90% of their MHC pool enriched in slow fibers (Andersen et al., 2000). Treadmill running (a form of endurance training), for instance, has been shown to alter the contractile properties of motor units and to promote endurance (Booth and Thomason, 1991).

The mechanisms involved in fiber type-remodelling are intensively investigated. Many lines of evidence point out the importance of calcium ions as a second messenger in fiber type remodelling (Bassel-Duby and Olson, 2006). The slow and fast muscle fibers differ in their calcium concentrations (100 -300 nM in slow fibers and 50 nM in fast fibers) (Chin and Allen, 1996; Westerblad and Allen, 1991), and nerve stimulation can remodel fiber type in a calcium-dependent fashion (Bassel-Duby and Olson, 2006). Various pathways involving calcineurin, 5'-AMP-activated protein kinase (AMPK), as well as the transcription factors nuclear factor of activated T cells (NFAT), myocyte enhancer factor 2 (MEF2) and, peroxisome proliferator activator receptor delta (PPARδ) have been implicated in muscle endurance and fiber type remodelling (Bassel-Duby and Olson, 2006; Wang et al., 2004). For example, it has been also shown that AMPK and PPARδ agonists can act as

exercise mimetics (Narkar et al., 2008). Further, the role of PGC1α (peroxisome proliferative activated receptor, gamma, coactivator 1 alpha, a master regulator of mitochondrial gene expression) in promoting exercise-induced endurance status has been widely studied (Yan, 2009). The role of Rcan1 (regulator of calcineurin 1) in controlling calcineurin and thus muscle fiber plasticity is well documented (Oh et al., 2005). Further, several protein kinases (p38γ MAPK- mitogen-activated protein kinase 12, etc.) have been implicated in regulating muscle endurance (Pogozelski et al., 2009). Recent studies have implicated a role for microRNAs in controlling fast and slow gene programs. Further, microRNAs are also implied in exercise-mediated skeletal muscle remodelling (Safdar et al., 2009). Endurance exercise promotes angiogenesis, and factors mediating exercise-induced angiogenesis (including VEGF (vascular endothelial growth factor)), have also been well characterized (Marini and Veicsteinas, 2010). The metabolic plasticity of the skeletal muscle has been well characterized and includes altered enzyme activity. For instance, increases in citrate synthase levels following endurance training were reported. In addition, at the systemic level, the exercised skeletal muscle acts as an endocrine organ regulating liver and adipose tissue function and for instance involves IL-6 released by skeletal muscle into the blood circulation (Pedersen and Febbraio, 2008).

The genetic factors mediating exercise induced cardiac protection are recently characterized. For example, C/EBPβ has been implied in regulating exercise-mediated cardiac protection. It is also known that exercise can induce histone modifications in the skeletal muscle (Bostrom et al., 2010). Further, some studies suggest that exercise could be neuroprotective in neuromuscular diseases, such as ALS (Carreras et al., 2010; Deforges et al., 2009). Exercise has been shown to induce metallothioneins (scavengers of reactive oxygen species) in the spinal cord, which may underlie part of the observed neuroprotective effects (Hashimoto et al., 2009). Moreover, a recent study has shown that improving muscle function by elevated PGC1α activity in ALS mouse model can improve muscle and motor functions, without extending overall life span (Da Cruz et al., 2012). Another study has shown that exercise can limit astrogliosis seen in ALS spinal cords (Deforges et al., 2009). The mechanisms by which exercise confers neuroprotection in MNs or other neurons still remain unclear.

Exercise has been shown to alter MN properties (Beaumont and Gardiner, 2003). In addition, exercise has also been shown to effect memory performance, hippocampal plasticity, among others (Gomes da Silva et al., 2012). Taken together, the factors involved in promoting exercise-induced muscle endurance and cardiac protection are well-established, but the mechanisms underlying exercise-mediated neuroprotection in MNs remain to be elucidated. Elucidating the mechanistic basis of neuromuscular plasticity is therefore of great importance in understanding (and eventually treating) neuromuscular, cardiovascular diseases and other diseases responsive to habitual changes in physical activity patterns.

2.5 Spinal motor neuronal modifications upon endurance training

CNS neurons can undergo adaptation in their basic properties when their use over time is altered. Learning is one such example, where adaptive changes at the molecular and cellular level can be observed in neurons (for example, spine density, dendritic complexities alter upon learning) (Leuner and Gould, 2010). MNs display similar adaptively towards alterations in neuromuscular activity (Gardiner et al., 2006). The properties of the MNs are matched to the properties of the muscle fibers they synapse with (Kernell et al., 1999). Skeletal muscle exhibits high degree of plasticity and various factors can influence the fiber type and affect fiber type transformations (Pette and Staron, 1997). As the discharge properties of MNs are matched to the muscle fiber types, it appears likely that when the muscle fibers change properties, the properties of MNs would also change. Indeed, it has been shown by physiological studies that the MNs are also plastic and change upon activity/reduced activity (Beaumont and Gardiner, 2003; Cormery et al., 2005). MNs show alterations in voltage threshold, resting membrane potential and AHP amplitude upon neuromuscular conditioning (Gardiner, 2006). Moreover, it has also been shown that activity can induce morphological changes in the peripheral nerve (Roy et al., 1983). However, the direction and extent of the changes observed in MNs are limited, when compared to the muscle fibers. Various factors can influence the properties of MNs, including exercise, disuse, neuromodulatory factors and growth factors (such as BDNF- brain derived neurotrophic factor) (Gonzalez and Collins, 1997; Heckman et al., 2009). Chronic electrical stimulation of motor nerves have

revealed that MNs become more excitable under these conditions, exhibiting decreased rheobase, increased input resistance, as well as altered AHP duration (Munson et al., 1997). Taken together, several studies indicate that MNs show adaptive plasticity towards altered neuromuscular activity levels, such as those induced by chronically elevated or reduced physical activity. Herein, motor neuronal adaptations to chronic activity can occur at multiple levels: physiological, morphological and metabolic.

2.5.1 Physiological changes

Both general and 'type specific (FMNT specific)' adaptations were reported from MNs of endurance trained rats (Beaumont and Gardiner, 2002; Gardiner, 2006). The extent and the type of adaptations were dependent on the type of endurance exercise (voluntary running versus forced running on a treadmill) (Gardiner, 2006). General adaptations, which were independent of exercise type, include hyperpolarization of voltage threshold (for action potential) by 6-7mV (similar to that seen with fictive locomotion) and of resting membrane potential (all MNs of endurance trained rats and slow MN of voluntary running rats) (Gardiner et al., 2006; Gardiner, 2006). Modelling (simulation) experiments suggest that fast sodium or delayed rectifier potassium channels (concentration and/or voltage dependence) may be involved in such a change of voltage threshold (Gardiner et al., 2006). Further changes include an increase in AHP amplitude (which was reported to be subtype-specific and exercise dependent (in slow MNs of voluntary trained rats). Further these studies also reported an increase in cell capacitance of fast MNs (of endurance trained rats) and a faster antidromic spike rise time (of endurance trained MNs) (Gardiner et al., 2005; Gardiner et al., 2006). Apart from the suggestions derived by modelling, no direct experimental evidence (altered gene transcripts, signalling pathways, etc) exists for the above-mentioned changes. Further, neurotrophic factors like brain derived neurotrophic factor (BDNF) were shown to alter the excitability of MN (Gonzalez and Collins, 1997). It is interesting to mention here that BDNF mRNA expression is upregulated in soleus muscle of endurance trained rats. Moreover, BDNF, its receptor TrkB were reported to be upregulated in lumbar spinal cord after exercise (Gomez-Pinilla et al., 2002). Recent electrophysiological studies have

reported a slower adaptation (spike frequency adaptation -SFA) in endurance trained MNs. Further, these neurons also have a lower F/I slope (frequency/current) (modest leftward shift in F/I curve) (MacDonell et al., 2012). Take together; these findings indicate that spinal alpha-MNs change their physiological properties upon endurance training.

2.5.2 Morphological changes

Studies have reported changes in MN dendritic arborization, soma/axon size and in NMJ morphology upon exercise. A study by Gazula et al., have reported an increase in dendritic arborization of MNs of spinally-transected rats following exercise (Gazula et al., 2004). Some studies have reported a decrease in the axonal diameters following exercise, while other studies yielded contradictory findings and reported an increase in axonal diameter under these conditions. When it comes to soma size, two studies have shown that soma size is increased upon endurance training and in one study cell capacitance was used as a measure of cell size (Beaumont and Gardiner, 2003; Gardiner, 2006). Numerous changes (both morphological and physiological) have been reported at the neuromuscular junction upon endurance training (Andonian and Fahim, 1988; Deschenes et al., 1993). The presynaptic terminal size was reported to be increased in both fast and slow terminals upon exercise. Further, an increase in acetylcholine receptors (on post synaptic side of both fast and slow muscles) was also reported. Endurance training was also reported to improve synaptic endurance and safety factor for neurotransmission (increased quantal content and decreased run-down upon repeated activation) (Desaulniers et al., 2001; Dorlochter et al., 1991). Safety factor refers to the capacity of the NMJ to maintain neuromuscular transmission under a variety of physiological conditions.

2.5.3 Metabolic changes/biochemical changes

An increase in the concentration of CGRP, was reported in the soma of MNs after endurance training in rats (Gharakhanlou et al., 1999). Further, a recent study reported an increase in CGRP and acetylcholine receptors at both fast and slow

twitch muscles in rats (following endurance or resistance training) (Parnow et al., 2012). When it comes to metabolic enzymes, maleic dehydrogenase was also reported to be increased in the somata of trained MNs whereas succinate dehydrogenase (SDH) was reported to be unchanged. Further, an increase in orthograde transport or both ortho and retrograde transport of proteins was reported in MNs following endurance training (Jasmin et al., 1987; Jasmin et al., 1988; Kang et al., 1995). Further, altered growth factor (and receptor) levels, including those of BDNF (in both muscles and MNs) were reported after running exercise (Gomez-Pinilla et al., 2002; Ogborn and Gardiner, 2010). Moreover, transcriptome analysis of lumbar MNs from voluntary trained mice has revealed various transcripts involved in neuronal signalling and excitability were altered following training (Ferraiuolo et al., 2009). The same study reported that genes (*Nova2*) predicted to alter electrical properties, are also differentially regulated in lumbar MNs upon training. Taken together, all these findings indicate that MNs do undergo adaptive plastic changes in response to endurance training.

2.6 Skeletal muscle responses upon hindlimb unloading

/unweighting

Decreased neuromuscular activity (or lack of) induces fiber type-transformations that are opposite in nature (slow-fast) to that induced by elevated activity (Pette and Staron, 2001). Various interventions such as spinal cord transection, prolonged bed rest, nerve blockade (by tetradotoxin (TTX), affects both fast and slow twitch fibers), neurotomy, immobilization, microgravity and hindlimb suspension/unweighting (HS) can induce lack of activity (or decreased activity) in the skeletal muscle (Gardiner P, 2001). For example, elimination of neural inputs to the muscle results in atrophy and bed rest is known to induce atrophy in limb muscles (LeBlanc et al., 1992). HS is a ground based model to simulate spaceflight (mimics spaceflight at several levels-muscle atrophy characteristic of space flight, atrophy of extensor muscles, etc.) and was developed at the Ames Research Centre (National Aeronautics and Space administration-NASA) (Morey-Holton and Globus, 2002). There are two methods to

achieve hindlimb unloading - a tail suspension model and whole body harness model. Both models relieve the hindlimbs 'off' the gravitational force of body weight. HS induces atrophy of the slow-twitch extensor muscles (extensor muscles are also affected, fast twitch and flexor muscles are relatively less affected) and the slow-twitch ankle extensor; soleus (postural muscle) is greatly affected and has been extensively studied following HS (Thomason and Booth, 1990). EMG studies on soleus following HS have shown that following an initial decrease, the EMG returned to normal values (Alford et al., 1987). This proposes that HS does not represent functional denervation and cannot be termed 'disuse'. However, a later study has shown that EMG patterns decrease and change in soleus muscle upon HS (Blewett and Elder, 1993). Studies have indicated that upon HS corticosterone levels, adrenal and thymus weights are altered (Thomason and Booth, 1990). Prolonged HS causes atrophy of the soleus muscle (decreased muscle mass), protein loss (degradation, role of ubiquitin proteasome system) and fiber type transformations. Fiber type transformations occur in the direction of fast (slow to fast). HS induces the expression on type IIx and IIb myosin heavy chains (resulting in altered twitch contraction times) in the soleus (type IIb, IIx/d normally low in soleus) muscle and a decrease in the number and size of type I fibers (Haddad et al., 1998; Thomason and Booth, 1990). Further, studies have pointed to the existence of hybrid fibers (different myosin heavy chains co-exist) in unloaded slow muscles. This fiber type shift (towards fast) is accompanied by changes in mechanical properties of the muscle. For example, unloading results in a decrease of cross sectional area, peak activated force and fiber specific force (Elder and McComas, 1987). An increase in unloaded shortening velocity and a shorter half-relaxation time were reported from unweighted soleus muscles. Further, unloading causes significant changes in the metabolic profile of the muscles. In general, HS results in weakening of soleus muscle accompanied by it gaining of some fast twitch features (increase in maximum unloaded shortening velocity, etc). An increase in the activity of glycolytic (lactate dehydrogenase, α-glycerophphosphate dehydrogenase, phosphofructokinase) enzymes is reported upon HS and this indicates an increased anaerobic capacity of the normally oxidative muscle (Thomason and Booth, 1990). Similar alterations were seen in humans (atrophy) subjected to microgravity (in space missions and in humans patients subjected to bed rest) (Fitts et al., 2001; LeBlanc et al., 1992). There is also an increase in the levels of muscle- creatine kinase and glyceraldehydes-3-phosphate

dehydrogenase upon HS (Cros et al., 1999). Further, a decrease in the quantity of RNA and a decrease in the rate of protein synthesis (and myofibrillar protein loss) were also reported the unloaded soleus muscle (Thomason and Booth, 1990). HS induces a change in the vascularization (reduced capillarity) of the soleus muscle (Desplanches et al., 1990). Transcriptional analysis of the unloaded soleus muscle has shown a significant change of transcripts involved in several aspects of muscle function (protein degradation, excitability, signal transduction, etc.) (Wittwer et al., 2002). Further, there is an increase in sodium current density in soleus muscle fibers upon HS, which may decrease resistance to fatigue (Desaphy et al., 2001). Further, HS induces activation of apoptosis and a reduction in number, proliferation of satellite cells (Wittwer et al., 2002). Signalling mechanisms underlying atrophy and remodelling (seen in HS) are well studied. The importance of calcium in fiber remodelling upon gravitational unloading is well appreciated with a role for calcineurin/NFAT pathway in counteracting fiber type transformations (Shenkman and Nemirovskaya, 2008). Further, HS is also shown to alter the electrophysiological properties of MNs. Detailed investigations into mechanisms underlying fiber type atrophy and remodelling has important clinical applications (for counteracting muscle waste).

2.7 Motor neuronal responses upon reduced activity

As mentioned above, various models of decreased neuromuscular use can result in marked alterations of muscle fiber types. Altered neuromuscular activity causes alterations in properties of central neurons. EMG studies have pointed a significant alteration of motor control in various studies of decreased neuromuscular activity and a few studies have provided direct evidence for altered motor function (morphological, physiological) upon decreased neuromuscular activity (Cormery et al., 2005). For example, intracellular recordings have shown that MN properties do change upon HS. Further, blocking tibial motor nerve fibers using TTX has demonstrated an increase in rheobase of some MNs (in cells with longest AHP durations, slow MNs) (Cormery et al., 2000). Further, unloading induces plastic changes (extensor hyperactivity) of neurons implicated in locomotor commands (Canu et al., 2001). Decreased neuromuscular activity by HS also alters the NMJ

(short period of interventions causes no changes, whereas long periods of intervention cause reduction in endplate dimensions) (Deschenes et al., 2006). Moreover, there is an alteration in the activity of AChE (soleus muscle, increase) and an elevation in the levels of Chat in the sciatic nerves of rats subjected to HS (Gupta et al., 1985). There are reports of altered SDH activity, soma size distribution. Studies have reported an alteration in dendritic development under conditions of decreased neuromuscular activity (Inglis et al., 2000). Further, a recent study has demonstrated changes in electrophysiological properties of dorsal root ganglion (DRG) neurons in rats subjected to HS (Ren et al., 2012). The changes in electrophysiological properties of MNs after HS are in a direction opposite to that induced by increased activity. For example, threshold for repetitive firing (increased, shift of F/I curve towards right), rheobase (increase in HS, decrease after running), spike amplitude (decrease in HS and increase after running) and AHP amplitude (decrease in HS and increase after running) change in MNs of animals subjected to HS (Cormery et al., 2005). Further changes include alterations in voltage threshold (depolarized, only in fast MNs) and minimum and maximum steady state firing frequencies (increased, only in slow MN). These studies also illustrate that changes in MNs after HS (like endurance training) can be either generic or type specific (fast versus slow). In general, reduced weight-bearing decreases the excitability of spinal MNs and to some degree promotes a shift in the properties from slow to fast. Taken together, these studies show that spinal MNs show adaptive changes in their properties upon decreased neuromuscular use.

2.8 Aim of the study

Motor neurons (MNs) are quite diverse and can be divided in to different functional subtypes (functional motor neuron subtypes, FMNTs). Despite the wealth of electrophysiological information available from spinal MNs, very little is known about molecular correlates and mechanisms underlying FMNT specification and function. In addition, what underlies the ability of MNs to adapt to chronically altered activity, such as during endurance exercise or sedentary lifestyle, remains unresolved. Given the beneficial effects of physical activity in neurodegenerative diseases like amyotrophic lateral sclerosis (ALS), understanding the underlying molecular correlates and mechanisms could provide important contributions for the development of therapeutic interventions.

To address these issues, in the initial part of my work, I have developed screens to gain insights in to the markers and molecular correlates accounting for functional diversity of MNs as seen in FMNTs. The gene expression differences between FMNTs were analyzed by transcriptional profiling of motor pools that were enriched in either fast or slow/αFR FMNTs.

To gain an insight in to the molecular correlates and mechanisms linked to the adaptive plasticity of MNs in response to altered neuromuscular activity levels, I have developed screens to study motor neuronal transcriptional profiles following chronic neuromuscular activity alteration, induced by endurance training and chronic hindlimb unweighting in mice.

The ultimate aim of the work is to evaluate the functional roles served by the candidate molecular correlates obtained from the above-mentioned screens in the context of FMNT diversity, plasticity and differential vulnerability towards neuromuscular diseases. These studies, apart from advancing our basic understanding of FMNT biology could further provide insights in pathology of neurodegenerative diseases like ALS.

III Materials and Methods

3.1 Animals

CD1 strain mice were used in this study and they belong to a standard lab strain carrying no genetic modifications.

3.1.1 Laboratory consumables and plastic ware

General consumables and plastic ware were purchased from Starlab GmbH, Eppendorf (Hamburg) and Sarstedt AG. Dissection instruments were purchased from Fine Science Tools GmbH. Glass micropipettes were purchased from World Precision Instruments*, Inc.*

3.1.2 Primary antibodies

Antibody name	Host species	Working dilution	Supplier
Tamnec1	Goat	1:500	Sigma Aldrich AG GmbH
vAChT	Rabbit	1:1000	Synaptic Systems GmbH
NeuN	Mouse	1:1000	Millipore AG
SC-71	Mouse	1:200	DSHB*
BF-F3	Mouse	1:200	DSHB*
BA-F8	Mouse	1:200	DSHB*
MY-32	Mouse	1:2000	Sigma Aldrich AG GmbH
c-Fos	Rabbit	1:750	Santa Cruz Biotechnology Inc

*DSHB: Developmental Studies Hybridoma Bank.

3.1.3 Secondary antibodies

Target species	Host	Conjugate	Working dilution	Supplier
Mouse	Donkey	Alexa fluorescent dye	1:1000	Invitrogen GmbH
Goat	Donkey	Alexa fluorescent dye	1:1000	Invitrogen GmbH
Rabbit	Donkey	Alexa fluorescent dye	1:1000	Invitrogen GmbH
Mouse	Goat	Alexa fluorescent dye	1:500	Invitrogen GmbH

3.1.4 Enzymes

Enzyme	Supplier
SuperScript III	Invitrogen GmbH
SuperScript II	Invitrogen GmbH

3.1.5 Kits

Kit	Supplier
iScript™cDNA Synthesis Kit	Bio-Rad GmbH
MouseRef-8 v2.0 Expression BeadChip Kit	Illumina, San Diego
TotalPrep RNA Amplification Kit	Illumina Inc.
RNeasy micro kit	Qiagen GmbH
RNA Clean & Concentrator TM-5 Kit	Zymo Research
Agilent RNA 6000 Pico Kit	Agilent Technologies
RNeasy MinElute Kit	Qiagen GmbH
Transcriptor High Fidelity cDNA Synthesis Kit	Roche GmbH
TargetAmp^{TM} 2-Round Biotin-aRNA Amplification Kit 3.0	Epicentre Biotechnologies

3.1.6 Solutions

Solution	Reagents
Antibody staining solution	PBS pH 7.2; 1% BSA; 0.5% Triton X-100

3.1.7 Chemicals and reagents

Name	Supplier
Bovine serum albumin (BSA)	Carl Roth GmbH
Cholera toxin subunit B conjugates	Invitrogen GmbH
Diethylpyrocarbonate (DEPC)	Carl Roth GmbH
Ethanol 99.9%	Carl Roth GmbH
Histoacryl Topical Skin Adhesive	B. Braun GmbH

Tissue-Tek O.C.T. compound	Sakura Finetek GmbH
RNase AWAY	Molecular Bioproducts
Paraformaldehyde (PFA)	Carl Roth GmbH
PBS pH 7.2	Invitrogen GmbH
Sucrose	Carl Roth GmbH
Triton X-100	Carl Roth GmbH
Trizol reagent	Invitrogen GmbH
β-Mercaptoethanol	Carl Roth GmbH
Glycerol	Carl Roth GmbH
Isopropanol	Carl Roth GmbH
Methanol	Carl Roth GmbH
VectaShield	Vector Labs Inc
Xylene	Carl Roth GmbH
2-methylbutane	Carl Roth GmbH
Ketamine	Medistar GmbH
Xylazine	Riemser AG
Myzotect Tincture	Hager Werken

3.1.8 Software

Program	Application	Supplier
Bead Studio	Microarray data analysis	Illumina, San Diego
Image J	Image processing	Abramoff et al., 2004
Photoshop CS5	Image processing	Adobe Inc
Prism	Data analysis	Graph Pad
Illustrator CS5	Image processing	Adobe Inc
IPA	Pathway/Network analysis	Ingenuity Systems
Panther	Molecular functions/biological process	pantherdb.org
DAVID	KEGG pathway mapping	http://david.abcc.ncifcrf.gov/home.jsp

3.2 Mouse animal experiments

All experiments were performed on mice in accordance with the animal protection law of Germany (Bezirksregierung Braunschweig, Germany) and were approved by the district government. Animals were fed *ad libitum* and were maintained by the animal facility of the ENI-Goettingen under the control of a veterinarian.

3.2.1 Retrograde tracing of motor neurons with cholera toxin subunit B

Alexa 555-conjugated cholera toxin subunit B (CTXB), a retrograde tracer was obtained as a lyophilized powder. The lyophilized powder was reconstituted in PBS to a final concentration of 1 µg/µl and was aliquoted and stored at -20^0C. Prior to the surgery CTXB was filled into glass injection capillary. Adult mice were anesthetized with an intraperitoneal injection of ketamine (100 mg/kg) and xylazine (10 mg/kg). Then, when the animals were under deep anaesthesia, the hair in the region of interest (around the desired muscles) was removed using a fine beard trimmer. The hair was blown away using a hair dryer and the exposed skin was cleaned using 70% ethanol, prepared in double-distilled water. The animal was the kept on a heating pad during the entire duration of the surgery. The skin was then incised using fine microscissors at appropriate area to expose the muscles of interest - tibialis anterior (TA) or soleus. The membranes surrounding the muscles were carefully cleaned ensuring no damage to the muscle. Then CTXB in the glass micropipette was injected into the muscles (at 3-4 locations in TA and 1-2 location in soleus muscles). Any spill was immediately cleared using a lint-free tissue paper. The wound was immediately sealed using tissue glue Histoacryl. A drop of PBS was applied to both the eyes to prevent drying and the animals were placed in a humidified chamber maintained at 32^0C until recovery. Following recovery, they were transferred to their respective home cages. Sample collection post injection depended on the experiment type. Minimum post operative time for sample collection was 7 days (for HS study), 10 days (for FMNT marker study) or 2 weeks (for endurance training study). The animals exhibited no necrotic scars or signs of illness post-operation (intramuscular injection). Weight gain was normal in all animals.

3.2.2 Endurance training

CD1 mice from 2-3 litters were pooled at P2 (post-natal day 2) and then were randomly redistributed to their mothers. Only male animals were used in all of endurance training experiments. Females were avoided because of possible hormonal variations which may make interpretations complex. The animals were weaned at P21. The males were grouped into control and training groups and were housed in individual cages and were maintained under standard conditions (12 hour light: dark cycles). All the animals were fed *ad libitum*. Weights were taken on the day of weaning and only animals of comparable weights were used in downstream experiments. The animals were acclimatized in individual cages for 3 days and were then subjected to forced endurance training on a motor driven speed regulated treadmill. The endurance training lasted for 7 weeks (first week was for acclimatization). During the first week, the animals were acclimatized to the treadmill and to the desired speed. The first week training durations lasted for about 15 minutes (min). Briefly, the mice were kept on a motorized treadmill with the motor on and speed maintained at zero. The shocking grid was turned off. Then after 5 minutes of acclimatization, the shocking grid was turned "on" and the speed was increased to 5 meters/minute (m/min) and was maintained at that speed for about 15 min. From the next day onwards, the speed was progressively increased until the desired training speed of 17 m/min was achieved (each day 3 speeds were used, and each speed was maintained for about 3-5 min). The actual training protocol started from the next week. The mice were kept on the treadmill with the motor on and after 5 min of acclimatization the shocking grid was turned on and the speed was progressively increased to 17 m/min (6-7 m/min for 2 minutes, 10 m/min for 2 minutes, and from then a ramp of 1 m/min until 17 m/min was reached) and this speed was maintained for 1 hour /day. The animals ran during the entire duration of 1 hour (hr).

Protocol: 17 m/min; 1 hr/day; 5 days/week; 6 weeks

After 4 weeks of training, a surgery was performed as described above to administer intramuscular injection of retrograde tracer CTXB. The animals were, then given 4 days to recover and were again subjected to training for 2 weeks. After the

completion of experiments, the animals were sacrificed either by cervical dislocation (for microarray experiments) or by transcardial perfusion with PBS and 4% PFA under ketamine/xylazine anaesthesia for immunohistochemical studies. Spinal cords, muscles and blood samples were collected from the animals and were processed as described in the following sections.

3.2.3 Hindlimb suspension

CD1 mice from 2-3 litters were pooled at P2 and then were randomly redistributed to their mothers. Only male animals were used in all of HS experiments. The animals were weaned at P21 and the males were grouped into control and suspension groups. Weights were taken on the day of weaning and only animals of comparable weights were used. The control animals were housed in normal home cages, whereas the animals in the suspension group were housed in special custom designed cages. All the animals were fed *ad libitum*. The animals were acclimatized to the new cages for 1 week. Then the animals were subjected to HS for 28 days using the method described by Morey (Morey-Holton and Globus, 2002). The following methodology was adopted. Animals were anesthetised by ketamine/xylazine and the tail was then cleaned with 70% ethanol and dried. Mizotect tincture was applied to the tail and was allowed to dry for approximately 10 min. Then a traction tape mounted on a plastic tab was attached from the base of the tail. The tape was attached in such a way, that the tail was exposed to air in the middle and tip. PBS was applied to the eyes to prevent drying and the animals were kept for recovery in a humidified chamber maintained at 32^0C. Upon recovery, they were transferred to the suspension cages. On the next day, the animals were hindlimb unweighted. The angle subtended was approximately 30-40 degrees and was maintained throughout the course of 4 weeks by periodically adjusting the height using knobs. The animals were able to roam around freely with their forelimbs. If the animal comes out of suspension, they were resuspended (but without anaesthesia). Weights were registered on the day of suspension and on the terminal day. After 3 weeks of suspension, a surgery was performed as described above (3.2.1) to administer intramuscular injection of retrograde tracer CTXB. The animals were given 10 hrs to recover completely from anaesthesia and were then resuspended for one more week. After the completion of experiments, the animals were sacrificed either

by cervical dislocation (for microarray experiments) or by transcardial perfusion with PBS and 4% PFA under ketamine/xylazine anaesthesia (for immunohistochemical experiments). Spinal cords, muscles and blood samples were collected from the animals and were processed as described in the following sections. If an animal lost more than 25% of body weight, the animal was excluded from analysis (this happened only twice during the current study). The animal experiments were done in collaboration with a Canadian group, following which; I have received the muscle and spinal cord samples for down stream experiments.

3.2.4 Tissue Processing

Mice were sacrificed either by cervical dislocation (for microarray studies) of by performing transcardial perfusion (with PBS and 4% PFA) under ketamine/xylazine anaesthesia for immunohistochemical studies. In mice sacrificed by cervical dislocation, the spinal cord (lumbar region) was immediately flash frozen in OCT compound with dry ice and was stored at -80^{0}C until cryosectioning for laser capture microdissection experiments. The muscles (TA and soleus) of these animals were either immediately kept in Trizol reagent for subsequent RNA extraction or were flash frozen in liquid nitrogen cooled 2-methylbutane and were stored at -80^{0}C until cryosectioning for fluorescence immunohistochemistry experiments. The spinal cords and ventral roots obtained from the animals, sacrificed by transcardial perfusion were post-fixed for an additional 60-90 min in the same fixative (4% PFA) on ice. Subsequently, they were washed for 4 hrs in PBS at 4^{0}C and were kept in either 20% or 30% sucrose (prepared in PBS) for overnight (12-16 hrs) at 4^{0}C. After the sucrose treatment, the spinal cords were equilibrated for 5-10 min in OCT compound and were placed into an embedding mould filled with OCT compound. Subsequently, the moulds were rapidly frozen using dry ice and were stored at -20^{0}C to -26^{0}C until cryosectioning. For cryosectioning, the OCT blocks (flash frozen or fixed samples) were removed from the moulds and were mounted on chucks and were sectioned in a CM 1510S cryostat. Cutting temperatures were adjusted to -18^{0}C to -22^{0}C. Section thickness depended on the downstream experiments. For laser capture experiments, the section thickness was 8 µm and the sections were cut in longitudinal orientation, for general immunohistochemistry, cross sections were used and the section thickness was 30-40 µm. For floating immunohistochemistry experiments (for c-Fos

experiments) the section thickness was 60 µm. All muscle sections were of 10 µm. Sections used in immunohistochemistry were collected on Superfrost Plus microscope slides and were air dried for 3-4 hrs and were stored for subsequent experiments at -20^0C. The sections used for laser capture were collected on Silane-Prep slides (Sigma-Aldrich GmbH) and were always kept at -20^0C (during sectioning) and were then immediately stored at -80^0C until further downstream processing.

3.2.5 Laser capture microdissection

Sample collection and initial processing until cryosectioning for laser capture microdissection was described in section 3.2.4. The following tissue processing steps was done in RNase free coplin jars. The slides with longitudinal spinal cord sections were removed from -80^0C and were fixed in ice cold 70% ethanol (prepared in DEPC- PBS) for about 1 min, followed by 3 washes in ice cold DEPC PBS. Then the slides were dehydrated by a ethanol gradient (30 seconds (sec) in ice cold 70% ethanol, 30 sec in ice cold 95% ethanol, 2 incubations of 1 min each in ice cold 100% ethanol) and subsequent dehydration steps were done using xylene (2 incubations of 1 min each). Xylene incubation step was critical for subsequent laser capture process. The processed slides were kept at room temperature and were directly used for laser capture process. The slides were kept at this stage for no more than 30 hrs. For the microdissection of fluorescently labelled motor neurons, I used Arcturus Veritas microdissection system (MDS Analytical Technologies) coupled with a fluorescent package. The Alexa 555 positive cells (retrogradely traced motor neurons) were microdissected from the longitudinal sections of lumbar spinal cord using an infrared (IR) laser. Using fluorescent excitation the outline of the cells to be captured was marked. Then fluorescent light was turned off and the cells were shot using an IR laser in transmission mode. IR laser settings (spot size, intensity were adjusted to ensure specific isolation of marked cells). HS transfer caps were used to capture motor neurons. Approximately 50 cells from several slides were collected per cap. Validation of the captured cells was done at the quality control station of the setup in both bright field and fluorescent channels. Upon capturing of the motor neurons, the cap was removed from the setup and the microdissected cells were lysed by in-situ 10 min incubation with 30 µl of RLT buffer (Qiagen GmbH), with intermittent mixing by pipetting. The sample was then collected by centrifugation into

a 500 µl microcentrifuge tube and was stored at -80^{0}C until further use. All the above steps were carried out under RNase free conditions. The setup and the chamber were cleaned with RNase Away to ensure RNase free working conditions. (Espina et al., 2006).

3.2.6 RNA purification from the laser-captured cells

For the isolation of total RNA from the laser-captured cells, RNeasy micro kit was used according to the manufacturer's protocol. Following elution, the RNA was concentrated on a Vacufuge concentrator (Eppendorf) to concentrate the RNA.

3.2.7 Quantification of RNA

The concentrated RNA was checked for quality and quantity on a Pico-chip using the Bioanalyzer2000 (Agilent Technologies). The analysis was done using Agilent RNA 6000 Pico Kit following the manufacturer's protocol and specifications.

3.2.8 Amplification and synthesis of biotin-labelled RNA from RNA of laser-captured cells for microarray hybridization

The amplification and biotin labelling was carried out using TargetAmp™ 2-Round Biotin-aRNA Amplification Kit 3.0. The manufacturer's protocol was strictly followed. As one microarray chip has eight individual slots, all eight samples to be hybridized on one chip were processed in parallel (using the same master mix and conditions) to minimize technical variations.

3.2.9 RNA Extraction from muscles

The animals were sacrificed by cervical dislocation and the muscles (TA and soleus) were isolated and immediately immersed in Trizol reagent kept on ice (in microcentrifuge tubes). The samples were then flash frozen in liquid nitrogen and were stored at -80^{0}C for not more than 1 month. Subsequently, RNA was extracted from the samples according to the manufacturer's protocol. The extracted RNA was quantified using NanoDrop (Perkin Elmer) and used for the subsequent experiments

(amplification and labelling-for microarray studies or for cDNA preparation; for qPCR studies)

3.2.10 Synthesis of biotin-labelled RNA for microarray hybridization

Illumina TotalPrep RNA amplification kit was used for generating the biotin-labelled aRNA from the muscle RNA samples. 100 ng of total RNA from each muscle was used as input. As one microarray chip has eight individual slots, all eight samples to be hybridized on one chip were processed in parallel (using the same master mix and conditions) to minimize technical variations. The reactions were carried out according to manufacture's protocol and specifications. In the final step the biotinylated aRNA was eluted with nuclease-free water and the concentration was determined using NanoDrop. The final concentration was adjusted to 200 ng/µl. The biotinylated-aRNA (amplified RNA) was stored at -80^{0}C until further use in microarray hybridization experiments.

3.2.11 Microarray Hybridization

A total of 1 µg of biotinylated-aRNA generated as described in 3.2.8 and 3.2.10, was used from each sample for hybridization. The aRNA samples were applied to MouseRef-8 v2.0 expression BeadChips and were processed following the manufacturer's protocol. Microarray hybridization, imaging and data analysis were performed and obtained from Dr. Lars Wittler and Dr. Phillip Grote at the Max-Planck Institute of Molecular Genetics, Berlin. I have received the expression profile data, in excel sheet format.

3.2.12 Quantitative PCR

Quantitative real-time PCR (qPCR) was performed using a Roche LightCycler 480. cDNA was generated from the RNA samples using either iScript™cDNA Synthesis Kit or Transcriptor High Fidelity cDNA Synthesis Kit. All qPCR reactions were performed using the Roche Universal Probe Library (UPL). The primers were designed using Assay design Center available with Roche. The genes were identified by NCBI reference sequence number and primers were designed for amplifying the longest transcript using Assay Design Center. Data was normalized to either of the

housekeeping genes (hypoxanthine phosphoribosyltransferase (*Hprt*) or alpha-tubulin 1B). Reactions were set up and run according to the Roche LightCycler protocol.

Roche Assay Design Center:

(https://www.roche-applied science.com/sis/rtpcr/upl/index.jsp?id=UP030000).

3.2.13 Pathway analysis

The processed microarray data (Illumina IDs, along with the respective fold change values, either upregulated, downregulated or up- and downregulated together) were uploaded to Ingenuity Pathway Analysis Suite (Ingenuity Systems). Data was analyzed with the default settings in the software except for stringency, which was kept "high" and selection of "experimentally verified" filters. The data was analyzed at multiple levels. The data was analyzed in the context of canonical pathways, molecular and physiological functions, diseases and networks. The data was exported using "export function" of the software and was modified for representation using Photoshop CS5. The microarray data was also analyzed using the freely available DAVID (Database for Annotation, Visualization and Integrated Discovery) bioinformatics resources. The gene list/Illumina IDs (of significantly (p-value <0.05) altered transcripts) were uploaded to DAVID and were analyzed using the default settings (Huang da et al., 2009a; Huang da et al., 2009b). The genes were mapped to KEGG (Kyoto Encyclopedia of Genes and Genomes) (Kanehisa and Goto, 2000) pathways by the functional annotation tool of DAVID. The pathways were copied to Adobe Illustrator CS5 and were processed for presentation. For Panther gene expression analysis, the gene list of significantly up- or downregulated genes was copied to the work space (with *Mus musculus* genome selected) and analyzed in the context of molecular functions and biological processes (Thomas et al., 2003). The pie charts generated, were copied to Adobe Illustrator CS5 and processed for presentation. Percentage 1 - is the percent of genes classified to the respective category over the total number of genes and Percentage 2 – is the percent of genes classified to the respective category (function or process) over total number of class (function or process) hits. Heat maps of differentially regulated transcripts were generated using Microsoft Excel with a freely available macro. Venn diagrams were generated using GeneVenn.

(http://simbioinf.com/mcbc/applications/genevenn/genevenn.htm)

3.3 Immunohistochemistry

The slides were removed from -20^{0}C and were thawed at room temperature for 5 min. Then, they were transferred to a dark humidified chamber and all subsequent steps were performed on slides kept in humidified chamber. The slides were then washed with PBS primarily to rehydrate the tissue and also to remove residual embedding medium. Washes were done 3 times, each for 10 min at room temperature. After washing, primary antibody solution (500-700 μl) was applied immediately. The primary antibodies were diluted in the antibody staining solution to a concentration mentioned in 3.1.6. The sections were then incubated in primary antibody overnight at 4^{0}C (14-16 hrs). The next day, the primary antibody solution was removed and the slides were thoroughly washed with PBS (3 washes X 10 min each). Then, the appropriate secondary antibody solution (700 μl) (3.1.3) was applied and the slides were incubated for 1 hr at room temperature. The secondary antibodies were also diluted in the antibody staining solution. All secondary antibodies were applied at a dilution of 1:1000. After 1 hr, the secondary antibody was removed and the slides were thoroughly washed with PBS (5 washes X 10 min each). The slides were then mounted with coverslips using either 50% glycerol (prepared in PBS) or with VectaShield to prevent fading and were stored at 4^{0}C until imaging. Drying was avoided at all stages of the procedure. 60 μm floating sections were processed in a similar fashion (procedural outline) as described above for slides, only that they were kept in 12 well plates. The sections were washed for 4-5 hrs on a horizontal shaker to remove excess OCT compound. Then they were incubated with primary antibody for 2 days at 4^{0}C on a shaker. Sections were then washed 2 times (each wash is about 4-5 hrs) with PBS and were subsequently incubated in secondary antibody for 1 day at 4^{0}C on a shaker. Following this, the sections were washed overnight in PBS at 4^{0}C on a shaker and were mounted in 50% glycerol (prepared in PBS). They were then stored at 4^{0}C until imaging. All antibodies used were diluted in the antibody staining solution. Muscle sections were collected on Superfrost plus microscope slides and were post-fixed with ice cold acetone or 2% PFA for 5-10 min in the cold room. They were then, subsequently

washed with PBS (3 washes x 10 min each). Then the sections were processed in the same fashion as described above.

3.3.1 Confocal microscopy

After fluorescence immunohistochemistry, the slides were imaged on a DMRIE2 microscope (Leica Microsystems) with a SP2 TCS scanner (Leica Microsystems). Images were taken using either 10X, 20X, 40X or 63X objectives (40X and 63X – oil immersion objectives). Images were acquired using the Leica software. All the pictures were obtained at an original resolution of 1024 x 1024 pixels. In case of muscle sections, 10x images were taken at different frames and were stitched later using the photomerge option in Adobe Photoshop CS5. In co- localization studies, sequential scanning (in between the lines) was performed in 2 or 3 different channels with the appropriate PMT detection settings, in order, to avoid signal bleed-through. Adjustments on signal quality were performed in the "QLUT" mode where both the gain and offset were adjusted to obtain the best representation of the signal. Pinhole settings were adjusted to obtain best signal without compromising confocality. 4-16 consecutive optical sections were obtained (depending on section thickness) by sequential scanning (in case, of double or triple labelling), throughout the z-axis of the section. Afterwards, the images were imported into the ImageJ software and maximum intensity stacked projections were obtained and were further processed using Adobe Photoshop CS5. All adjustments in Photoshop CS5 (brightness, contrast, etc) were applied uniformly across the image. Further, the templates for presentation were made in either with Adobe Photoshop CS5 or with Adobe Illustrator CS5 software.

3.3.2 Soma-size quantification

The soma areas of motor neurons of mouse lumbar spinal cords were quantified on maximum intensity projections (obtained as described in 3.3.1) of optical sections. Imaging was done using Leica confocal laser scanning microscope. The images were obtained at a magnification of 20X and an original resolution of 1024 x 1024 pixels. Quantification was done on lumbar spinal cord cross sections double-stained for Tamnec1 and vAChT. Motor neuronal soma was outlined using Adobe Photoshop CS5 and the number of pixels in the outlined soma was noted. Presence of nucleus

was not used as a criterion. The pixel number was further converted into μm^2 (calculated from the scale bar and original resolution data). Soma-size distribution graphs represent grouped data from 3 animals. Soma-size distributions were plotted using GraphPad Prism software.

3.3.3 c-Fos quantification

The image acquisition and processing is described in section 3.3.1. The c-Fos intensity (strong versus weak versus absent) was manually quantified in a double-blind manner. Motor neurons in these experiments were identified by CTXB label. After counting the graphs was constructed with GraphPad Prism software.

3.3.4 Quantification of serum corticosterone levels

Quantification of serum corticosterone levels was done using ImmuChem[TM] Double Antibody Corticosterone ^{125}I RIA kit. All these experiments were done in collaboration with Prof. Dr. Hubertus Jarry (University Klinikum, Goettingen). The data obtained was analyzed using GraphPad Prism software.

3.3.5 Statistics

All statistical analysis was done using GraphPad Prism 5.0 software unless otherwise stated. Wherever applicable, student's t-test was used to calculate significance. Error bars in the figures indicate either standard deviation or standard error of mean.

IV Results

4.1 Strategy to isolate predominantly fast or slow motor neurons in adult mouse

All the motor neurons (MNs) innervating a single muscle are clustered to form a motor pool in the spinal cord. Functional motor neuron type status (FMNT status) is accurately matched to the type of the muscle fibers they innervate, and hence the motor pool composition reflects the fiber composition of the respective muscle. Mammalian muscles are heterogeneous in their fiber type composition, and hence their motor pools are also heterogeneous and contain different relative proportions of αFF, αFI, αFR, αS, β and γ motor neurons (innervating type IIb, IIx/d, IIa, I muscle fibers, respectively). This, together with the scattered anatomical organization of the FMNTs in the spinal cord, makes the task of identifying specific markers or gene signatures for FMNTs difficult. However, certain muscles in the rodents and other mammals are relatively enriched in either fast or slow muscle fiber types. For example, the soleus muscle in cats and rats is highly enriched in slow (type I) muscle fibers (Kernell, 2006). Therefore, the soleus motor pool in these animals is relatively enriched in αS (slow) MNs. Further, the neurons within a motor pool can be specifically retrogradely traced using intramuscular injections of tracers like cholera toxin subunit B (CTXB) or dextran-conjugates (Fig. 4) (Gramsbergen et al., 1996). When these tracers are coupled with fluorescent labels, it enables specific visualization of these neurons, thereby facilitating their isolation with the aid of techniques like laser capture microdissection. Further, transcriptional analysis can be performed on these isolated neurons, enabling one to identify specific markers and gene signatures for specific for different FMNTs. So, choosing the right muscle is of paramount importance in identifying markers for different FMNTs. The mouse model, with its genome sequenced and the relative ease of manipulating its genome through established gene targeting or transgenic technology, offers the system of choice to study the functional importance of FMNT-specific markers or gene signatures obtained in a screen such as the one mentioned above.

4.2 Characterization of tibilalis anterior (fast) and soleus (slow) muscles of CD1 mouse

To identify novel FMNT markers, I have chosen to retrogradely trace, identify and isolate mouse tibialis anterior (TA) and soleus MNs and perform transcriptome analysis on these isolated MNs. Mouse TA, is a predominantly fast muscle enriched in fast muscle fibers, and hence its motor pool is enriched in fast MNs. TA is used in dorsiflexion, whereas mouse soleus is a mixed muscle and it has both type I and type IIa muscle fibers and, hence its motor pool enriched in αS and αFR motor neurons. Because muscle fiber type composition can vary between strains (Totsuka et al., 2003), and since I have used CD1 mice in all my experiments, I made a thorough characterization of its TA and soleus muscles. As a prerequisite to comment upon the type status of the FMNTs present in their motor pools, I first characterized TA and soleus muscles of CD1 mice using immunohistochemistry by using fiber type specific monoclonal antibodies on 10 μm cross sections and by quantitative PCR (qPCR). The results are shown in Figs. 2 and 3. MY-32 antibody recognizes an epitope on myosin heavy chain and it stains fast (type II) fibers. TA is virtually entirely composed of MY-32 positive fast muscle fibers (Fig. 2A and Fig. 3A), whereas soleus has approximate equal proportions of fast (MY-32 positive) and slow (MY-32 negative) fibers (Fig. 2B and Fig. 3B). Fast muscle fibers are further classified into type IIb (encoded by *Myh*4 gene), type IIx/d (encoded by *Myh*1 gene) and type IIa (encoded by *Myh*2 gene) fibers. So, to further gain an insight into the fast fiber type composition of TA and soleus, I performed immunohistochemistry on TA and soleus using type IIb, IIa specific monoclonal antibodies (type IIb, Fig. 2C-D and type IIa, Fig. 2E-F and Fig. 3C-D). BF-F3 antibody recognizes myosin heavy chain IIb and it stains fast (type IIb) muscle fibers. TA is highly enriched in type IIb muscle fibers (Fig. 2C), whereas soleus which is generally considered as a slow-twitch muscle is entirely devoid of type IIb muscle fibers (Fig. 2D). TA also has type IIa muscle fibers as revealed by immunostaining with SC-71 antibody (Fig. 2E and Fig. 3C). SC-71 antibody recognizes myosin heavy chain IIa and stains type IIa muscle fibers. Further, the type IIa muscle fibers in TA are concentrated primarily deep in the muscle (Fig. 3C). Soleus on the other hand has approximate equal proportions of type IIa positive and type IIa negative slow fibers (Fig. 2F and Fig. 3D). Finally, I performed immunostaining to check the slow muscle fiber type composition of TA

and soleus using BA-F8 antibody. BA-F8 antibody recognizes slow myosin and it stains slow muscle fibers. It can be seen that TA is entirely devoid of type I fibers (Fig. 2G and Fig. 3E) whereas soleus is enriched in type I fibers (Fig. 2H and Fig. 2F). Further, qPCR performed on cDNA made from RNA extracted from TA and soleus muscles indicate an abundance of fast transcripts *Myh*4 and *Myh*1 in TA (Fig. 2I, J, respectively), confirming the immunohistochemistry results. *Myh*7 (slow) transcripts and *Myh*2 transcripts are abundant in soleus (Fig. 2L and K) congruent with the immunohistochemistry results shown in Fig. 2H and F. Taken together, these results clearly indicate that TA of CD1 mouse is a predominant fast muscle highly enriched in type IIb muscle fibers and entirely devoid of slow muscle fibers. On the other hand, the soleus of CD1 mice has approximate equal proportions of type I and type IIa muscle fibers. This fiber type repertoire also indicates the abundance of fast motor neurons (αFF) in TA motor pool as opposed to type αS and αFR in soleus motor pool. Thus, by retrograde tracing TA muscle of CD1 mice I can label a high proportion of fast MNs (αFF) and by retrograde tracing soleus muscle I can label approximate equal proportions of αs and αFR MNs (Fig. 4). These results thus form the foundation for interpreting FMNT screening results. From here onwards, TA MNs will be referred to as 'fast' MNs (used interchangeably) and soleus MNs will be referred to 'αs/ αFR' MNs (used interchangeably).
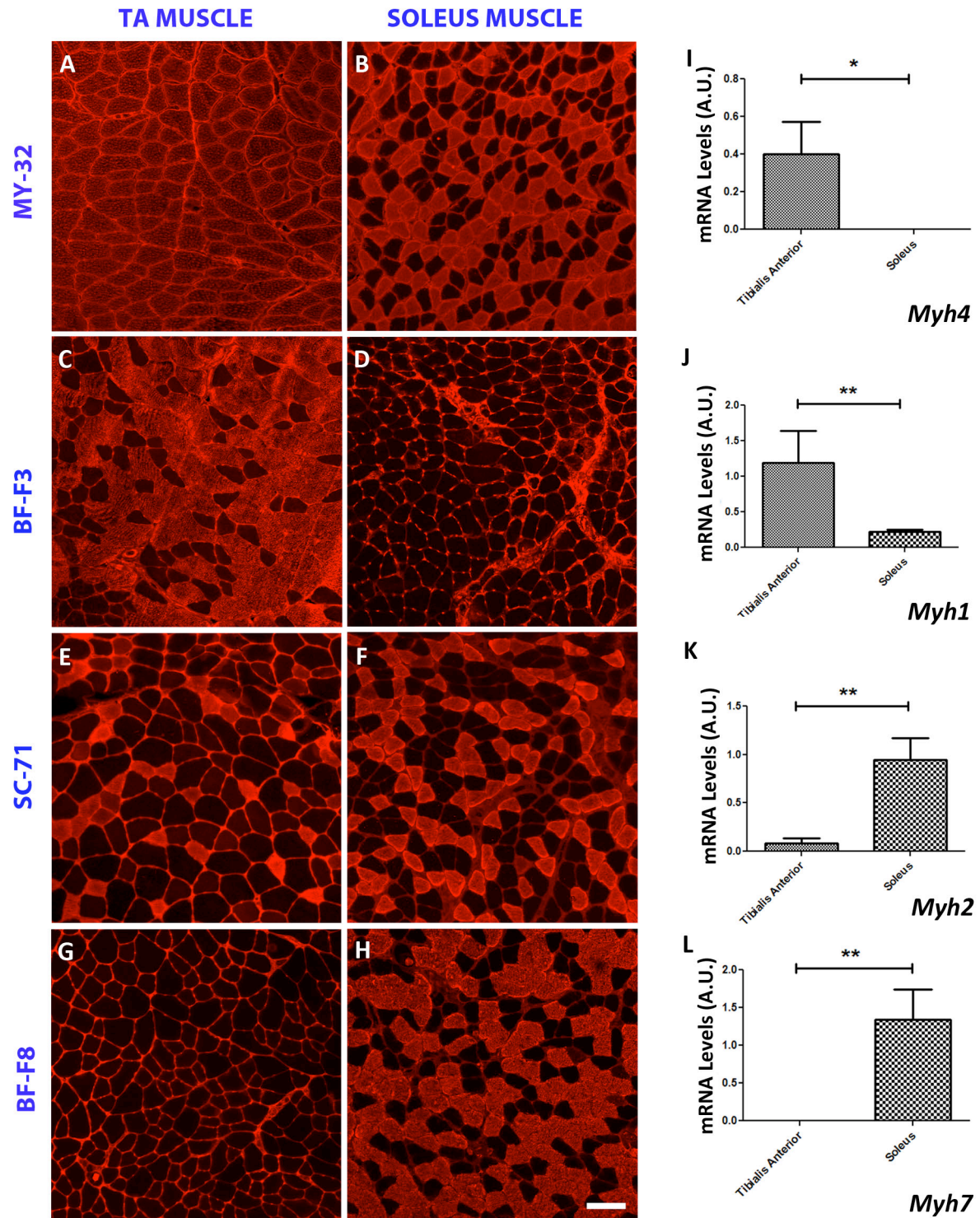
Figure 2: Characterization of TA and soleus muscles of CD1 mouse. Immunohistochemical analysis of mouse TA and soleus muscle cross-sections with MY-32 (A and B), BF-F3 (C and D), SC-71 (E and F) and BF-F8 (G and H) antibodies. qPCR analysis of *Myh4* (I), *Myh1* (J), *Myh2* (K) and *Myh7* (L) transcripts expression in mouse TA and soleus muscles. Section thickness is 10 μm and the scale bar represents 100 μm.
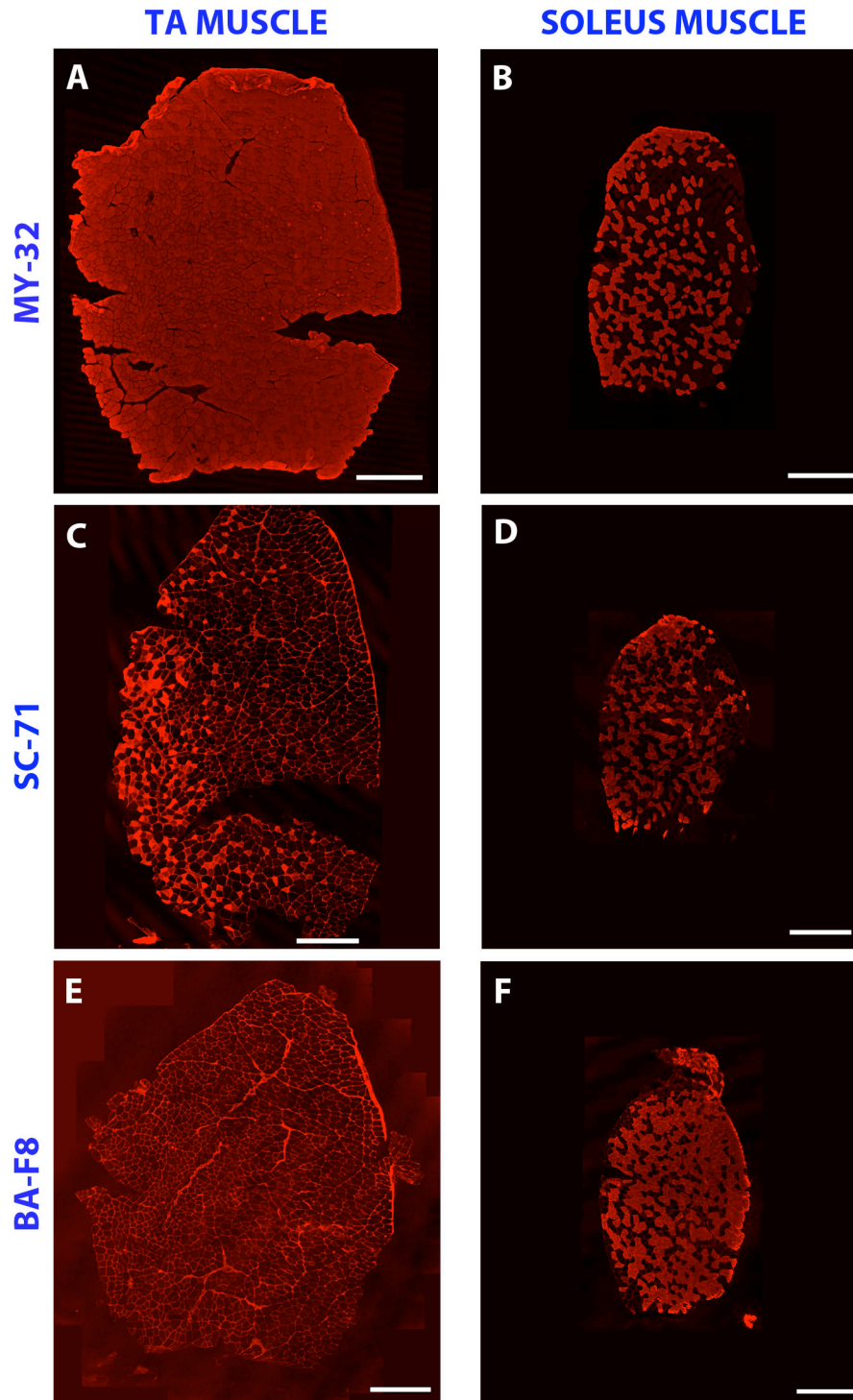
Figure 3: Immunohistochemical characterization of TA and soleus muscles of CD1 mouse. Cross-sections representing whole muscle cross sectional area were immunostained with MY-32 (A and B), SC-71 (B and C) and BA-F8 (E and F) antibodies. Section thickness is 10 µm and the scale bar represents 500 µm.

4.3 Retrograde tracing of adult TA and soleus motor neurons of CD1 mouse

In order to perform the FMNT screen, I should first identify and isolate MNs from muscles enriched in fast or slow fibers. To this end, I retrogradely traced adult TA and soleus MNs by intramuscular injections of fluorescently conjugated CTXB (Alexa 555) into TA and soleus muscles (Fig. 4A). I performed the intramuscular injections at P60, followed by a 10 day tracing and recuperation period prior to collecting spinal cords for MN isolation. All the traced (labelled) MNs are positive for vAChT (vesicular acetylcholine transporter, labels all cholinergic neurons (MNs in this context) (Arvidsson et al., 1997)) immunostaining (Fig. 4-1). This tracing process thus allowed me to identify MNs (fast versus αS/ αFR MNs) of TA and soleus muscles for downstream experiments (FMNT screen).
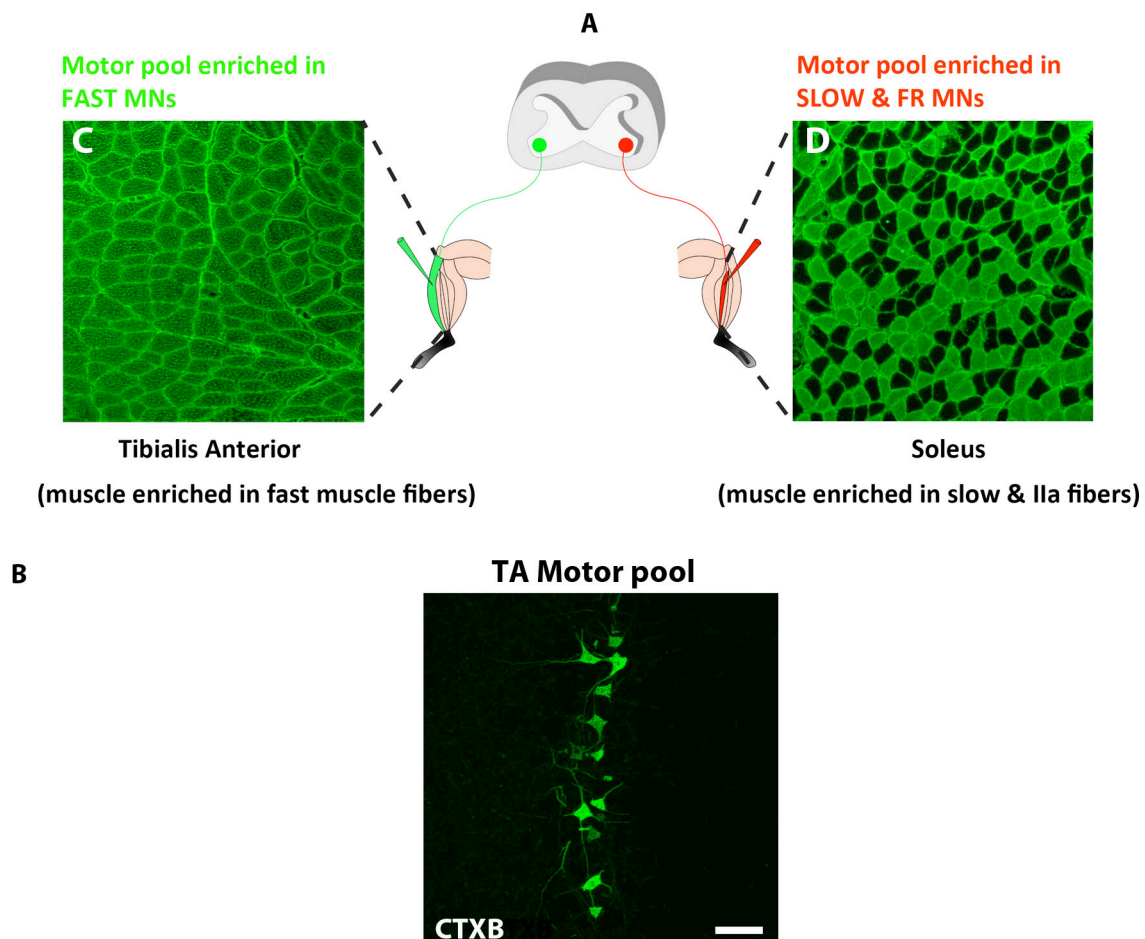
Figure 4: Schematic representation of retrograde tracing of TA and soleus motor neurons. Intramuscular injection of fluorescently conjugated CTXB in mouse TA (A, represented by green micropipette) and soleus muscles (A, represented by red micropipette). TA muscle fibers represented in 'C' and soleus muscle fibers represented in 'D' are immunostained with MY-32 antibody. Retrogradely traced TA, soleus MNs are represented by 'green' and 'red' circles in the spinal cord. Adult mouse spinal cord longitudinal section

showing retrogradely traced TA MNs is shown in B. Section thickness is 30 µm and the scale bar represents 100 µm.
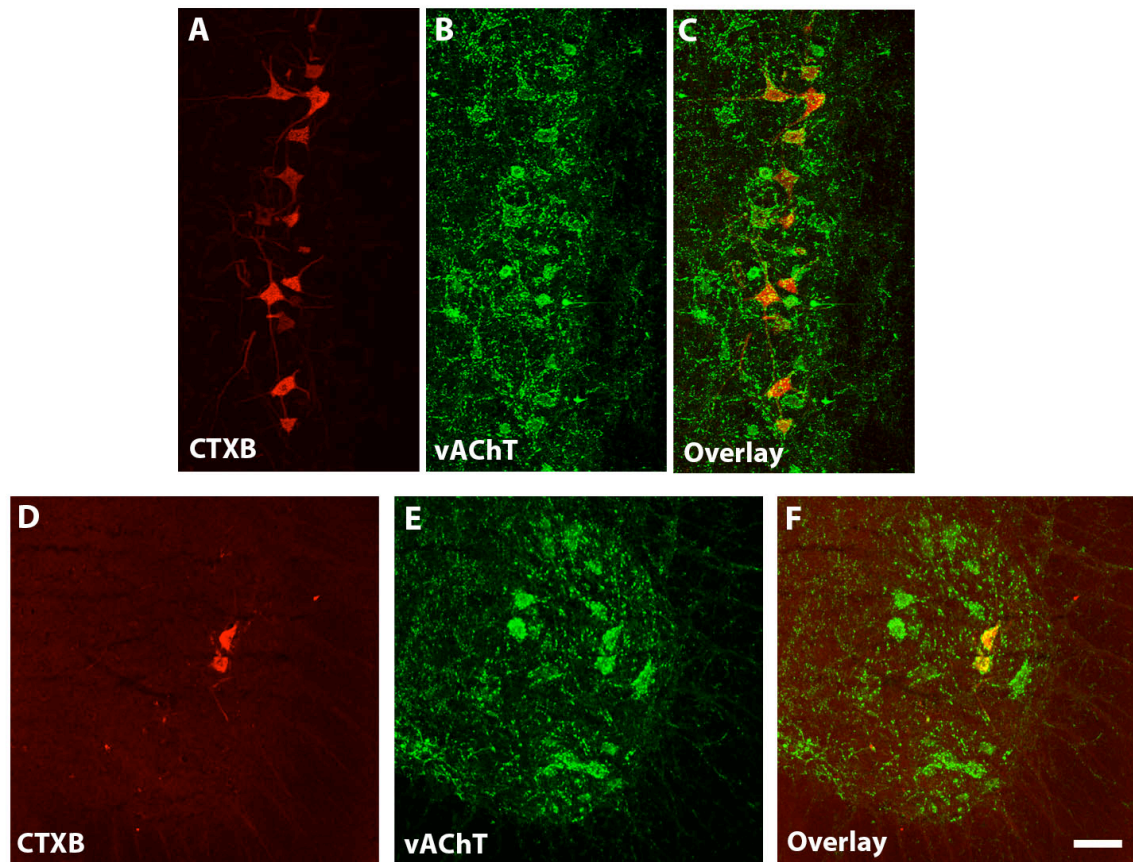
Figure 4-1: Retrogradely traced TA motor neurons. Retrogradely traced TA MNs in the spinal cord are represented in red (A and D). vAChT immunostaining of spinal cord sections represented in green (B and E). Overlay of A, B and D, E is shown in C, F, respectively. A, B and C represent longitudinal sections of adult spinal cord (P70) and D, E and F represent cross sections of adult spinal cord. Section thickness is 30 µm and the scale bar represents 100 µm.

4.4 Screen to identify markers and gene signatures of adult fast and slow motor neurons (FMNT screen)

Screening outline: By injecting muscles (n=12 animals, bilateral for TA and n=12 animals, bilateral for soleus) enriched in fast (TA) and slow (soleus) fiber types, with fluorescently conjugated (Alexa 555) CTXB, I could visualize their respective MNs (fast or αs/ αFR FMNTs) in the spinal cord (Fig. 4-1 and Fig. 5B). Following retrograde tracing, I have isolated the labelled MNs by using laser capture microdissection with low-energy infrared lasers (Fig. 5C), followed by extracting RNA from these cells. After pooling samples from 3 animals, the RNA samples were amplified and labelled (biotin labelling) using commercially available kits facilitating linear amplification (Fig. 5D). The samples were subsequently hybridized to Illumina BeadChip microarrays (MouseRef-8 v2 Expression BeadChip) (Fig. 5E). The raw data (Fig. 5F) obtained was processed to obtain expression and fold change values (Fig. 5G). This screening paradigm thus represents a new methodology to identify gene signatures/markers of muscle-specific MNs (in this case, fast and αs/ αFR MNs).
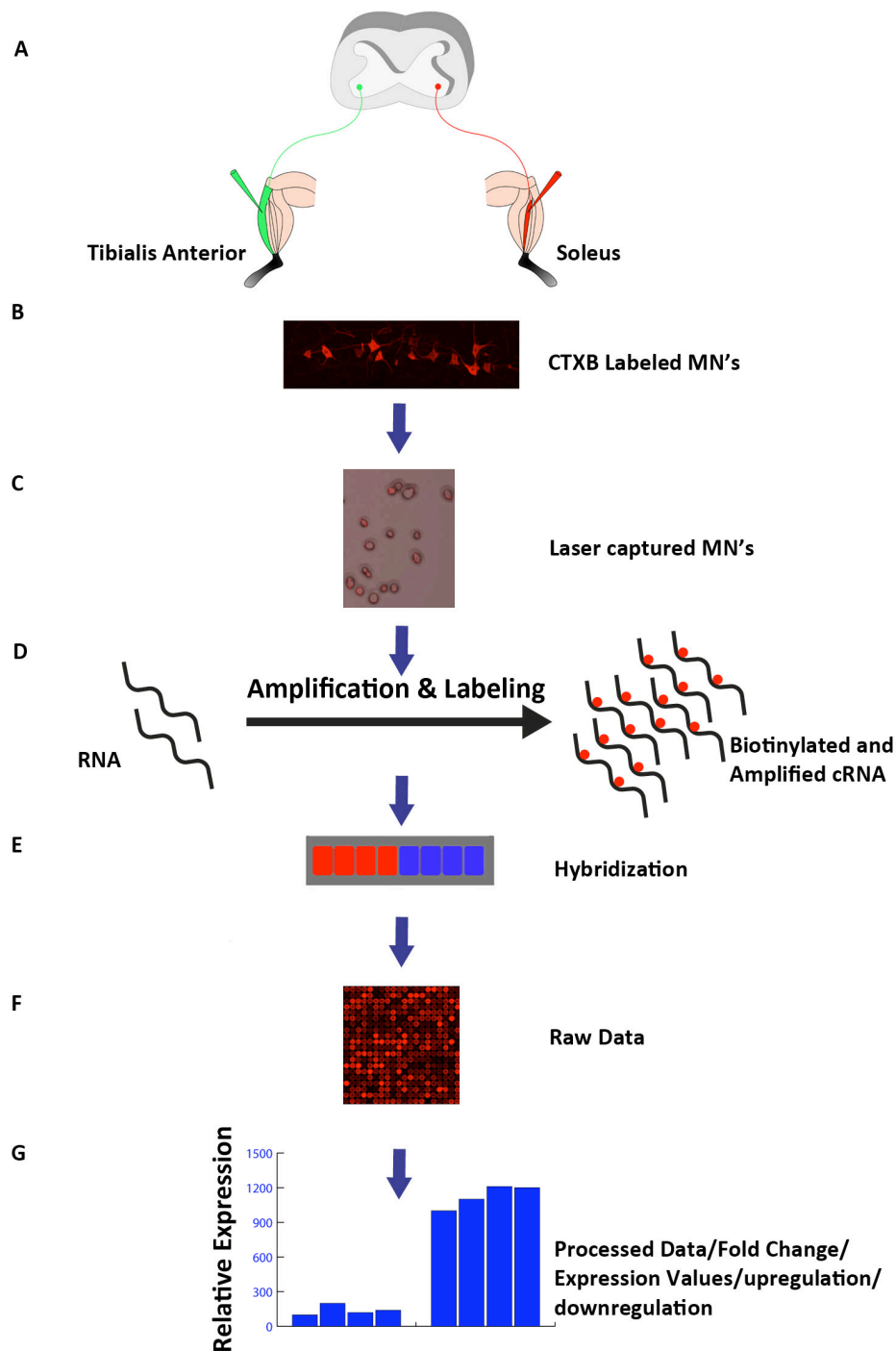
Figure 5: Schematic representation of the screen for adult FMNT population. At P60 the TA (fast) and soleus (I/IIa) muscles were injected (intramuscular) with fluorescently conjugated CTXB (A). At P70, the spinal cords are isolated and processed for cryosectioning to enable visualization of retrogradely traced MNs (fluorescently labelled) (B). The fluorescently labelled cells are isolated by laser capture microdissection (C). RNA was extracted from the laser-captured cells and was amplified (and biotin labelled) (D). The biotinylated RNA was hybridized to Illumina BeadChip microarrays (E). The raw expression data (F) was processed to obtain expression, fold change values (G).

Screening results

The results of the FMNT-screen are shown in Fig. 6 and Fig. 7. Whole transcriptome analysis of fast and αs/ αFR MNs has revealed that 503 transcripts are enriched in fast (TA) MNs and 929 transcripts are enriched in αS/αFR (soleus) MNs (Fig. 6A). 4984 transcripts (Fig. 6A) were expressed by both types of neurons and contains generic MN (*Chat*, etc.) and housekeeping (*Tuba1b*, *Gapdh,* etc.) genes. The transcripts which are expressed in an exclusive fashion (503 for TA and 929 for soleus) contain transcripts specific to fast and slow MNs (FMNT markers), pool specific transcripts, spinal level (lumbar) specific markers and extensor-flexor specific transcripts. Further downstream analysis (Fig. 9) are essential to validate the above mentioned candidates potential for being bona fide fast or slow MN markers. Heatmaps represent an elegant way of visualizing transcriptome data. Each value in the data set is colour-coded to graphically represent enrichment. So, I have generated heatmaps of the TA (fast MNs), soleus (αS + αFR MNs) enriched genes obtained from the screen. The heatmaps are shown in Fig. 6B. Red represents enrichment (abundance) and blue represents low abundance of the genes/transcripts. This data, represents a unique 'gene signature set' for TA and soleus MNs.
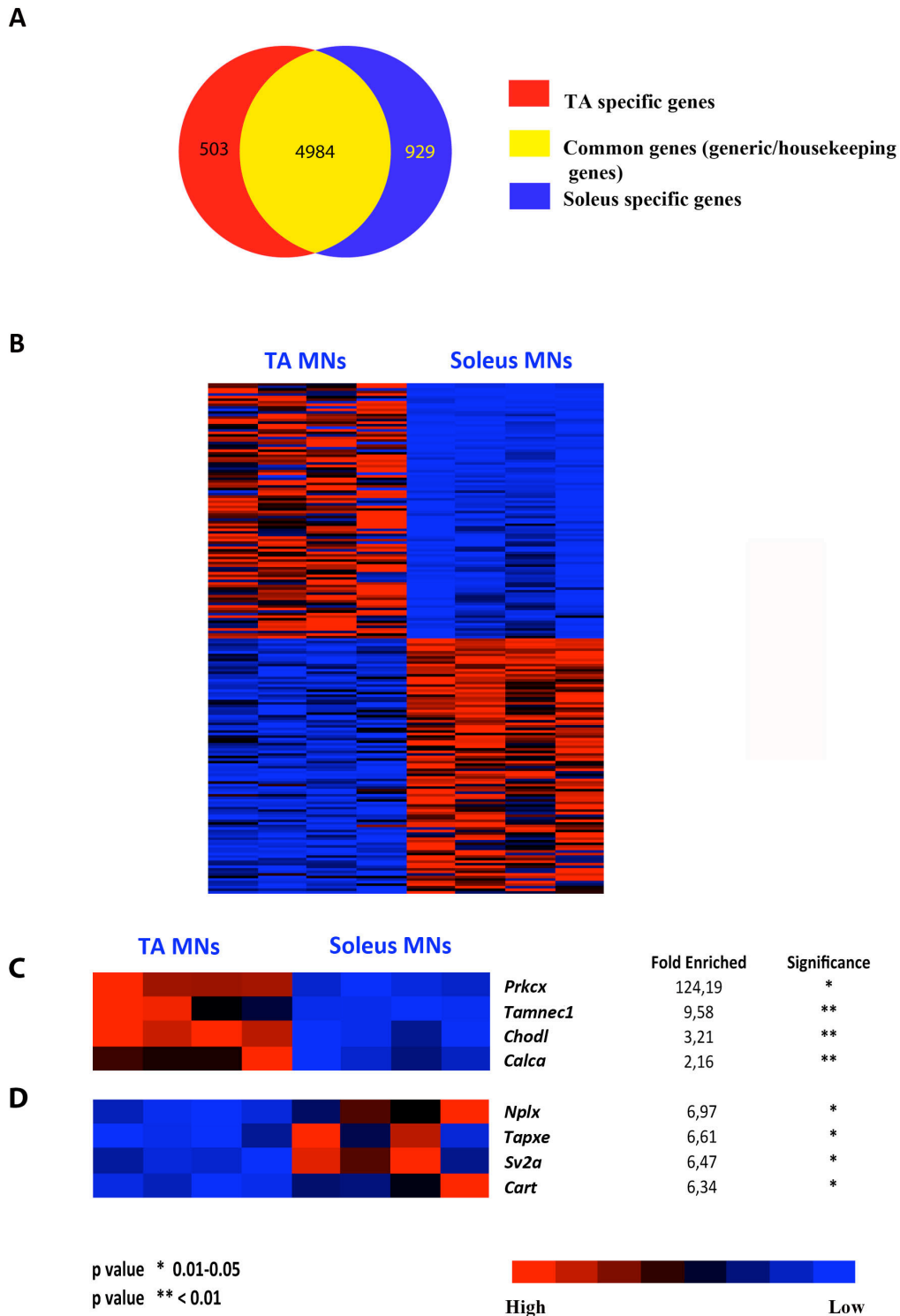
Figure 6: Expression analysis of fast and slow/FR enriched motor pools (TA and soleus) of adult mouse (FMNT screen expression analysis). Venn diagram representing gene expression in fast (TA) and slow/FR (soleus) MNs of adult mouse (A). Heatmaps (B) of selected genes that are significantly enriched in either TA or soleus MNs. Heatmaps of selected candidates with fold change (FDC) and significance values (TA enriched, C; soleus enriched, D). The threshold level for gene expression was set to 100 relative units to avoid false positive results. Red represents high level of expression and blue represents low level of expression. p-value criteria are shown in the bottom left-hand side of the image.

4.5 Comparison of expression levels of selected genes from adult FMNT screen

The expression data from the microarray analysis revealed that *Prkcx* (protein kinase C-x, Fig 6C and Fig. 7B) and Tamnec1 (tibialis anterior MN-enriched collagenase 1, Fig. 6C and Fig. 7A) are highly enriched in TA MNs. Collagenase1 proteins have been implicated in neuronal plasticity and ALS (Fujioka et al., 2012). On the other hand, *Cart* (cocaine and amphetamine regulated transcript, Fig. 6D and Fig. 7D), *Nplx* (neuropeptide ligand x, Fig. 6D and Fig. 7C), and *Tapxe* (T-cell activating protein x-e, Fig. 6D and Fig. 7E) are enriched in soleus as opposed to TA MNs. Further, *Calca* (calcitonin gene-related peptide 1, Fig. 6C and Fig. 7F) and *Chodl* (chondrolectin, Fig. 6C and Fig. 7G) transcripts which were already proposed to be fast markers are highly enriched in TA MNs. Similarly, *Sv2a* (synaptic vesicle glycoprotein 2A, Fig. 6D and Fig. 7H), a recently identified putative slow MN marker is enriched in soleus MNs. Generic markers like *Chat* (choline acetyltransferase, Fig. 7I) and housekeeping genes like *Gapdh* (glyceraldehyde-3-phosphate dehydrogenase, Fig. 7J) and *Tuba1b* (tubulin, alpha 1B, Fig. 7K) show no differential expression suggesting that the above mentioned expression differences are indeed true. Further, *Gfap* (an astroglial marker, glial fibrillary acidic protein, Fig. 7L) expression is negligible (far below threshold and not differentially enriched) and suggests that the laser capture process excluded astroglial contamination. Gamma-MNs are also present in motor pools and they account for approximately 30% of MNs in most motor pools (Friese et al., 2009; Shneider et al., 2009). Known gamma-MN markers like *Gfra1* (glial cell line-derived neurotrophic factor family receptor alpha 1) (Fig. 7M) and *Htr1d* (5-hydroxytryptamine (serotonin) receptor 1d, Fig. 7N) show low expression and are not differentially enriched, indicating that differentially expressed genes identified through the screen did not associate with the distinction between alpha or gamma MN classes. (*Tamnec1-* gene; Tamnec1-protein).
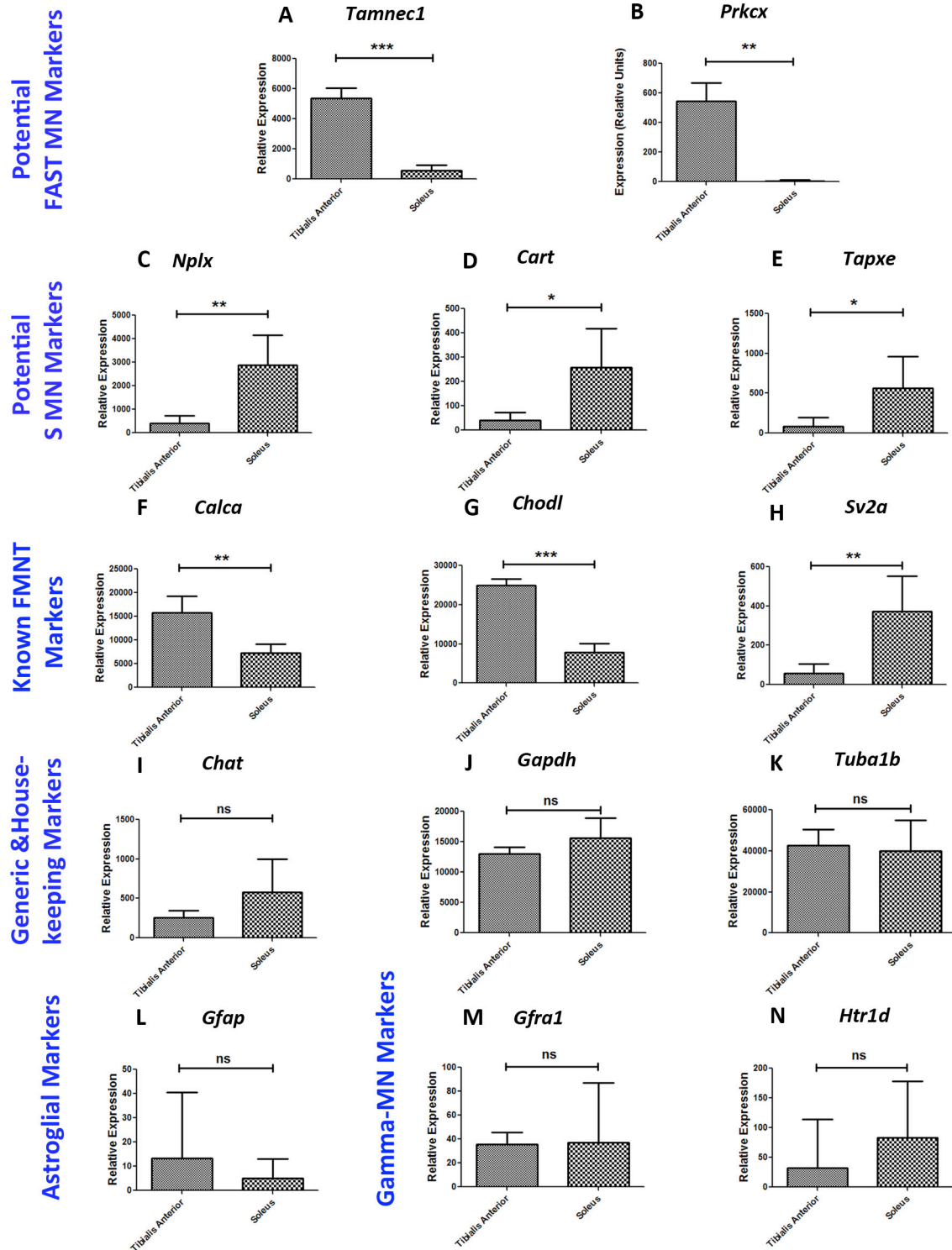
Figure 7: Comparison of expression levels of selected genes from adult FMNT screen. Comparison of expression levels of differentially enriched genes between TA and soleus motor neurons. TA enriched transcripts (A, B, F and G). Soleus enriched transcripts (C, D, E and H). Known fast MN markers (F and G). Known Slow MN marker (H). Generic MN marker (I). Housekeeping genes (J and K). Astroglial marker (L). Gamma-MN markers (M and N). Significance is calculated using student's t-test (* p-value <0.05, ** p-value <0.01, *** p-value <0.001, ns – no significance).

4.6 Immunohistochemical verification of Tamnec1 expression in TA and soleus motor neurons

The expression data (from microarray) for *Tamnec1* was verified at the protein level by using immunohistochemistry (Fig. 8) on spinal cord sections containing retrogradely traced MNs (green, Fig. 8A and D). The antibody against Tamnec1 specifically recognizes this protein and does not cross react with other collagenases. Immunohistochemical analysis revealed that Tamnec1 is expressed in all TA MNs (Fig. 8G) and is absent in soleus MNs (Fig. 8H). This clearly validates the array expression data (Fig. 8 A*o*) at the protein level and also points the reliability of the FMNT screen. However, a thorough downstream analysis (Fig. 9) is further required to establish Tamnec1's potential for being a bona fide 'fast MN' marker.
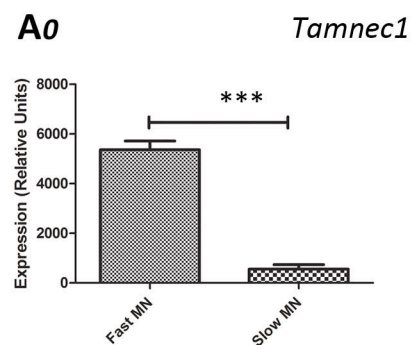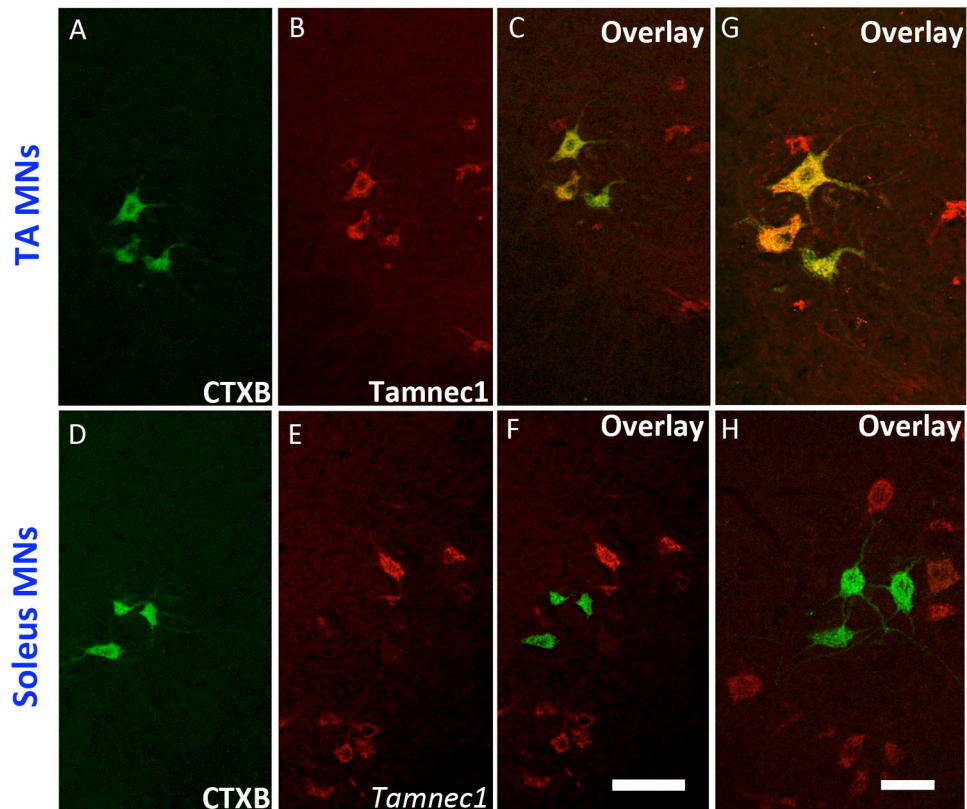
Figure 8: Immunohistochemical analysis of Tamnec1 expression in TA and soleus motor neurons. TA and soleus MNs were identified by retrograde tracing (green, A, D, F and H) with intramuscular injection (of TA, soleus muscles, respectively) of fluorescently conjugated CTXB. Tamnec1 expression in cross sections of adult mouse spinal cord is represented in red (B, C, E, F, G and H). C, F and G, H represent overlay images. Section thickness is 30 µm. Scale bar represents 100 µm for A- F and 50 µm for G and H. Array expression profile of Tamnec1 is shown in Ao.

4.7 Requirements to be fast and slow motor neuronal specific marker

The expression data obtained from the above-mentioned screen (FMNT screen, TA and soleus MN expression data) might contain transcripts which can be either pool specific, column specific, level specific or extensor–flexor specific. Further, the expression data might also contain markers of gamma-MNs (in addition to bona fide 'fast or slow' MN markers). Therefore, a thorough downstream analysis is required to establish a candidate from the FMNT screen as a bona fide 'fast or slow' MN marker. To meet these criteria, a candidate gene should be expressed at all levels (cervical, thoracic, lumbar and sacral) of the spinal cord since fast and slow MNs are present scattered (subset of MNs) at all levels of the spinal cord. Further, the candidate should be present in all motor columns (medial motor column and lateral motor column) since fast and slow MNs do not show a bias for columnar organization. They should also be expressed in multiple motor pools (not only TA versus soleus). Further it should not have an extensor-flexor bias; in that it should not be specific to either extensor or flexor MNs (the said candidate should have a scattered expression in motor neurons, not regionalized to either physiological extensor or flexor areas). Further, its expression should be excluded from gamma-MNs, and its presence should be confirmed in alpha-MNs. If a candidate meets all the above requirements and further if it is highly expressed in fast motor pools as opposed to slow motor pools, the said candidate can then be considered as a bona fide fast or slow MN marker. Further, correlation with muscle fiber type along with a thorough electrophysiological characterization will provide the ultimate proof for a candidates potential to be a fast or slow MN marker. The summary of the screen to identify bona fide fast or slow MN markers from the FMNT screen is summarized in Fig. 9. As an initial screen, the expression pattern of the candidates (MN presence, expression at all levels, etc.) can be verified using mouse spinal cord atlas (http://mousespinal.brain-map.org/). Its scattered mRNA expression at all levels and enrichment in TA MNs (Fig. 8 G) prompted me to test Tamnec1's potential for being a bona fide fast MN marker.

Gene List from Adult TA and Soleus MN Screen

divison/level specific (if 'yes'- removed from list)

NO

column speficic (if 'yes' removed from list)

NO

pool specific (if 'yes' remove from list)

NO

extensor/flexor specific (if 'yes' remove from list)

NO

expression in gamma-MNs (if 'yes' remove from list

NO

expression in alpha-MNs (if 'not' remove from list)

YES

enrichment in fast/slow motor pools-correlation with fiber type (if 'not' remove from list

YES

Scattered Expression Large Soma-Size

BONA FIDE 'FAST'/'SLOW' MARKERS

Figure 9: Criteria to identify bona fide fast or slow motor neuronal markers. Criteria to identify bona fide fast or slow MN markers from adult TA and soleus MN gene expression data (from FMNT screen).

4.8 Expression analysis of Tamnec1 in adult mouse spinal cord

Immunohistochemical analysis of Tamnec1 expression at different rostro-caudal levels of adult spinal cord.

I have tested the expression pattern of Tamnec1 in adult spinal cord cross sections. The results of the expression analysis are shown in Fig. 10. Tamnec1 expression is shown in red (Fig. 10B, E, H and K). Tamnec1 presence in MNs was confirmed by co-staining with vAChT (green Fig. 10A, D, G and J) (overlay-Fig. 10C, F, I and L). These results clearly demonstrate that Tamnec1 is present in a subset of MNs at all levels (cervical, Fig. 10C; thoracic, Fig. 10F; lumbar, Fig 10I; sacral, Fig.10L) of the adult spinal cord. Further, Tamnec1 expression shows no bias for medial motor column (MMC) versus lateral motor column (LMC) (MMC, yellow arrows in Fig. 10B, H; LMC, blue arrows in Fig.10B, H) and no bias for extensor versus flexor MNs (physiological extensor area pointed with red arrow in Fig. 10H; physiological flexors area pointed with white arrow in Fig. 10H). Further, the expression of Tamnec1 was quite specific to MNs (very few cells in the dorsal horn were positive for Tamnec1). These results clearly show that Tamnec1 meets many criteria (summarized in Fig. 9) for being certified as a bona fide fast MN marker.
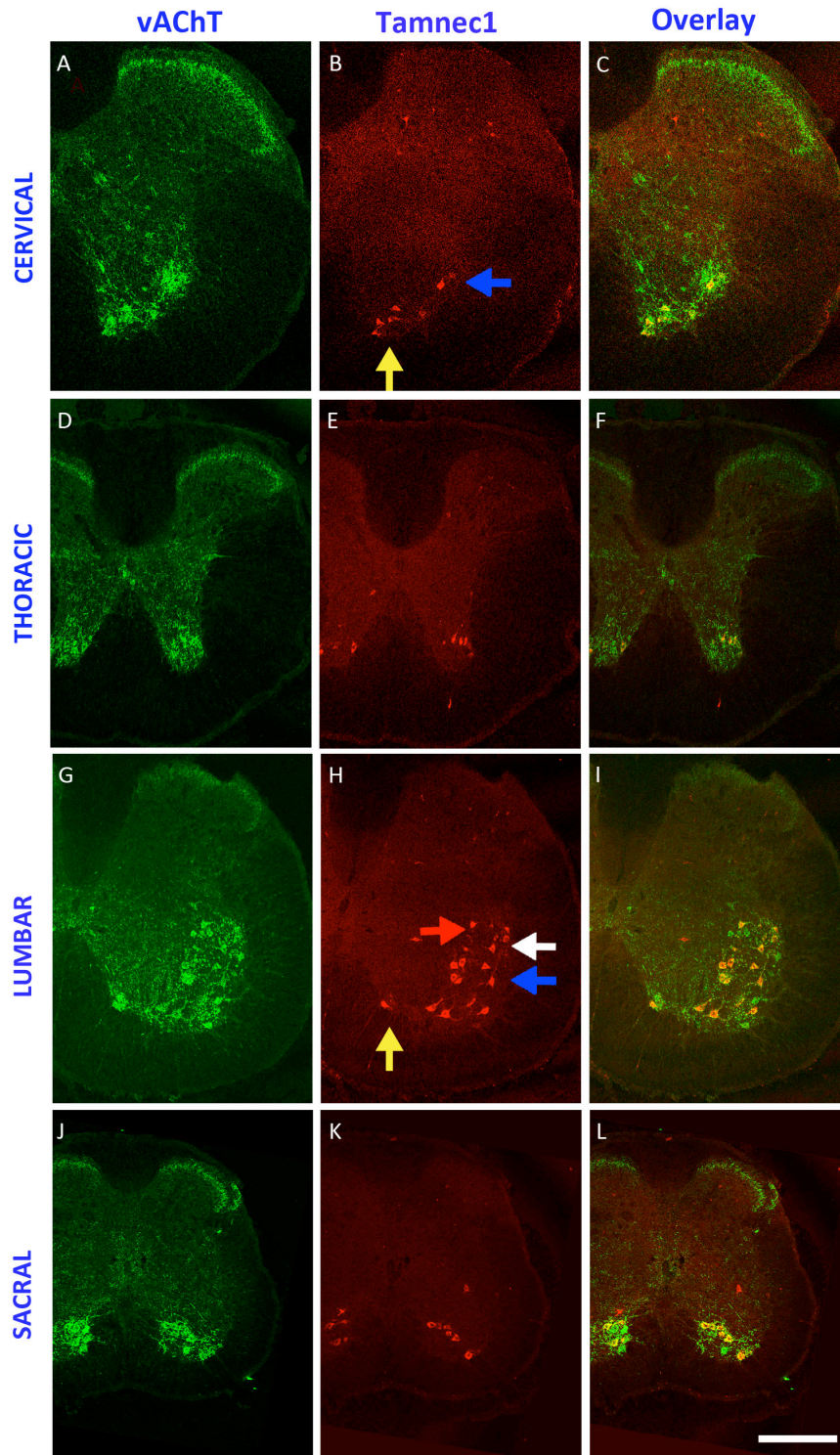
Figure 10: Immunohistochemical analysis of Tamnec1 expression at different rostro-caudal levels of adult spinal cord. vAChT immunostaining on cross sections of adult spinal cord is represented in green (A, D, G, and J). Tamnec1 expression on the same sections is represented in red (B, E, H and K). Overlay images are shown in C, F, I and L. Yellow arrows point medial motor column MNs whereas blue arrows point at lateral motor column MNs. Red arrows represent location of physiological extensor MNs while the white arrows represent location of physiological flexor MNs. Section thickness is 30 µm and the scale bar represents 500 µm.

4.9 Tamnec1 expression in different motor pools

One of the requirements for being a bona fide 'fast' MN marker is that, the said marker should be expressed in many motor pools and should also be enriched in fast motor pools (Fig. 9). To verify the expression pattern of Tamnec1 in multiple motor pools, I chose to check the expression of Tamnec1 in two fast motor pools (TA and rectus femoris (RF), Fig. 11G-I and J-L, respectively) and one slow/αFR (soleus) motor pool neurons (Fig. 11D-F). TA and RF are fast twitch muscles (high number of type IIb fibers) and hence their motor pools are highly enriched in fast MNs. On the other hand soleus is a slow twitch muscle (having type I and IIa fibers) and hence its motor pool is enriched in αS and αFR MNs. These MNs can be retrogradely traced using CTXB (green, Fig. 11D, G, J and F). Immunohistochemical analysis clearly show that all retrogradely traced MNs of TA (Fig. 11I) and RF (Fig. 11L) are Tamnec1 positive, while Tamnec1 expression is absent in soleus MNs (Fig. 11F). Further, quantification of double positive MNs clearly shows that all TA (n=24 from 2 animals) and RF (n=10 from 1 animal) MNs are positive for Tamnec1 (Fig. 12-1). Majority of soleus MNs (Fig. 12-1) are negative for Tamnec1 (n=22 from 2 animals, 1 MN/animal is double positive). These results indicate that Tamnec1 is enriched in motor pools of fast muscles and is absent from a majority of MNs in the soleus motor pool. This further strengthens its candidature as a bona fide 'fast MN marker'. These results also rule out shank versus thigh bias as RF is a thigh muscle and TA is a shank muscle. Further, these results also indicate that Tamnec1 could potentially be a αFF and/or αFI MN marker since TA (Fig. 2C and I) and RF muscles are enriched in type IIb muscle fibers (and their motor pools are enriched in αFF MNs) . Soleus, on the other hand is devoid of type IIb fibers and has approximate equal proportions of type I and type IIa fibers (Fig. 2D and I, Fig 2F, respectively) (and its motor pool has αS and αFR MNs). Thus, if Tamnec1 is a general fast MN marker, its expression is expected to be found in approximately 50% of soleus MNs, and this is not the case (Fig. 12-1). This hints at Tamnec1 expression in being specific to either αFF or αFI MNs.
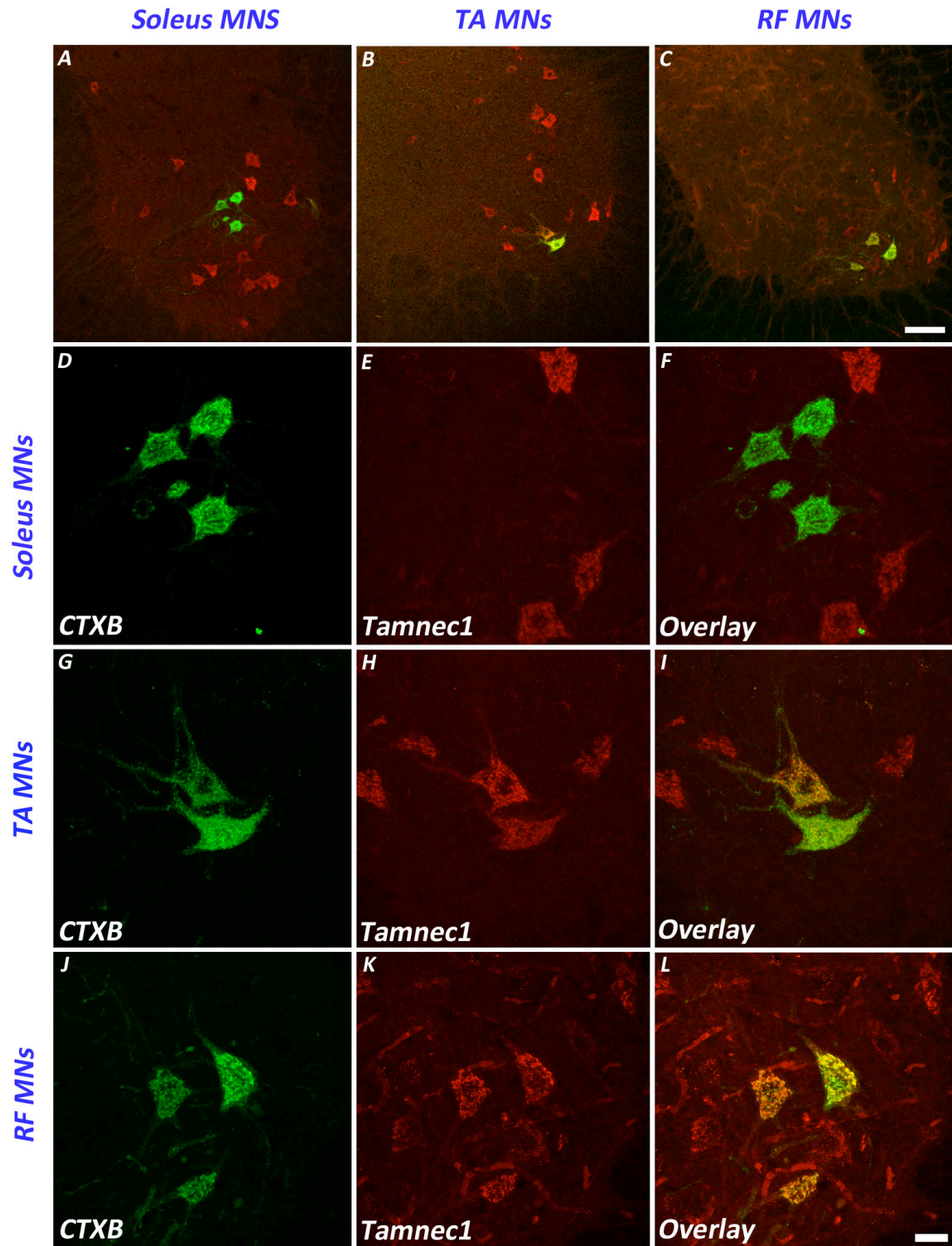
Figure 11: Tamnec1 expression in different motor pools. TA, RF and soleus MNs were identified by retrograde tracing (green, D, G, J and F) with intramuscular injection (of TA, RF, soleus muscles, respectively) of fluorescently conjugated CTXB. Tamnec1 expression in cross sections of adult mouse spinal cord is represented in red (E-L). Overlay images are shown in (A, B, C, F, I and L). A, B and C represent images acquired at lower magnification. Section thickness is 30 μm and the scale bar represents 100 μm in A, B, C and 25 μm in D-L.

4.10 Soma size-distribution of Tamnec1 positive lumbar motor neurons

Soma-size distributions of MN population give important insights into their type status. For example, alpha versus gamma-MNs can be distinguished by their soma-sizes. Gamma-MNs have small soma sizes compared to alpha-MNs. Further, slow MNs have smaller soma-size as opposed to fast MNs, which have a bigger soma-size (Ishihara et al., 1988). Since Tamnec1 has met many of the general criteria for being a bona fide fast MN marker, I quantified the soma-size distribution of Tamnec1 expressing lumbar MNs together with the soma-size of whole lumbar motor neuronal population (identified by vAChT immunostaining, red, Fig. 12-2). The soma-size distribution curve (Fig. 12-2) shows that Tamnec1 expression is enriched in large soma-size population (blue, Fig 12-2) and is excluded from the gamma-MN population (Fig. 12-2, small soma size peak). A total of 482 cells from lumbar spinal cords of 3 animals (n=3) were analyzed. The soma-size of all MNs, irrespective of the presence of nucleus was measured, which explains Tamnec1 distribution in a few small cells in the alpha peak. This result indicates that Tamnec1 expressing MNs are big in terms of soma-size. This suggests that Tamnec1 could indeed be a bona fide fast MN marker. However, a more stringent analysis of soma size distributions at all spinal levels has to be done to make a concrete statement regarding Tamnec1 expression and type status.
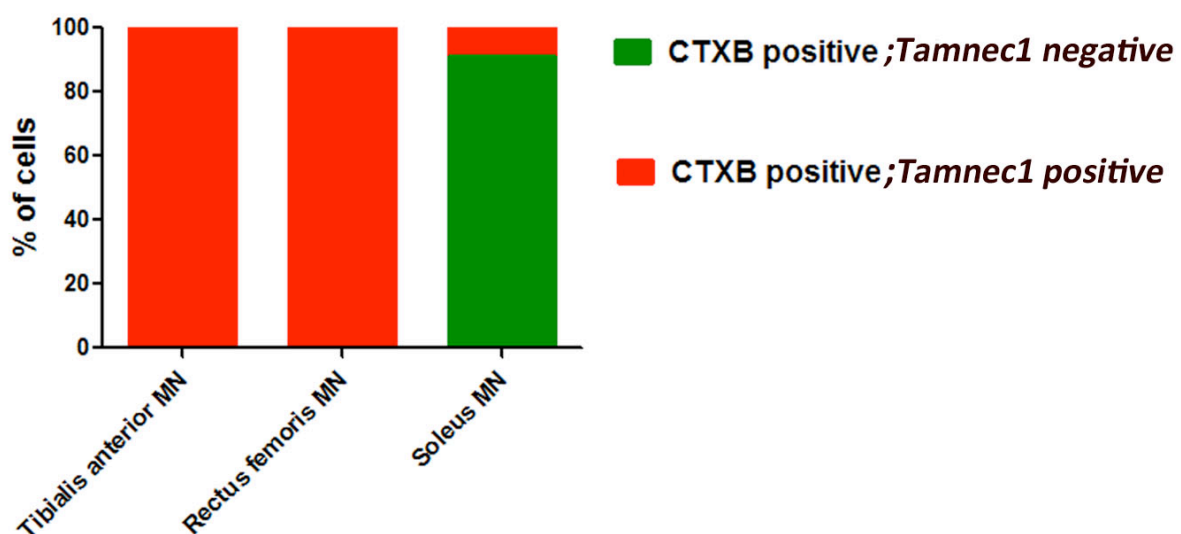
Figure 12-1: **Quantification of TAMNEC1 expression in different motor pools.** Tamnec1 expression was quantified (and expressed as percentage of cells) in MNs retrogradely traced by intramuscular injection of fluorescently conjugated CTXB (into TA, RF and soleus muscles). Double positive MNs (CTXB positive & Tamnec1 positive) are represented in red whereas MNs which are CTXB positive but Tamnec1 negative are represented in green.
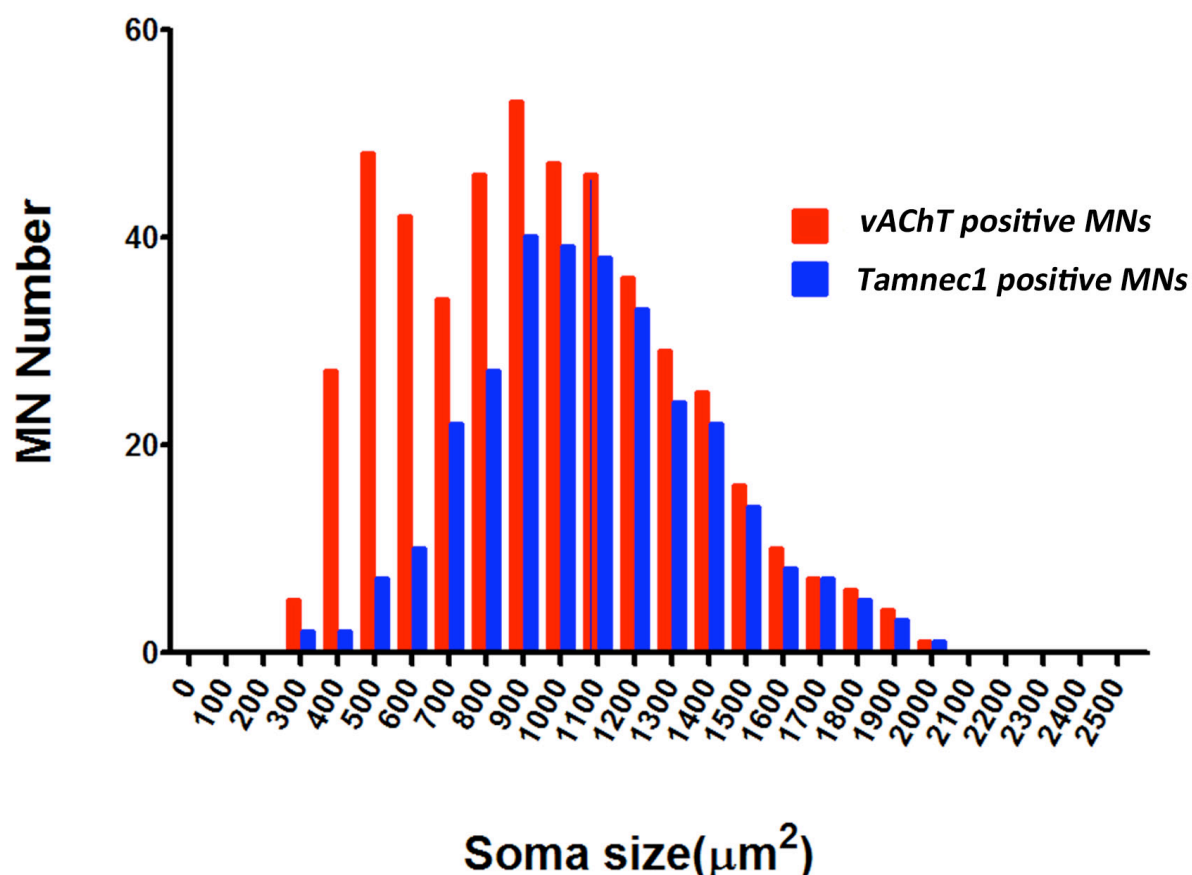
Figure 12-2: Soma size distribution of Tamnec1 positive lumbar motor neurons. Soma-size distribution of Tamnec1 positive MNs represented by blue bars. vAChT positive motor neurons are represented by red bars. The soma size is expressed in μm^2. Y-axis represents motor neuronal number.

4.11 Tamnec1 is expressed in alpha motor neurons and absent in gamma motor neurons

In a motor pool, alpha-MNs are numerous in comparison to gamma-MNs . Alpha and gamma-MNs can be distinguished by differences in their soma size and by expression of certain markers like NeuN, Err3, Gfrα1, 5ht1d and osteopontin (OPN). Alpha-MNs express OPN and high levels of NeuN and low/no levels of Err3. On the

other hand, gamma-MNs express low/no levels of NeuN and high levels of Err3. Since fast and slow MNs are subtypes of alpha-MNs, they express high levels of NeuN and low/no levels of Err3. To check whether Tamnec1 is expressed in alpha-MNs, I have done immunohistochemical analysis on adult mouse lumbar spinal cord sections with NeuN, Tamnec1 and vAChT antibodies (Fig. 13). vAChT immunostaining labels all spinal MNs (green, Fig. 13C). The results clearly show that all Tamnec1 expressing MNs are of the alpha type as revealed by the presence of NeuN in Tamnec1 expressing MNs (yellow arrows in Fig. 13D). Tamnec1 expression is absent in gamma-MNs (white arrows, Fig. 13) characterized by no NeuN expression (vAChT positive, NeuN negative, white arrows in Fig. 13D). Further, Tamnec1 expression is absent in some alpha-MNs (vAChT positive, NeuN positive and Tamnec1 negative, red arrows in Fig.13D) which may be of the slow type. Further, Tamnec1 expressing MNs express low (yellow arrow in Fig. 14G and white arrows in Fig. 13F) or no (white arrow in Fig. 14G) levels of Err3 indicating they are of the alpha-MN type. High levels of Err3 expression is indicated by yellow arrows in Fig. 14F and by blue arrow in Fig. 14G). Few Tamnec1 positive neurons (1-2 per section) express high levels of Err3 (indicated by blue arrow in Fig. 14 F) and these may be beta-MNs. These results shows that Tamnec1 is expressed in a subset of alpha-MNs (Fig. 13D) and is absent from gamma-MNs (Fig. 13 and 14G).
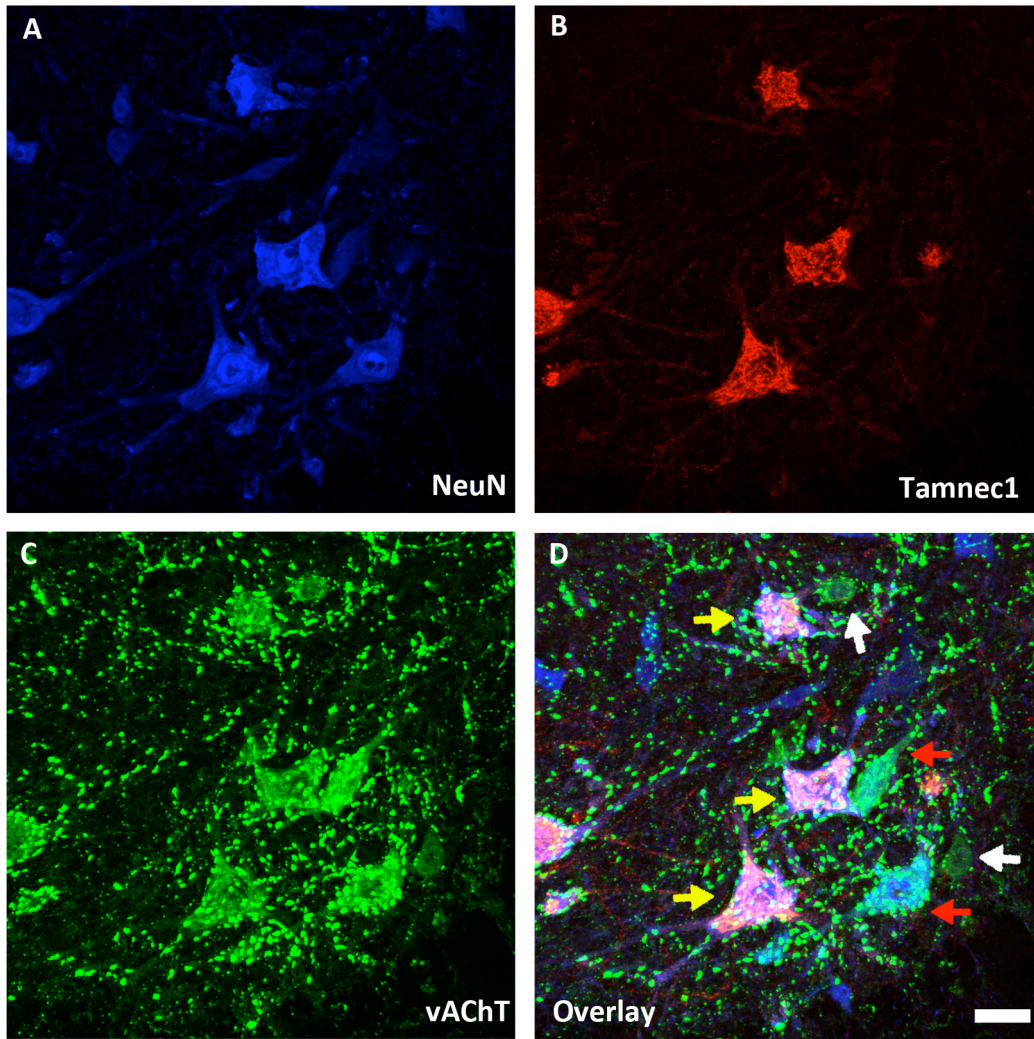
Figure 13: Tamnec1 is expressed in alpha motor neurons. NeuN expression in adult spinal cord sections is shown in blue (A) and Tamnec1 expression on the same sections is shown in red (B). MNs are identified by vAChT immunostaining shown in green (C). Overlay image is seen in D. Yellow arrows point NeuN[+]; Tamnec1^{+}; vAChT[+] MNs while the red arrows point NeuN[+]; vAChT[+] MNs. The white arrows point NeuN[-]; vAChT[+] MNs. Section thickness is 30 µm and the scale bar represents 25 µm.
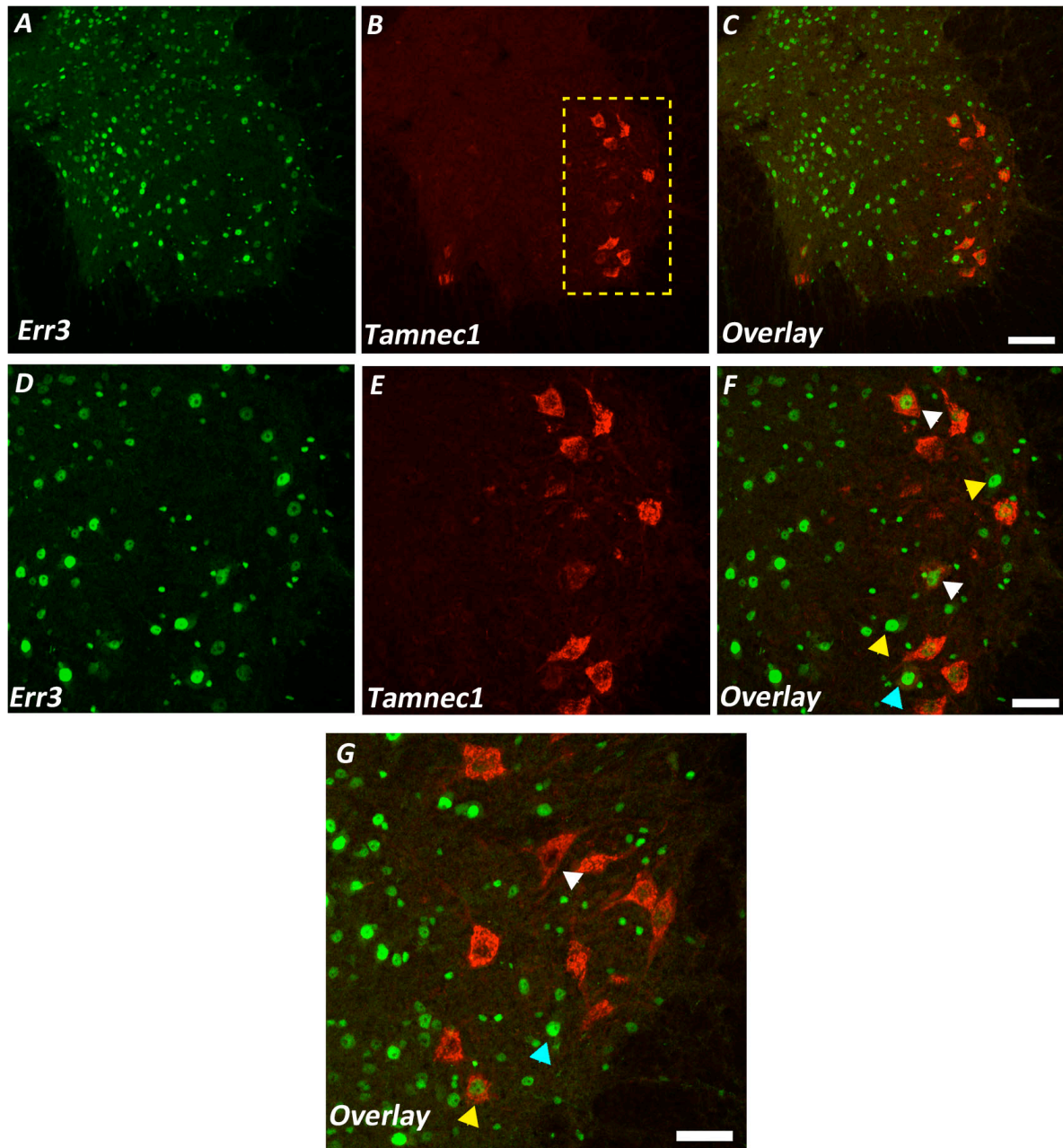
Figure 14: Tamnec1 positive motor neurons express low (or no) levels of Err3. Immunostaining showing the expression of Err3 (green, A and D) and Tamnec1 (red, B and E) in adult spinal cord sections. Overlay image is shown in C and F. Yellow arrows in 'F' point cells expressing high levels of Err3. White arrows in 'F' point cells expressing Tamnec1 and low levels of Err3. The blue arrow in 'F' points Tamnec1 positive neuron expressing high levels of Err3. The general trend of Err3 expression in Tamnec1 positive neurons is shown in 'G'. The white arrow in 'G' points Tamnec1 positive; Err3 negative neuron whereas the yellow arrow in 'G' points Tamnec1 positive neuron having low levels of Err3. Blue arrow in 'G' points cell with high Err3. Scale bar represents 100 μm in A-C and 50 μm in D-G.

Taken together, all these results indicate the candidature of Tamnec1 as a bona fide fast MN marker.

Summary of the results indicating Tamnec1's candidature as a bona fide fast MN marker (based on the criteria outlined in Fig 9).

Criteria for being a bona fide fast or slow MN marker	TAMNEC1 Status (fulfilled versus not fulfilled) for being bona fide FAST MN marker	Supporting Figures
Expression at all rostro-caudal levels (YES versus NO)	YES; fulfilled	10
Scattered expression (subset of MNs) (YES versus NO)	YES; fulfilled	10, 13 D
Column specificity (YES versus NO)	NO; fulfilled	10
Extensor-flexor bias (YES versus NO)	NO; fulfilled	10
Pool specificity (YES versus NO)	NO; fulfilled	11,10
Expression in gamma-MNs (YES versus NO)	NO; fulfilled	13, 14
Expression in alpha-MNs (YES versus NO)	YES; fulfilled	13
Enrichment in FAST motor pools and absence in slow motor pools (YES versus NO)	YES; fulfilled	11

4.12 Endurance training

Skeletal muscle is highly plastic and various paradigms can result in muscle fiber transformations (CLFS, endurance training, disuse, etc). Endurance training leads to myofiber transitions in the direction of 'slow' type (fast to slow (oxidative)), although the magnitude of shift is limited by intrinsic differences between fiber types. Upon alteration of activity, the spinal MNs also show adaptive plasticity, including alterations in electrophysiological properties. These adaptations can be both, general or type-specific, involving changes in FMNT-dependent properties. For instance, changes in cell capacitance are limited to fast MNs upon endurance training (Gardiner, 2006). However, the molecular correlates of spinal MN plasticity are largely unknown and remain to be elucidated. To address this, I have designed a screen to elucidate the transcriptional profile of type specific (Fast/TA MNs) MNs following endurance training, which would eventually lead us to understand the molecular correlates underlying MN plasticity. The schematic representation of the screen is shown in Fig. 15. CD1 mice were subjected to forced treadmill running on a speed-regulated treadmill. A total of 24 male CD1 mice were used for transcriptional analysis (n= 12 control group and n=12 training group). Starting from P28 mice were acclimatized to treadmill running for 7 days until acclimatization to the final speed of 17 meter/minute (m/min) was achieved. This speed was chosen as it was moderate in intensity, with the possibility of translating it to ALS mouse models. Following initial training, the mice were subjected to regular training for 1 hour per day, 5days per week for a total of 6 weeks. The controls were housed in regular home cages for the entire duration of training. During daily training sessions, the speed was achieved by gradually increments. After 4 weeks of training a surgery was performed (on controls and trained animals) to administer intramuscular injections in TA muscle with the aim of retrogradely tracing TA MNs (Fig. 15A). Animals were then given 4 days of rest, to recover from the surgery. Following this, they were trained on the treadmill for another 2 weeks. After completion of the training the spinal cords and muscles were collected from age-matched controls and endurance trained animals and were further processed for transcriptional analysis. I have isolated the labelled MNs (Fig. 15B and C) by using laser capture microdissection.
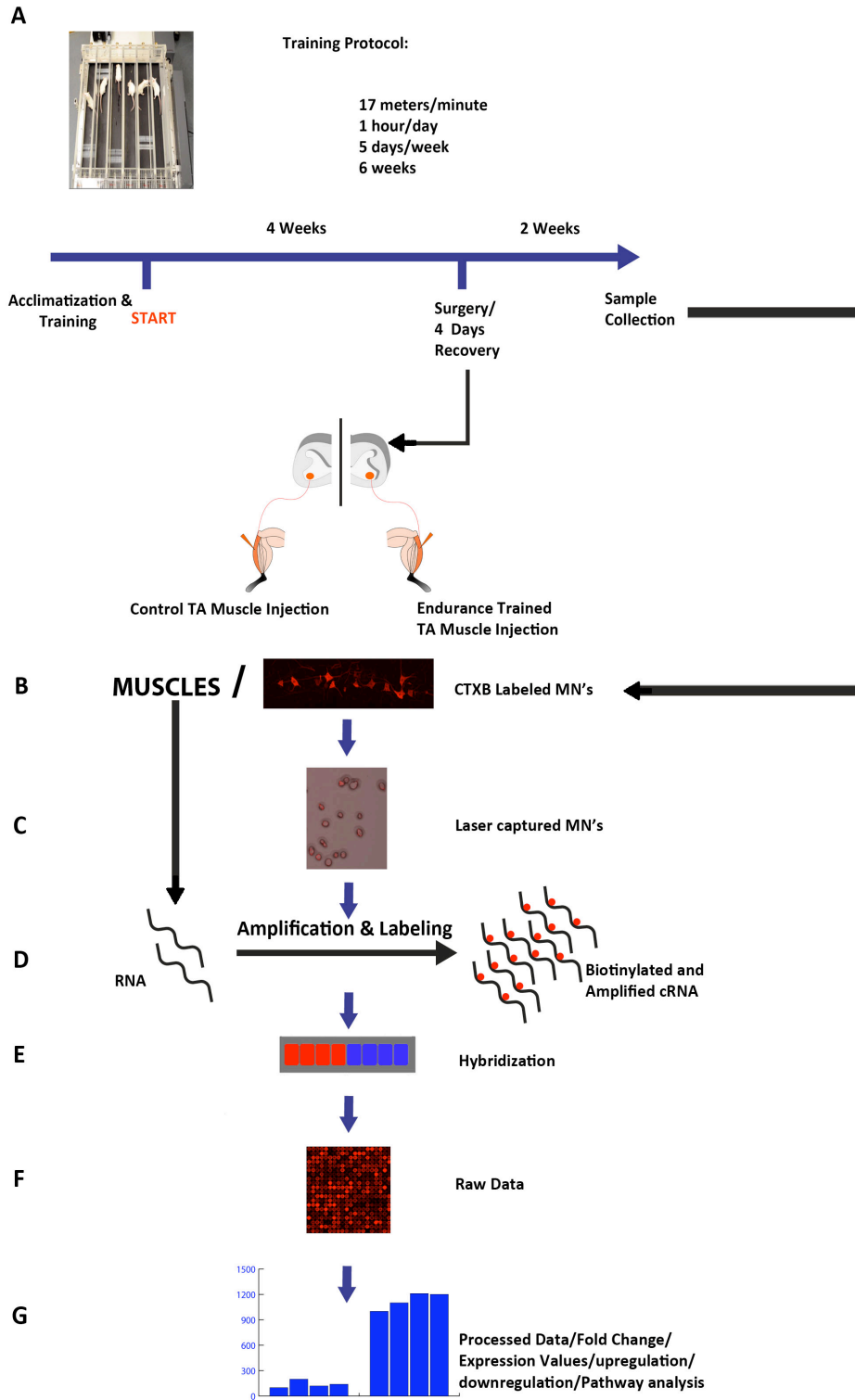
Figure 15. Schematic representation of the endurance trained TA motor neuronal and muscle screen. Schematic representation of endurance training protocol and paradigm (with intramuscular injections 4 weeks after the start of training) (A). After 6 weeks of training, the spinal cords were isolated and processed for cryosectioning to enable visualization of retrogradely traced MNs (fluorescently labelled) (B). The fluorescently labelled cells were isolated by laser-capture microdissection (C). RNA was extracted from the laser captured cells and was amplified (and biotin labelled) (D). The biotinylated RNA was hybridized to Illumina BeadChip microarrays (E). The raw expression data (F) was processed to obtain expression and fold change values (G).

69

This screening paradigm represents a new methodology to identify altered gene signatures/correlates of "type specific" motors in response to endurance training. In parallel to the MNs, the muscles isolated from the endurance training animals and age-matched controls were also analyzed for altered gene signatures by using microarray profiling with the aim of achieving a functional correlation of muscle and MN transcriptomes induced by activity. The results of the muscle and motor neuronal screen are mentioned below. The general health of the trained animals was assessed in terms of body weights and serum corticosterone levels (indicators of stress (Rattner et al., 1980)) and was compared with age matched controls (Fig. 16). There was no detectable difference in the body weights of endurance trained animals (not normalized with the amount of food intake) as compared to age-matched controls (Fig. 16A). The levels of serum corticosterone levels (ng/ml) were also not measurably different (Fig. 16B) as compared to age-matched controls indicating that long duration endurance trained animals cope with stress (however, initial stress cannot be ruled out and was not measured).
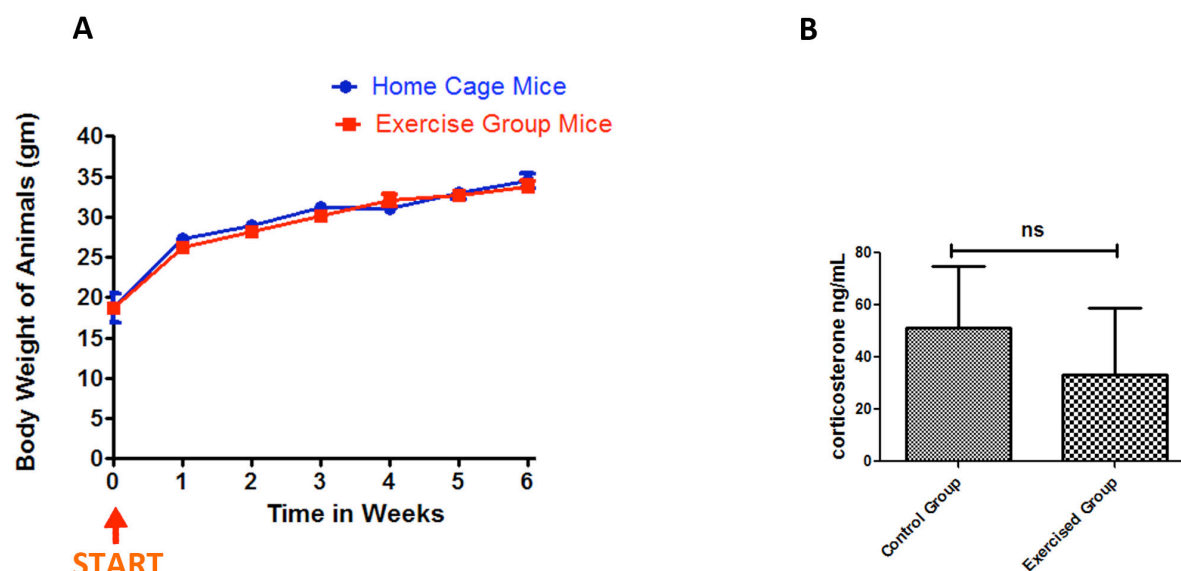
Figure 16: General health of endurance trained animals. Body weights of endurance trained animals as compared to age matched controls (A). Serum corticosterone levels (B). Significance is calculated using student's t-test (ns-no significance).
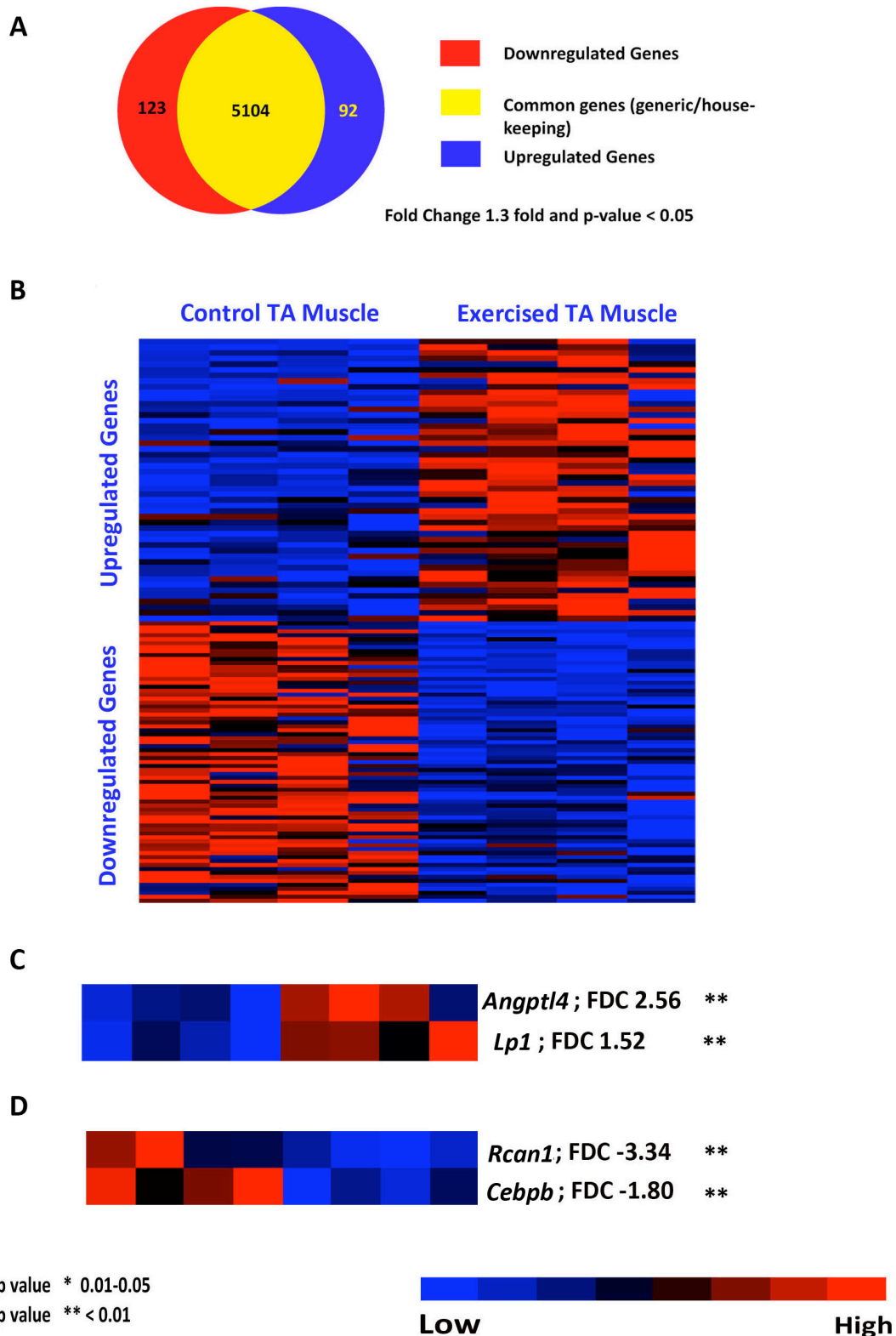
Figure 17. Expression analysis of control versus endurance-trained TA muscles. Venn diagram representing gene expression changes in endurance trained mouse TA muscle (versus controls) (A). Heatmaps (B) of selected genes that are significantly up or downregulated post endurance training) in mouse TA muscles. Heatmaps of selected candidates with fold change (FDC) and significance values (upregulated, C; downregulated, D).The threshold level for gene expression was set to 100 relative units to avoid false positive results. Red represents high level of expression and blue represents low level of expression. p-value criteria are shown in the bottom left-hand side of the image.

4.13 Transcriptional profiling of TA muscle following 6 weeks of endurance training

The results of the transcriptional profiling of TA muscle following 6 weeks of endurance training are shown in Figs. 17-21. After 6 weeks of endurance training 123 transcripts were significantly downregulated and 92 transcripts were significantly upregulated. 5104 transcripts expressed at substantial levels showed no detectable differential expression (Fig. 17A-D). Some of the differentially regulated genes (also verified by qPCR) are as follows; *Angptl4* (angiopoietin-related protein 4, Fig. 18E and I) and *Lp1* (low density lipoprotein receptor related protein 1, Fig. 18F and J) are upregulated following 6 weeks of endurance training in TA muscles whereas *Rcan1* (regulator of calcineurin 1, Fig. 18G and K) and *Cebpb* (CCAAT/enhancer binding protein, beta, Fig.18 H and L) are downregulated. Angptl4 is induced by PPAR (peroxisome proliferator-activated receptor) and plays a role in lipid metabolism and in angiogenesis (Hato et al., 2008). Rcan1 (downregulated in the present study) was shown to be important in muscle plasticity and fiber remodelling and is involved in calcineurin pathway (Oh et al., 2005). Deregulation of Rcan1 (involved in calcineurin pathway) indicates that TA muscle fibers are at a stage in fiber remodelling.

The expression levels of myosin heavy chain genes remain unchanged in TA muscle after 6 weeks of endurance training (Fig. 18A-D). The fast fiber content of TA also remains unchanged after 6 weeks of endurance as revealed by MY-32 antibody staining of control versus trained TA muscle (Fig. 18M-N). This indicates that the exercise paradigm was not of either sufficient intensity or duration to induce a fiber transformation. However, changes in Rcan1 (involved in calcineurin pathway) indicate that the muscle is at a state of possible fiber remodelling. Further, panther gene expression analysis of differentially expressed (upregulated, Fig. 19; downregulated, Fig. 20) genes in the context of molecular functions (Fig. 19A and C, Fig. 20A and C) and biological process (Fig. 19B and D, Fig. 20B and D) revealed that the up or downregulated genes have a variety of molecular functions (ion channel activity, catalytic activity, etc) and participate in various biological processes like metabolism, transport, etc. Further, Ingenuity network analysis revealed that genes altered upon 6 weeks of endurance training are involved in lipid metabolism network (Fig. 21), indicating a probable alteration in metabolic status of the muscle.

Taken together, these results indicate that TA muscle is at an early step of fiber remodelling after 6 weeks of endurance training and is undergoing a change in its metabolic profile.
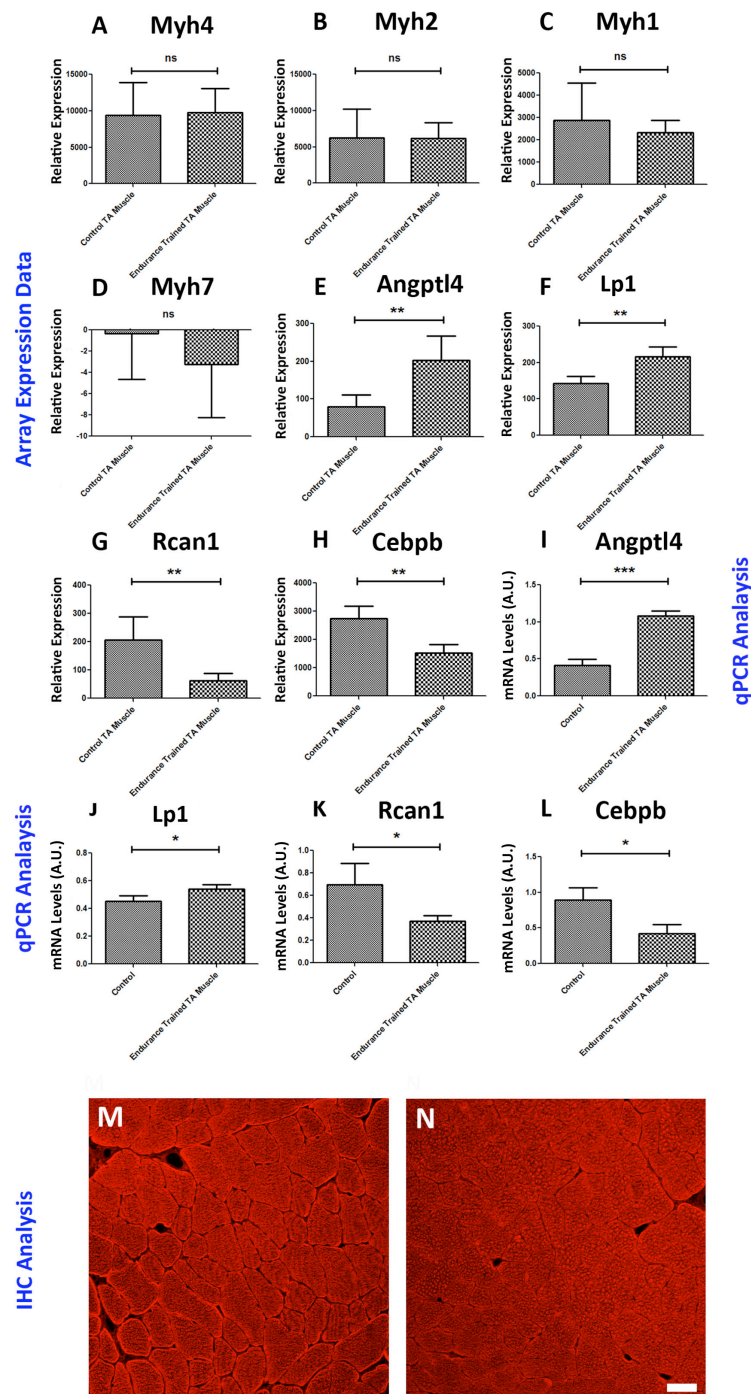
Figure 18: Comparison and verification of expression levels of selected genes from endurance trained TA muscle (versus control TA muscle). Comparison of expression levels of genes between control and endurance trained TA muscles. Expression profile of myosin heavy chain genes (A-D). Upregulated genes (E-F). Downregulated genes (G-H). qPCR verification of up or downregulated genes (I-J and K-L, respectively). Immunohistochemical analysis using MY-32 antibody on mouse TA (control (M); endurance trained (N)) muscle cross sections. Section thickness is 10 µm and the scale bar represent 50 µm. Significance is calculated using student's t-test (* p-value <0.05, ** p-value <0.01, *** p-value <0.001, ns – no significance).

Panther Analysis of Genes Upregulated in TA Muscle (Endurance Training)

A **Molecular Function**

B **Biological Process**

Total genes 77; Total function hits 77

Total genes 77; Total process hits 143

C

Sr. No	Molecular Function	No. of Genes	Percentage 1	Percentage 2
1	ion channel activity (GO:0005216)	1	1.3%	1.3%
2	transporter activity (GO:0005215)	4	5.1%	5.2%
3	translation regulator activity (GO:0045182)	1	1.3%	1.3%
4	transcription regulator activity (GO:0030528)	7	9.0%	9.1%
5	enzyme regulator activity (GO:0030234)	4	5.1%	5.2%
6	catalytic activity (GO:0003824)	17	21.8%	22.1%
7	receptor activity (GO:0004872)	9	11.5%	11.7%
8	structural molecule activity (GO:0005198)	7	9.0%	9.1%
9	binding (GO:0005488)	27	34.6%	35.1%

Legend for A:
- binding (GO:0005488)
- catalytic activity (GO:0003824)
- enzyme regulator activity (GO:0030234)
- ion channel activity (GO:0005216)
- receptor activity (GO:0004872)
- structural molecule activity (GO:0005198)
- transcription regulator activity (GO:0030528)
- translation regulator activity (GO:0045182)
- transporter activity (GO:0005215)

D

Sr. No	Biological Process	No. of Genes	Percentage 1	Percentage 2
1	cell communication (GO:0007154)	17	21.8%	11.9%
2	cellular process (GO:0009987)	25	32.1%	17.5%
3	transport (GO:0006810)	11	14.1%	7.7%
4	cellular component organization (GO:0016043)	6	7.7%	4.2%
5	apoptosis (GO:0006915)	1	1.3%	0.7%
6	system process (GO:0003008)	8	10.3%	5.6%
7	reproduction (GO:0000003)	2	2.6%	1.4%
8	response to stimulus (GO:0050896)	10	12.8%	7.0%
9	developmental process (GO:0032502)	15	19.2%	10.5%
10	metabolic process (GO:0008152)	29	37.2%	20.3%
11	cell cycle (GO:0007049)	3	3.8%	2.1%
12	cell adhesion (GO:0007155)	5	6.4%	3.5%
13	immune system process (GO:0002376)	11	14.1%	7.7%

Legend for B:
- apoptosis (GO:0006915)
- cell adhesion (GO:0007155)
- cell communication (GO:0007154)
- cell cycle (GO:0007049)
- cellular component organization (GO:0016043)
- cellular process (GO:0009987)
- developmental process (GO:0032502)
- immune system process (GO:0002376)
- metabolic process (GO:0008152)
- reproduction (GO:0000003)
- response to stimulus (GO:0050896)
- system process (GO:0003008)
- transport (GO:0006810)

Figure 19: Panther analysis of gene expression profiles. Classification of genes 'upregulated' after endurance training in TA muscle (A-B). Guides (legends) to follow the pie charts represented in A, B (C is the legend for A and D is the legend for B). Percentage 1 indicates percent of gene hit against total genes and percentage 2 indicates percent of gene hit against total process hits.

Panther Analysis of Genes Downregulated in TA Muscle (Endurance Training)

A **Molecular Function**

B **Biological Process**

Total genes 110; Total function hits 116

Total genes 110; Total process hits 202

C

Sr. No	Molecular Function	No. of Genes	Percentage 1	Percentage 2		
1	binding (GO:0005488)	39	35.8%	33.6%		binding (GO:0005488)
2	receptor activity (GO:0004872)	6	5.5%	5.2%		catalytic activity (GO:0003824)
3	enzyme regulator activity (GO:0030234)	8	7.3%	6.9%		enzyme regulator activity (GO:0030234)
4	structural molecule activity (GO:0005198)	10	9.2%	8.6%		motor activity (GO:0003774)
5	catalytic activity (GO:0003824)	35	32.1%	30.2%		receptor activity (GO:0004872)
6	transcription regulator activity (GO:0030528)	16	14.7%	13.8%		structural molecule activity (GO:0005198)
7	motor activity (GO:0003774)	1	0.9%	0.9%		transcription regulator activity (GO:0030528)
8	transporter activity (GO:0005215)	1	0.9%	0.9%		transporter activity (GO:0005215)

D

Sr. No	Biological Process	No. of Genes	Percentage 1	Percentage 2		
1	cell communication (GO:0007154)	25	22.9%	12.4%		apoptosis (GO:0006915)
2	cellular process (GO:0009987)	35	32.1%	17.3%		cell adhesion (GO:0007155)
3	localization (GO:0051179)	1	0.9%	0.5%		cell communication (GO:0007154)
4	transport (GO:0006810)	7	6.4%	3.5%		cell cycle (GO:0007049)
5	cellular component organization (GO:0016043)	8	7.3%	4.0%		cellular component organization (GO:0016043)
6	apoptosis (GO:0006915)	6	5.5%	3.0%		cellular process (GO:0009987)
7	system process (GO:0003008)	10	9.2%	5.0%		developmental process (GO:0032502)
8	response to stimulus (GO:0050896)	8	7.3%	4.0%		generation of precursor metabolites and energy (GO:0006091)
9	developmental process (GO:0032502)	24	22.0%	11.9%		immune system process (GO:0002376)
10	generation of precursor metabolites and energy (GO:0006091)	2	1.8%	1.0%		localization (GO:0051179)
11	metabolic process (GO:0008152)	53	48.6%	26.2%		metabolic process (GO:0008152)
12	cell cycle (GO:0007049)	9	8.3%	4.5%		response to stimulus (GO:0050896)
13	immune system process (GO:0002376)	8	7.3%	4.0%		system process (GO:0003008)
14	cell adhesion (GO:0007155)	6	5.5%	3.0%		transport (GO:0006810)

Figure 20: Panther analysis of gene expression profiles. Classification of genes 'downregulated' after endurance training in TA muscle (A-B). Guides (legends) to follow the pie charts represented in A, B (C is the legend for A and D is the legend for B). Percentage 1 indicates percent of gene hit against total genes and percentage 2 indicates percent of gene hit against total process hits.

Ingenuity Analysis - Lipid Network

Figure 21: Ingenuity analysis of differentially regulated genes. Genes differentially regulated upon endurance training in TA muscle are mapped to lipid network. Genes highlighted in red are upregulated and genes highlighted in green are downregulated. Gene names are provided in appendix 1.

4.14 Transcriptional profiling of TA motor neurons following 6 weeks of endurance training

TA MNs are recruited upon endurance training as indicated by the upregulation of the neural activity-induced immediate early gene product c-Fos (Flavell and Greenberg, 2008) in TA MNs, following 1 week of endurance training (Fig. 22). Similar c-Fos elevation of c-Fos was seen in MNs after exercise (Grondard et al., 2008).
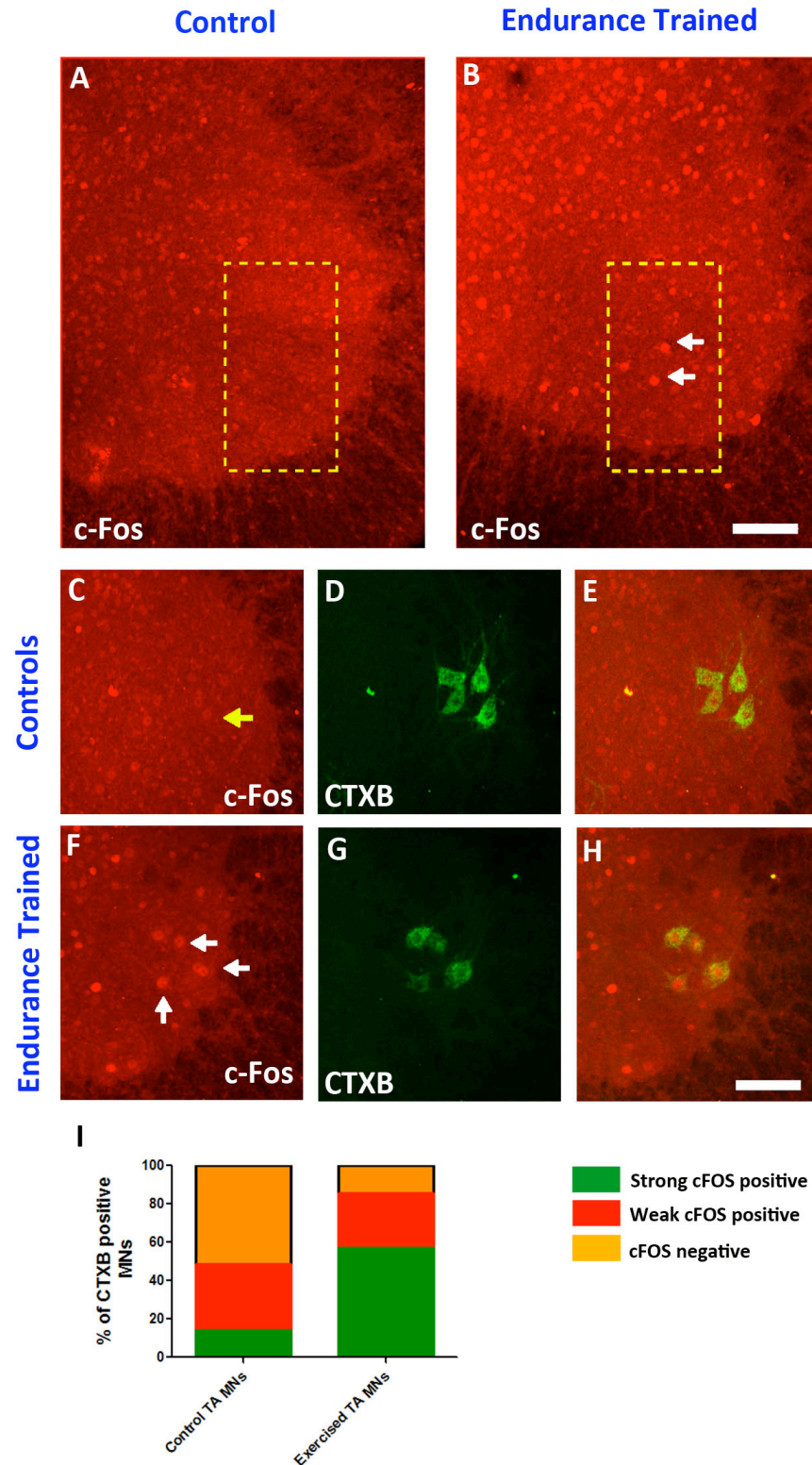
Figure 22: c-Fos expression analysis in control versus endurance trained TA motor neurons. c-Fos expression in control (A) and endurance trained spinal cord (B). Expression in TA MNs (C-H). MNs were identified by retrograde tracing with fluorescently conjugated CTXB (green, D and G). C-Fos expression is shown in red (C and F). Overlay images (E and H). C-E represent spinal cord sections from controls and F-H represent spinal cord sections from endurance trained animals. Section thickness is 60 μm and the scale bar represents 100 μm. Quantification of c-Fos positive TA MNs (control versus endurance trained, identified by CTXB tracing, CTXB positive MNs) is shown in I.
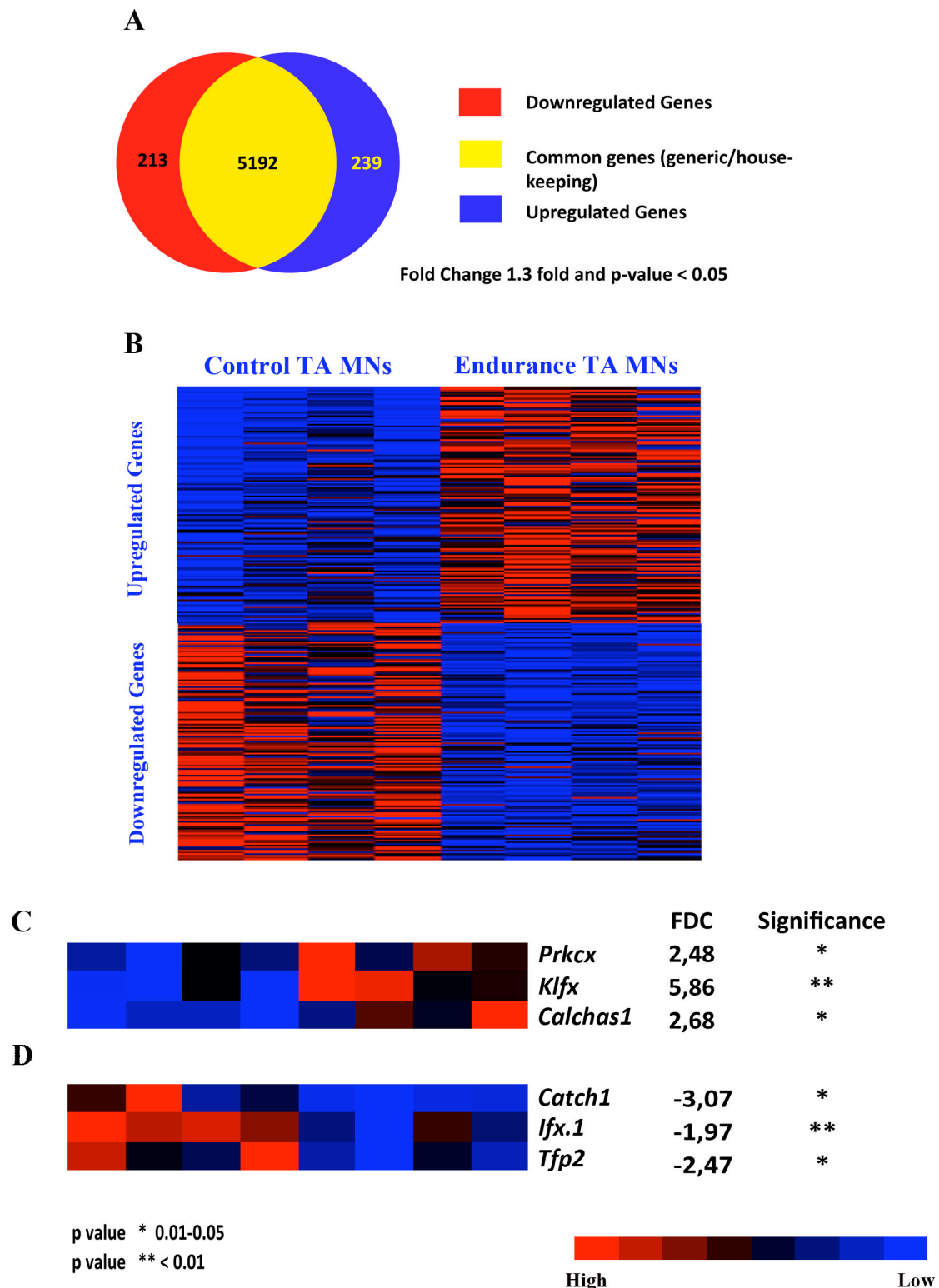
Figure 23: Expression analysis of control versus endurance trained TA motor neurons. Venn diagram representing gene expression changes in endurance trained mouse TA MNs (versus controls) (A). Heatmaps (B) of selected genes that are significantly up or downregulated post endurance training in mouse TA MNs. Heatmaps of selected candidates with fold change (FDC) and significance values (upregulated, C; downregulated, D). The threshold level for gene expression was set to 100 relative units to avoid false positive results. Red represents high level of expression and blue represents low level of expression. p-value criteria are shown in the bottom left-hand side of the image.

I next proceeded to investigate the transcriptional profile of TA MNs following 6 weeks of endurance training. The results of the screen are shown in Figs. 23 – 28. After 6 weeks of endurance training 213 transcripts were significantly downregulated, and 239 transcripts were significantly upregulated in TA MNs. 5192 significantly expressed transcripts showed no differential expression (Fig. 23A). Heatmap representation of significantly (p-value <0.05) up (Fig. 23B and C) or downregulated (Fig. 23B and D) genes is shown in Fig. 23 B-D. Among the differentially regulated transcripts *Prkcx* (protein kinase c x, 2.48 fold), *KlfX* (kruppel like factor x, 5.86 fold) and *Calchas1* (calcium channel alpha subunit 1, 2.68 fold) were upregulated (Fig. 24A, B and Fig. 23C), and *Catch1* (cation channel 1, 3.07 fold), *Ifx.1* (translation initiation factor 1, -1.97 fold) and *Tfp2* (transcription factor 2, -2.47 fold) were downregulated (Fig. 24 C, D and Fig. 23 D). Notably, neither the fast MN marker genes *Chodl, Tamnec1* (Fig. 24E, F, respectively), nor the putative slow MN-marker *Sv2a,* showed significant differential expression (Fig.24 L), indicating that the fast MNs of the TA did not undergo wholesale change of their type status following 6 week endurance training. Further, generic MN marker genes like *Chat* (Fig. 24 G) and housekeeping genes like *Gapdh*, Hprt (Fig. 24 H, I, respectively) showed no change following training. *Prkcx* encodes an isoform of protein kinase C and members of the PKC family play a important role in neuronal signalling and plasticity (Tanaka and Nishizuka, 1994) Thus, upregulation of *Prkcx* (an isoform of PKC) after endurance training indicates a similar role for it in shaping motor neuronal plasticity. Further, panther gene expression analysis of differentially regulated (upregulated, Fig. 25; downregulated, Fig. 26) genes in the context of molecular functions (Fig. 25A and C, Fig. 26A and C) and biological process (Fig. 25B and D, Fig. 26B and D) revealed that the up or down-regulated genes have a variety of molecular functions, including ion channel activity (highlighted in red), motor activity, transcriptional regulator activity, among others, and participate in various biological processes, such as energy metabolism or intracellular transport. KEGG (Kyoto encyclopedia of genes and genomes) pathway analysis using DAVID (Database for Annotation, Visualization and Integrated Discovery) revealed that some of the altered (upregulated) genes encode proteins involved in MAPK and neurotrophin signalling pathways (Fig. 27A). MAPK signalling pathway with upregulated genes is shown in Fig. 27B).
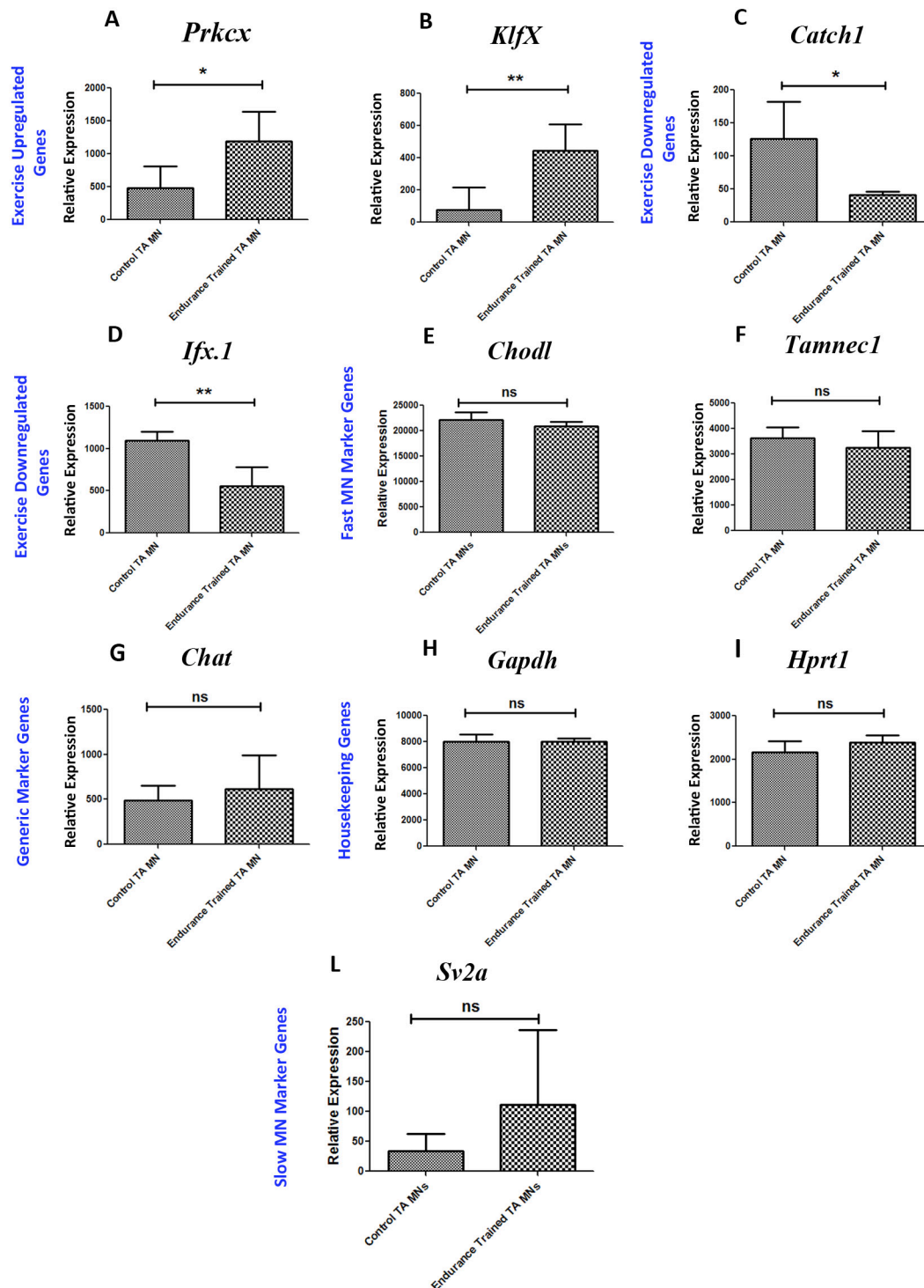
Figure 24: Comparison of expression levels of selected genes from endurance trained TA motor neurons (versus control TA motor neurons). Comparison of expression levels of endurance altered motor neuronal genes. Upregulated genes (A and B). Downregulated genes (C and D). Fast motor neuronal marker (E and F). Generic motor neuronal marker (G). Housekeeping genes (H and I). Slow motor neuronal marker (L). Significance is calculated using student's t-test (* p-value <0.05, ** p-value <0.01, *** p-value <0.001, ns-no significance).

Panther Analysis of Genes Upregulated in MNs (Endurance Training)

A Molecular Function

B Biological Process

Total genes 203; Total function hits 202

Total genes 203; Total process hits 299

C

Sr. No	Molecular Function	No. of Genes	Percentage 1	Percentage 2
1	ion channel activity (GO:0005216)	4	2.0%	2.0%
2	transporter activity (GO:0005215)	13	6.4%	6.4%
3	translation regulator activity (GO:0045182)	2	1.0%	1.0%
4	transcription regulator activity (GO:0030528)	19	9.4%	9.4%
5	enzyme regulator activity (GO:0030234)	7	3.4%	3.5%
6	catalytic activity (GO:0003824)	70	34.5%	34.7%
7	motor activity (GO:0003774)	2	1.0%	1.0%
8	receptor activity (GO:0004872)	7	3.4%	3.5%
9	antioxidant activity (GO:0016209)	1	0.5%	0.5%
10	structural molecule activity (GO:0005198)	14	6.9%	6.9%
11	binding (GO:0005488)	63	31.0%	31.2%

Legend (C):
- antioxidant activity (GO:0016209)
- binding (GO:0005488)
- catalytic activity (GO:0003824)
- enzyme regulator activity (GO:0030234)
- Ion channel activity (GO:0005216)
- motor activity (GO:0003774)
- receptor activity (GO:0004872)
- structural molecule activity (GO:0005198)
- transcription regulator activity (GO:0030528)
- translation regulator activity (GO:0045182)
- transporter activity (GO:0005215)

D

Sr. No	Biological Process	No. of Genes	Percentage 1	Percentage 2
1	cell communication (GO:0007154)	35	17.2%	11.7%
2	cellular process (GO:0009987)	48	23.6%	16.1%
3	localization (GO:0051179)	1	0.5%	0.3%
4	transport (GO:0006810)	38	18.7%	12.7%
5	cellular component organization (GO:001604	8	3.9%	2.7%
6	apoptosis (GO:0006915)	7	3.4%	2.3%
7	system process (GO:0003008)	10	4.9%	3.3%
8	reproduction (GO:0000003)	2	1.0%	0.7%
9	response to stimulus (GO:0050896)	8	3.9%	2.7%
10	homeostatic process (GO:0042592)	1	0.5%	0.3%
11	developmental process (GO:0032502)	18	8.9%	6.0%
12	generation of precursor metabolites and energy	2	1.0%	0.7%
13	metabolic process (GO:0008152)	97	47.8%	32.4%
14	cell cycle (GO:0007049)	10	4.9%	3.3%
15	immune system process (GO:0002376)	10	4.9%	3.3%
16	cell adhesion (GO:0007155)	4	2.0%	1.3%

Legend (D):
- apoptosis (GO:0006915)
- cell adhesion (GO:0007155)
- cell communication (GO:0007154)
- cell cycle (GO:0007049)
- cellular component organization (GO:0016043)
- cellular process (GO:0009987)
- developmental process (GO:0032502)
- generation of precursor metabolites and energy (GO:00060
- homeostatic process (GO:0042592)
- immune system process (GO:0002376)
- localization (GO:0051179)
- metabolic process (GO:0008152)
- reproduction (GO:0000003)
- response to stimulus (GO:0050896)
- system process (GO:0003008)
- transport (GO:0006810)

Figure 25: Panther analysis of gene expression profiles. Classification of genes 'upregulated' after endurance training in TA MNs (A-B). Guides (legends) to follow the pie charts represented in A, B (C is the legend for A and D is the legend for B). Percentage 1 indicates percent of gene hit against total genes and percentage 2 indicates percent of gene hit against total process hits. Ion channel percentage is highlighted in red (A and C).

Panther Analysis of Genes Downregulated in MNs (Endurance Training)

A **Molecular Function**

B **Biological Process**

Total genes 187; Total function hits 194

Total genes 187; Total process hits 319

C

Sr. No	Molecular Function	No. of Genes	Percentage 1	Percentage 2
1	ion channel activity (GO:0005216)	8	4.3%	4.1%
2	transporter activity (GO:0005215)	7	3.7%	3.6%
3	translation regulator activity (GO:0045182)	2	1.1%	1.0%
4	transcription regulator activity (GO:0030528)	18	9.6%	9.3%
5	enzyme regulator activity (GO:0030234)	7	3.7%	3.6%
6	catalytic activity (GO:0003824)	72	38.5%	37.1%
7	motor activity (GO:0003774)	3	1.6%	1.5%
8	receptor activity (GO:0004872)	4	2.1%	2.1%
9	structural molecule activity (GO:0005198)	15	8.0%	7.7%
10	binding (GO:0005488)	58	31.0%	29.9%

Legend (C):
- binding (GO:0005488)
- catalytic activity (GO:0003824)
- enzyme regulator activity (GO:0030234)
- Ion channel activity (GO:0005216)
- motor activity (GO:0003774)
- receptor activity (GO:0004872)
- structural molecule activity (GO:0005198)
- transcription regulator activity (GO:0030528)
- translation regulator activity (GO:0045182)
- transporter activity (GO:0005215)

D

Sr. No	Biological Process	No. of Genes	Percentage 1	Percentage 2
1	cell communication (GO:0007154)	31	16.6%	9.7%
2	cellular process (GO:0009987)	52	27.8%	16.3%
3	localization (GO:0051179)	1	0.5%	0.3%
4	transport (GO:0006810)	26	13.9%	8.2%
5	cellular component organization (GO:0016043)	11	5.9%	3.4%
6	apoptosis (GO:0006915)	7	3.7%	2.2%
7	system process (GO:0003008)	16	8.6%	5.0%
8	reproduction (GO:0000003)	1	0.5%	0.3%
9	response to stimulus (GO:0050896)	12	6.4%	3.8%
10	regulation of biological process (GO:0050789)	1	0.5%	0.3%
11	homeostatic process (GO:0042592)	1	0.5%	0.3%
12	developmental process (GO:0032502)	18	9.6%	5.6%
13	generation of precursor metabolites and energy	5	2.7%	1.6%
14	metabolic process (GO:0008152)	96	51.3%	30.1%
15	cell cycle (GO:0007049)	18	9.6%	5.6%
16	immune system process (GO:0002376)	21	11.2%	6.6%
17	cell adhesion (GO:0007155)	2	1.1%	0.6%

Legend (D):
- apoptosis (GO:0006915)
- cell adhesion (GO:0007155)
- cell communication (GO:0007154)
- cell cycle (GO:0007049)
- cellular component organization (GO:0016043)
- cellular process (GO:0009987)
- developmental process (GO:0032502)
- generation of precursor metabolites and energy (GO:0006091)
- homeostatic process (GO:0042592)
- immune system process (GO:0002376)
- localization (GO:0051179)
- metabolic process (GO:0008152)
- regulation of biological process (GO:0050789)
- reproduction (GO:0000003)
- response to stimulus (GO:0050896)
- system process (GO:0003008)
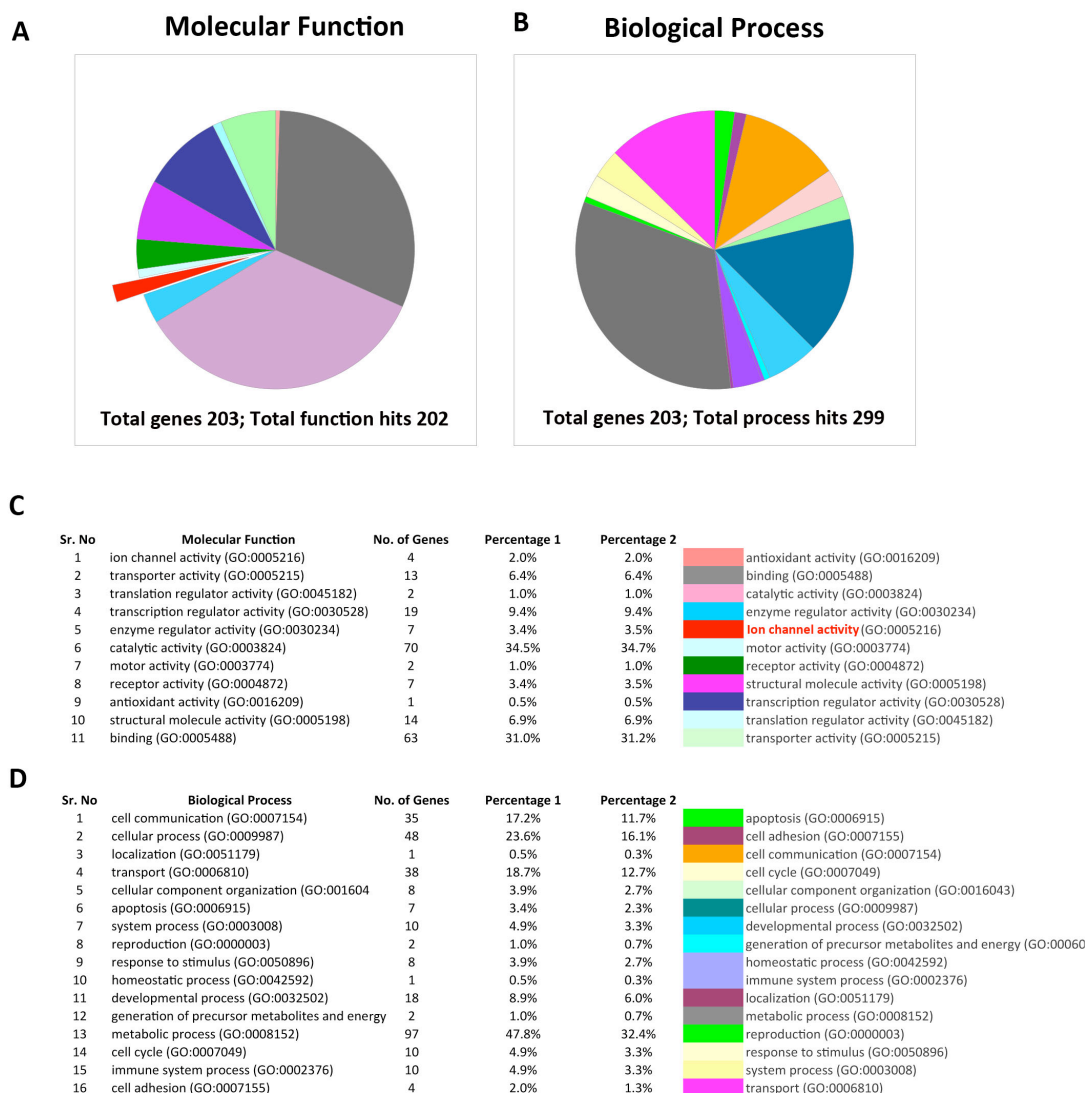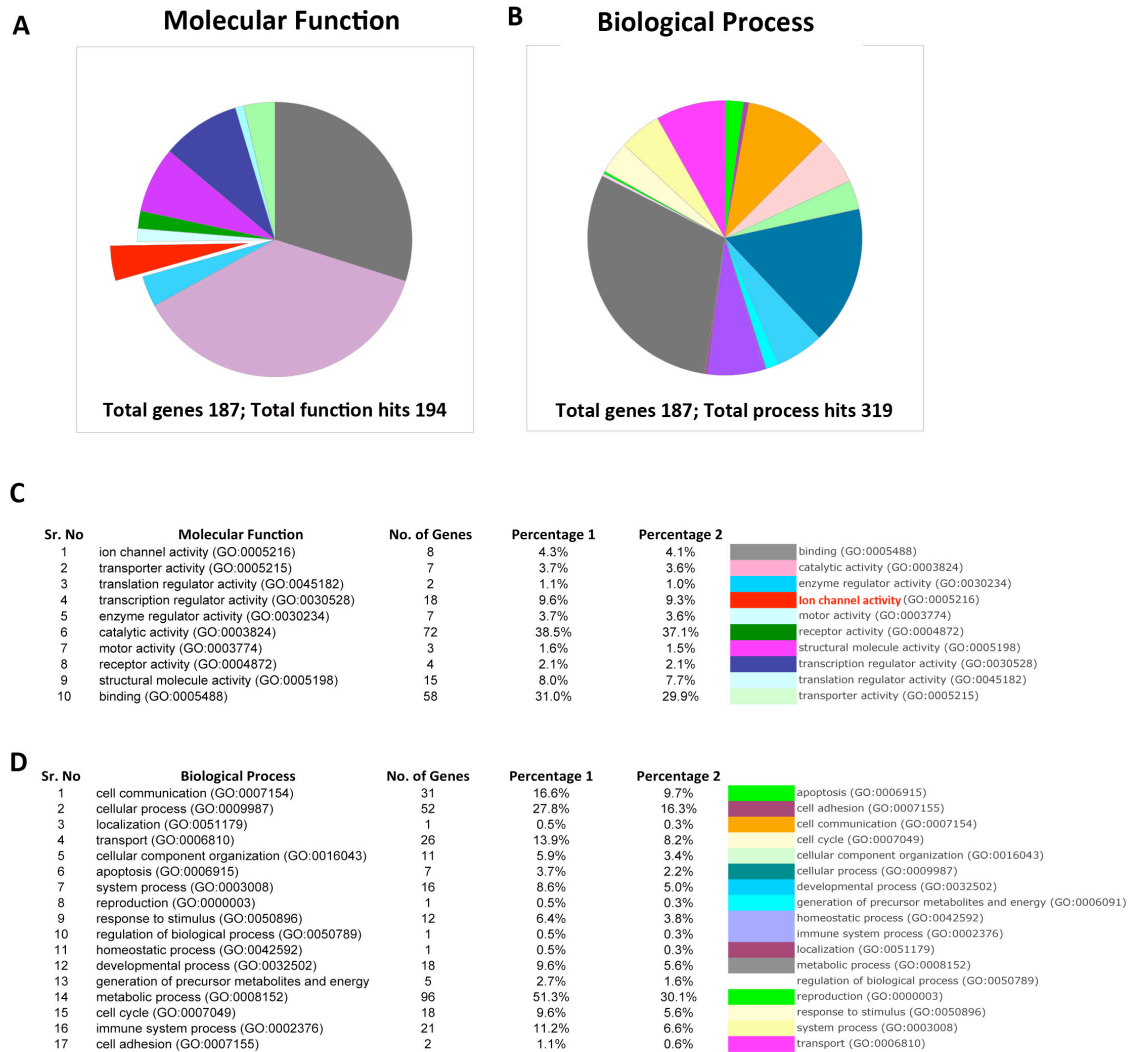- transport (GO:0006810)

Figure 26: Panther analysis of gene expression profiles. Classification of genes 'downregulated' after endurance training in TA MNs (A-B). Guides (legends) to follow the pie charts represented in A, B (C is the legend for A and D is the legend for B). Percentage 1 indicates percent of gene hit against total genes and percentage 2 indicates percent of gene hit against total process hits. Ion channel percentage is highlighted in red (A and C).

A

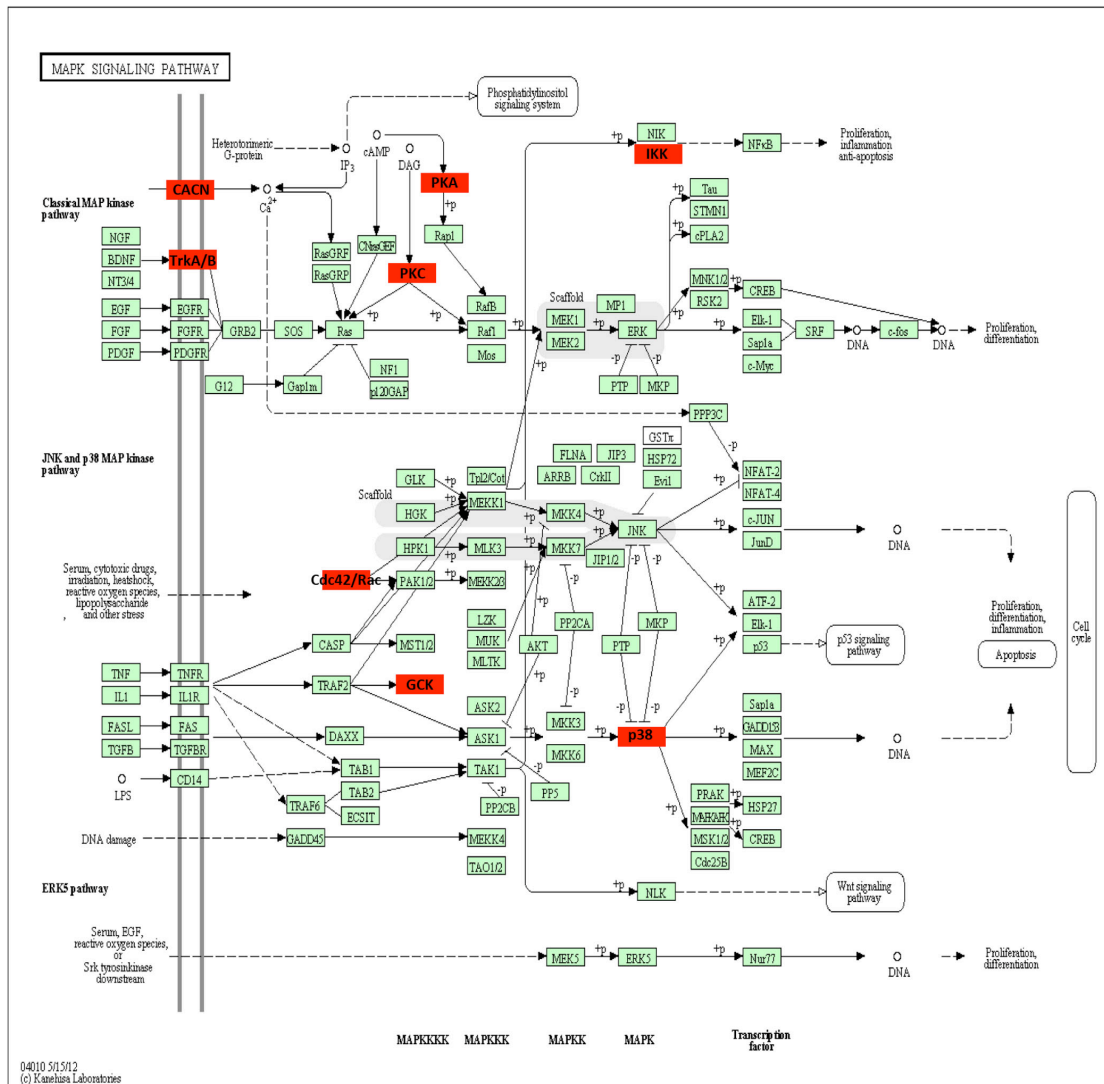| Category	Pathway	No. of Genes	p-value
KEGG_PATHWAY	GnRH signaling pathway	6	8.0E-3
KEGG_PATHWAY	MAPK signaling pathway	9	2.0E-2
KEGG_PATHWAY	Neurotrophin signaling pathway	5	5.1E-2
KEGG_PATHWAY	Ubiquitin mediated proteolysis	6	3.0E-2

B

Figure 27: DAVID pathway analysis of genes upregulated after endurance training in TA motor neurons. Upregulated genes participate in the mentioned pathways (A). KEGG pathway for MAPK signalling (B). Upregulated genes are represented in red boxes. Gene names are provided in appendix 2.

Ion channels represent an interesting class of proteins which regulate the excitability of neurons and several ion channel transcripts (4 transcripts upregulated Fig. 25A and C, 8 transcripts downregulated, Fig. 26A and C) are altered in TA MNs following 6 weeks of endurance training. The following ion channel transcripts are upregulated following endurance training in TA (fast MNs) – *Sodchas1* (sodium channel alpha subunit 1, 2.99 fold, Fig. 28A), *Potch1* (calcium activated potassium channel 1, 2.4 fold, Fig. 28B), *Calchs1* (calcium channel subunit 1, 3.96 fold, Fig. 28C) and *Calchas1* (calcium channel alpha subunit 1, 2.68 fold, Fig. 28D). The upregulation of *Sodchas1* (sodium channel) was verified by qPCR (Fig. 28E). Further, these channels along with *Eaarip* (excitatory amino acid receptor interacting protein, upregulated in endurance trained TA MNs) were not upregulated in either the brain (Fig. 29A-D) or in the liver tissue (Fig. 29E). This result indicates that these adaptations (upregulation of ion channel transcripts) were specific to MNs and are a part of the adaptive response to neuromuscular training. All of these channels were shown to regulate excitability of neurons, and thus an upregulation in their transcripts might underlie plastic adaptations, such as increased excitability and AHP changes that occur in MNs following endurance training.
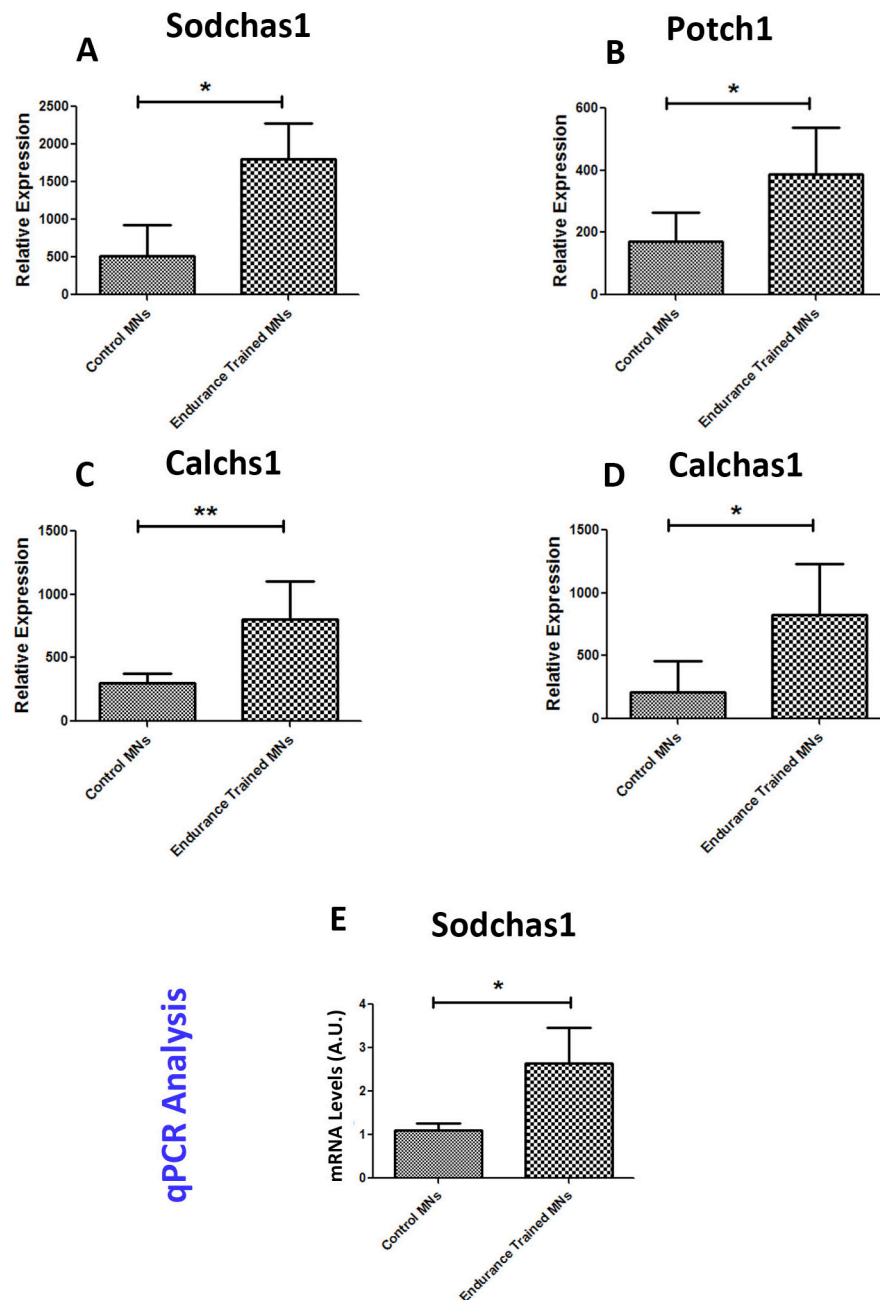
Fig. 28: Upregulated ion channel transcripts in TA motor neurons following 6 weeks of endurance training. Comparison of expression levels of ion channel transcripts (versus controls) following endurance training (A-D). qPCR validation of sodium channel upregulation (E). Significance is calculated using student's t-test (* p-value <0.05, ** p-value <0.01, *** p-value <0.001).
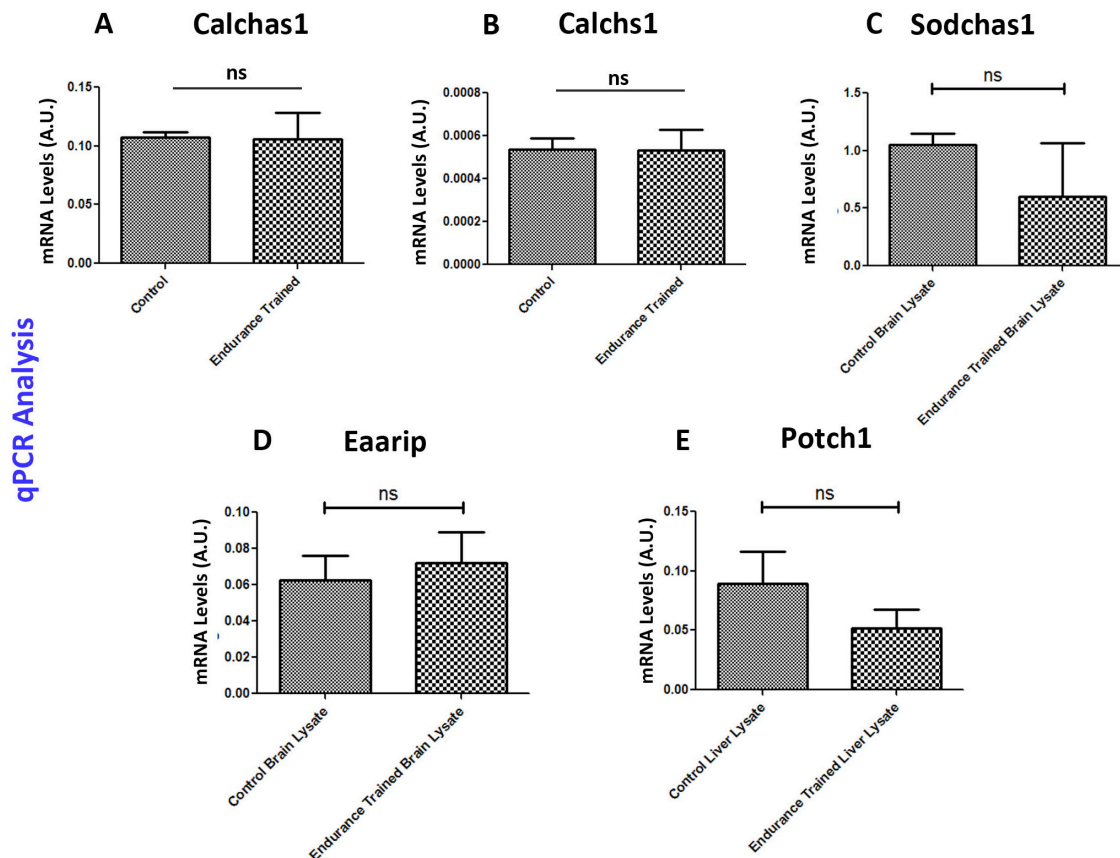
Fig. 29: Comparison of ion channel transcripts expression in brain and liver tissue following 6 weeks of endurance training. qPCR analysis of ion channel transcripts expression following endurance training in brain (A-D) and liver (E) tissues. Significance is calculated using student's t-test (ns – no significance).

4.15 Hindlimb suspension

Muscle and MNs are altered following HS and for instance, spinal MNs display reduced excitability following HS. However, the molecular correlates underlying this adaptive plasticity are unknown. To address this, I have designed a screen to elucidate the transcriptional profile of soleus MNs (along with soleus muscles) following HS which would eventually lead us to understand the molecular correlates underlying MN plasticity following decreased neuromuscular use. Soleus muscles were chosen because several studies reported that soleus muscle is greatly affected following HS; in terms of fiber type transitions (slow to fast). The schematic representation of the screen is shown in Fig. 30. CD1 mice were subjected to HS in custom designed cages. A total of 16 male CD1 mice were used for transcriptional

analysis (n= 8 controls and n=8 HS group). Starting from P28, mice were subjected to HS by tail suspension method for 4 weeks. The controls were housed in regular home cages for the entire duration of HS (4 weeks). After 3 weeks of HS a surgery was performed (on controls and HS animals) to administer intramuscular injections (Fig. 30A) in soleus muscle with the aim of retrogradely tracing soleus MNs. Then, on the following day the animals were suspended again for 1 week. After completion of HS the spinal cords and muscles were collected from age-matched controls and HS animals and were processed for transcriptional analysis. This screening paradigm represents a new methodology to identify molecular correlates of plasticity in MNs following HS. The muscles isolated from the HS animals and age matched controls were also analyzed for altered gene signatures by using microarray profiling with the aim of achieving a functional correlation of muscle and MN transcriptomes induced by decreased neuromuscular use. The results of the muscle and MN screen following HS are shown in Figs. 32-39. The general health of the trained animals was assessed in terms of their body weights and serum corticosterone levels in comparison to age-matched controls (Fig. 31). There was significant difference in the body weights of HS (not normalized with the amount of food intake) as compared to age-matched controls (Fig. 31A). The levels of serum corticosterone levels (ng/ml) were also significantly different (Fig. 31B) as compared to age- matched controls. Similar changes were reported in animals subjected to HS (Thomason and Booth, 1990)**.** These observations also indicate a possible stress factor in these animals

4.16 Transcriptional profiling of soleus muscle following 4 weeks of hindlimb suspension

The results of the transcriptional profiling of soleus muscle following 4 weeks of HS are shown in Figs. 32-35-1. After 4 weeks of HS, 411 transcripts were downregulated and 381 transcripts were upregulated in the soleus muscle. 4895 transcripts showed no differential expression (Fig. 32A). Heatmap representation of significantly (p-value <0.05) up- or downregulated genes is shown in Figs. 32B-D. The threshold level for gene expression was set to 100 relative units to avoid false positive results. Upregulated transcripts include (also verified by qPCR) include *Myh4* (Fig. 33A and G), *Myh1* (Fig. 33B and H), *Actn3* (Fig. 33D and J) and *Pvalb* (Fig. 33E

and K). *Myh7* (Fig. 33C and I) and *Fabp3* (Fig. 33F and L) were downregulated following HS in soleus muscles. Increase in *Myh4* transcripts and a decrease in *Myh7* transcripts showed that soleus muscle is undergoing fiber type transitions towards a "fast type". Further, immunohistochemical analysis (Fig. 34) reveals that slow myosin (as assessed by BA-F8 immunostaining) content in soleus is decreased (Fig. 34A-D) and fast fiber content (as assessed by MY-32 immunostaining) is increased (Fig. 34E and F) following HS, confirming array and qPCR data. Soleus muscle also showed atrophy upon 4 weeks of HS (Fig. 34A and B). A decrease in *Fabp3* indicates a decrease in oxidative potential of soleus muscle. Further, Ingenuity pathway analysis (Fig. 35-1) revealed that many transcripts (such as *Acadl*, acyl-CoA dehydrogenase, long chain) involved in fatty acid metabolism are downregulated following HS in soleus muscles. KEGG pathway mapping (Fig. 35) revealed that genes involved in PPAR signalling such as *Cpt1*- (carnitine palmitoyltransferase 1) are downregulated in soleus muscle following HS. These results clearly indicate a decreased oxidative potential of soleus muscle (a predominantly oxidative muscle). Taken together, all these results clearly indicate that soleus muscle undergoes significant changes following 4 weeks of HS.
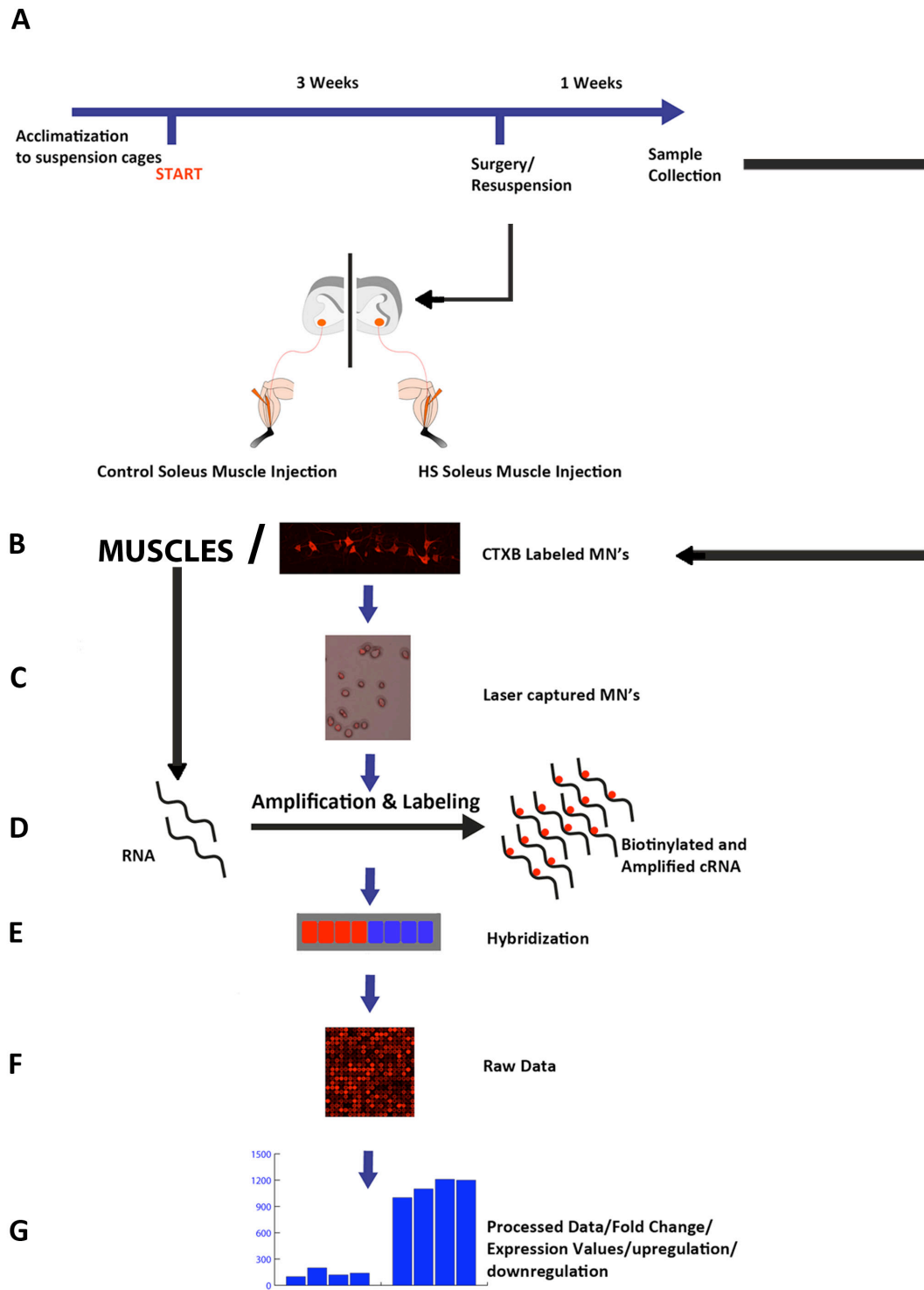
Figure 30: Schematic representation of soleus motor neuronal and muscle screen following 4 weeks of hindlimb suspension. Schematic representation of HS protocol and paradigm (A). After HS, the spinal cords were isolated and processed for cryosectioning to enable visualization of retrogradely traced MNs (B). The fluorescently labelled cells were isolated by laser capture microdissection (C). RNA was extracted from the laser captured cells and was amplified (and biotin labelled) (D). The biotinylated RNA was hybridized to Illumina BeadChip microarrays (E). The raw expression data (F) was processed to obtain expression and fold change values (G).
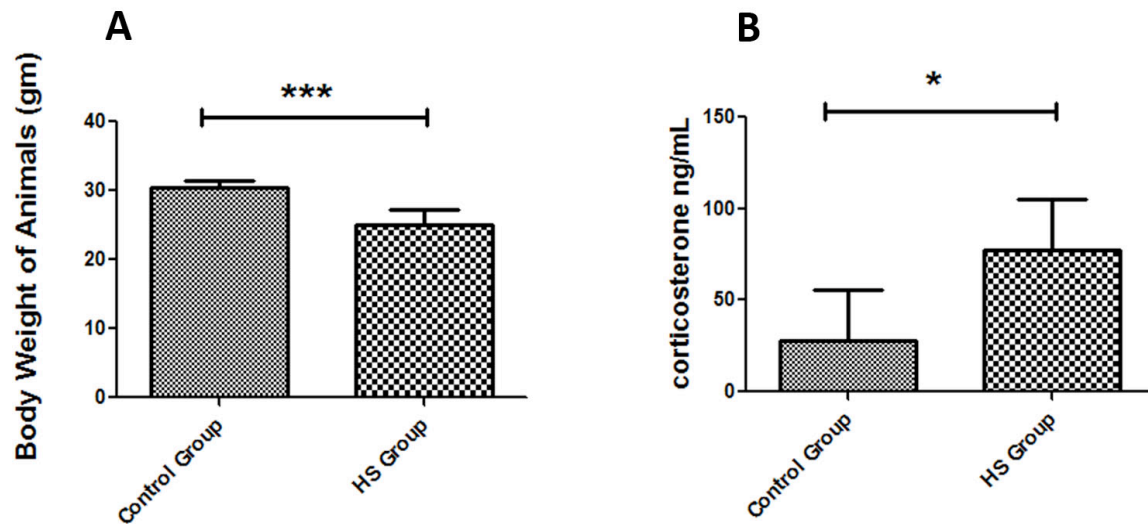
Figure 31: General health of hindlimb suspended animals. Terminal body weights of HS group in comparison with age-matched controls (A). Serum corticosterone levels (B). Significance is calculated using student's t-test (* p-value <0.05, *** p-value <0.001).
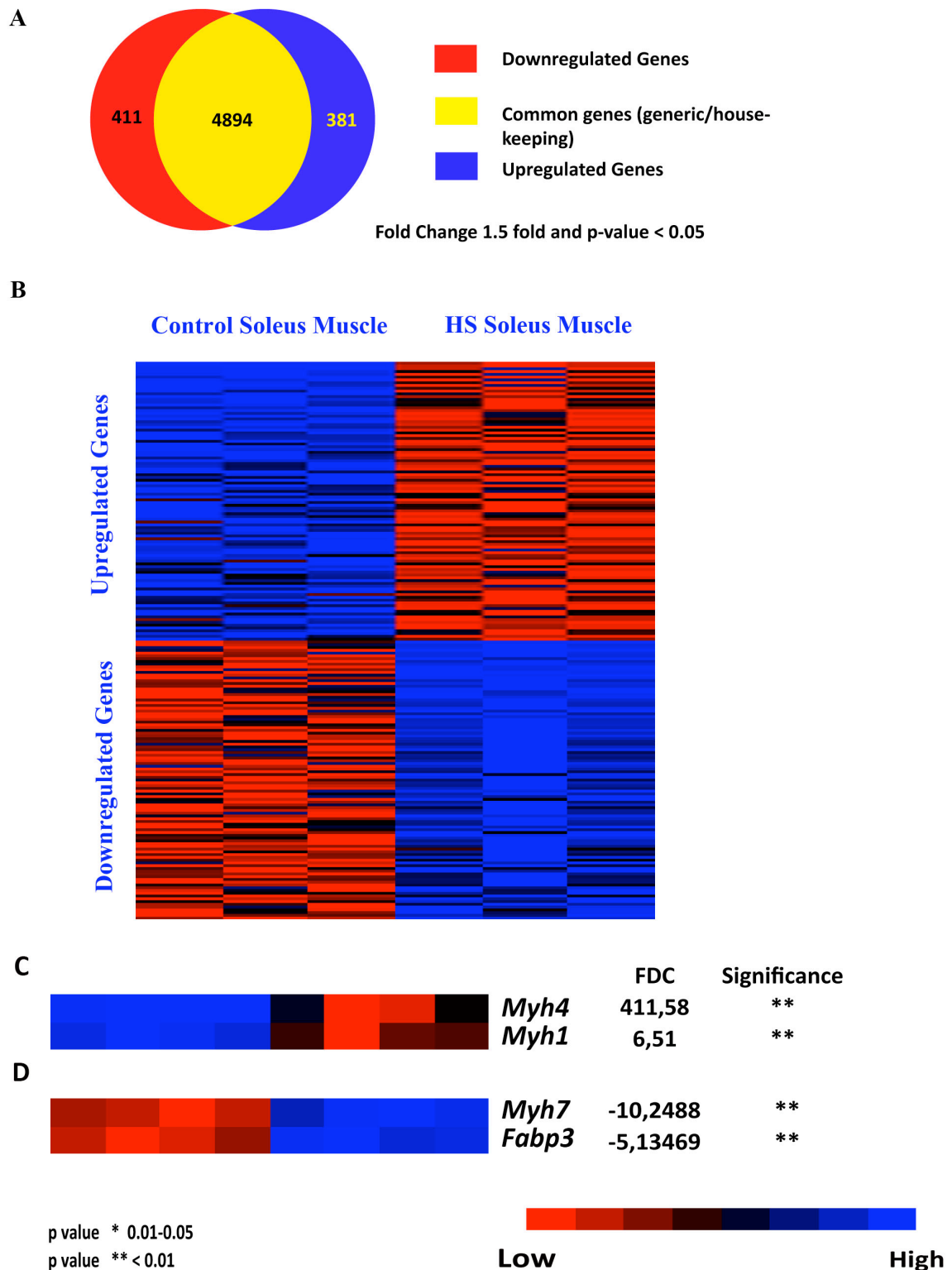
Figure 32: Expression analysis of control versus hindlimb suspended soleus muscles. Venn diagram representing gene expression changes (versus controls) in hindlimb suspended soleus muscle (A). Heatmaps of selected genes that are significantly up or downregulated post HS in mouse soleus muscle (B). Heatmaps of selected candidates with fold change (FDC) and significance values (upregulated, C; downregulated, D).The threshold level for gene expression was set to 100 relative units to avoid false positive results. Red represents high level of expression and blue represents low level of expression. p-value criteria are shown in the bottom left-hand side of the image.
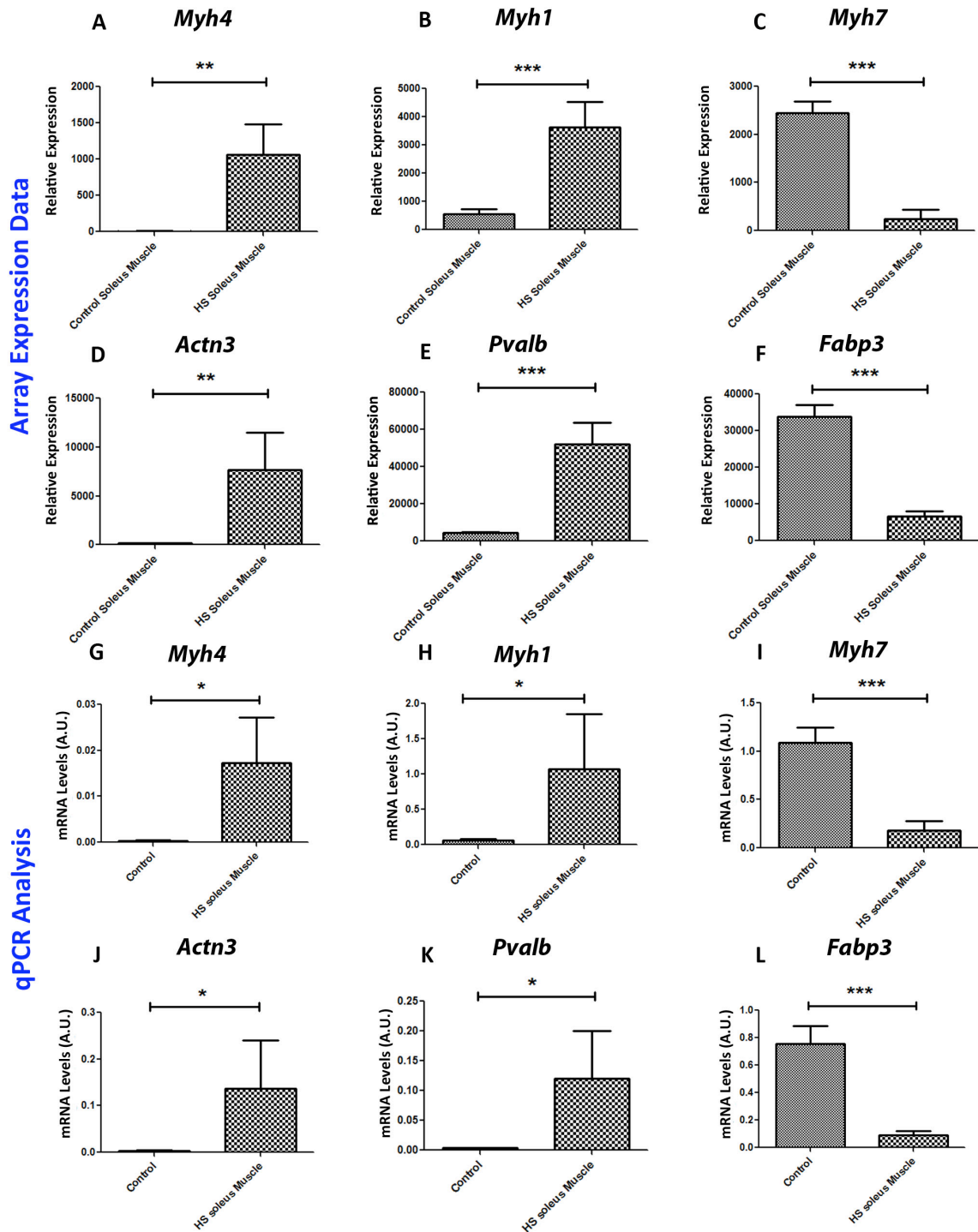
Figure 33: Comparison and verification of expression levels of selected genes from hindlimb suspended soleus muscle (versus control soleus muscle). Comparison of expression levels of genes between control and hindlimb suspended soleus muscles. Upregulated genes (A, B, D and E). Downregulated genes (C, F). qPCR verification of up or downregulated genes (G, H, J, K and I, L, respectively). Significance is calculated using student's t-test (* p-value <0.05, ** p-value <0.01, *** p-value <0.001).

Control Soleus Muscle **HS Soleus Muscle**
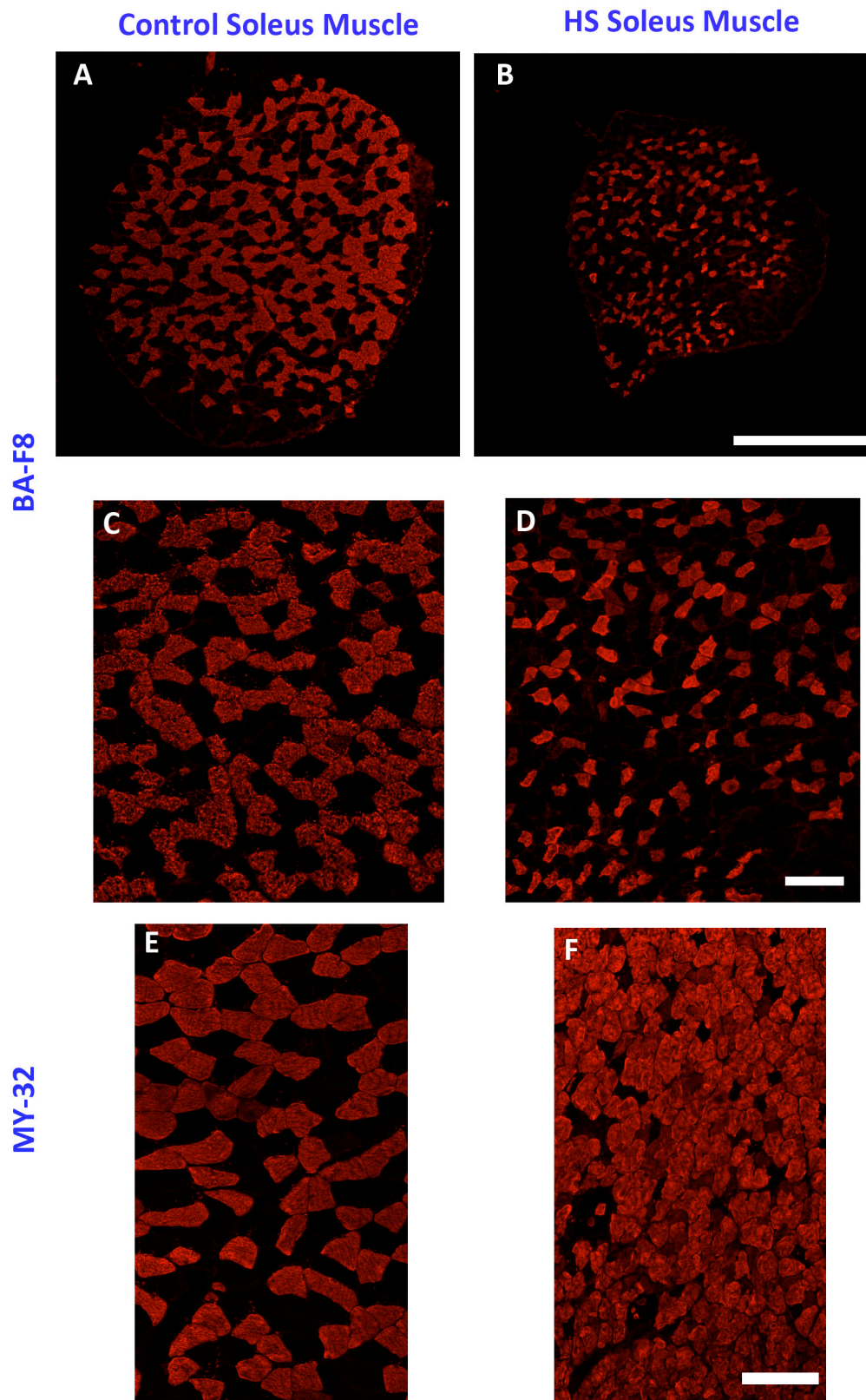
Figure 34: Immunohistochemical analysis of mouse soleus muscle after 4 weeks of hindlimb suspension. Control soleus muscle (A, C and E). Hindlimb suspended soleus muscle (B, D and F). BA-F8 (A-D) and MY-32 (E and F) immunostaining on cross sections of mouse soleus muscle. Section thickness is 10 µm. The scale bar represents 500 µm in A, B and 100 µm C-F.
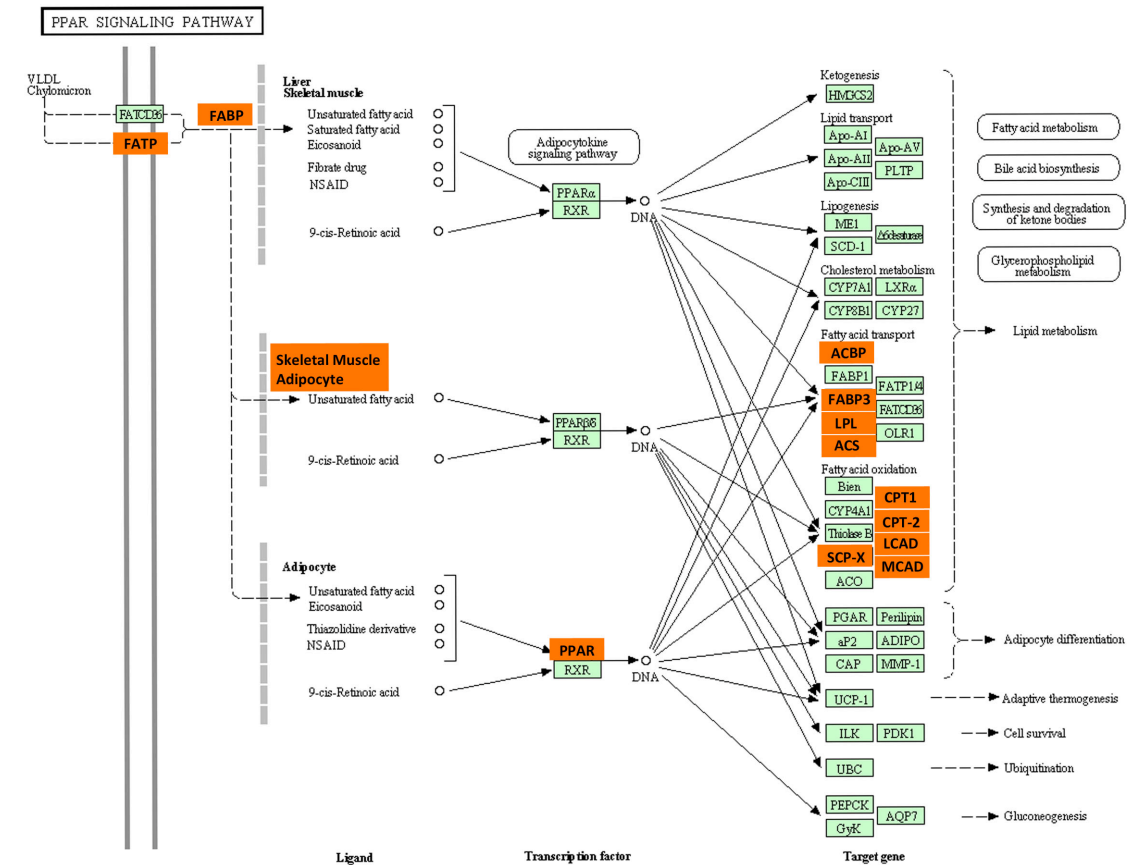
Figure 35: Genes downregulated after HS in soleus muscles are mapped to PPAR signalling pathway. KEGG pathway for PPAR signalling. Downregulated genes are represented in red boxes. Gene names are provided in appendix 3.

Ingenuity Pathway - Fatty Acid Metabolism
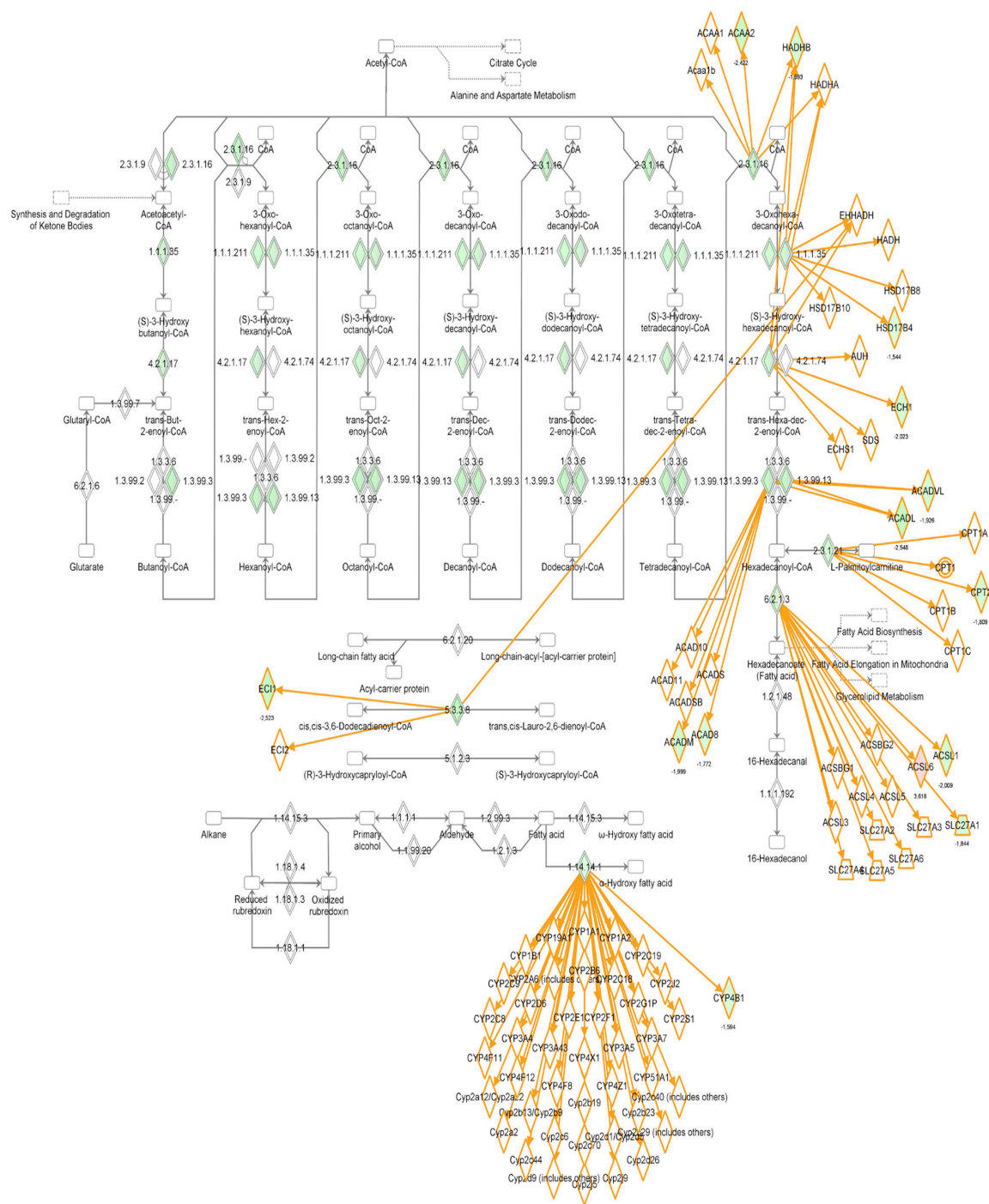
Figure 35-1: Ingenuity pathway analysis of differentially regulated genes (in soleus muscle upon HS). Genes differentially regulated upon HS in soleus muscle are mapped to fatty acid metabolism pathway. Genes highlighted in green are downregulated and genes highlighted in red are upregulated. Fold change values shown in brackets. Gene names are shown in appendix 4.

4.17 Transcriptional profiling of soleus motor neurons following 4 weeks of hindlimb suspension

The results of the soleus MN screen are shown in Figs. 36 – 39. After 4 weeks of HS, 192 transcripts were downregulated and 278 transcripts were upregulated in soleus MNs. 4612 transcripts show no differential expression (Fig. 36A). Heatmap representation of significantly up (Fig. 36B and C) or downregulated (Fig. 36B and D) genes is shown in Fig. 36 B-D. The threshold level for gene expression was set to 100 relative units to avoid false positive results. Upregulated transcripts include, *Grep* (growth response gene 1, 237 fold), *Cabuf* (Calcium buffering gene, 7.1 fold) and *Svap* (synaptic vesicle associated protein, 1.87 fold) (Fig. 37A, B, C and Fig. 36C, respectively). *Syap2* (synaptic vesicle associated protein 2, -4.2 fold) and *Cdkx* (cyclin dependent kinase x, -4.9 fold) were downregulated (Fig. 37D and Fig. 36D, respectively). Neither the fast marker gene (*Chodl,* Fig. 37E) nor the slow marker gene *Sv2a* (Fig. 37H) showed differential expression. Further, generic motor neuronal marker genes like *Chat* (Fig. 37F) and housekeeping genes like *Gapdh* (Fig. 36G) showed no change following HS. Further, panther gene expression analysis of differentially expressed (upregulated, Fig. 38; downregulated, Fig. 39) genes in the context of molecular functions (Fig. 38A and C, Fig. 39A and C) and biological process (Fig. 38B and D, Fig.39B and D) revealed that the up or down regulated genes have a variety of molecular functions (ion channel activity (4 transcripts, indicated by red in Fig. 38A and C), motor activity (3 transcripts), transcriptional regulator activity, etc) and participate in various biological processes like metabolism, transport, cell communication, etc. Notably, 4 ion channels transcripts are upregulated upon HS in soleus MNs (Fig. 38A and C, highlighted in red).
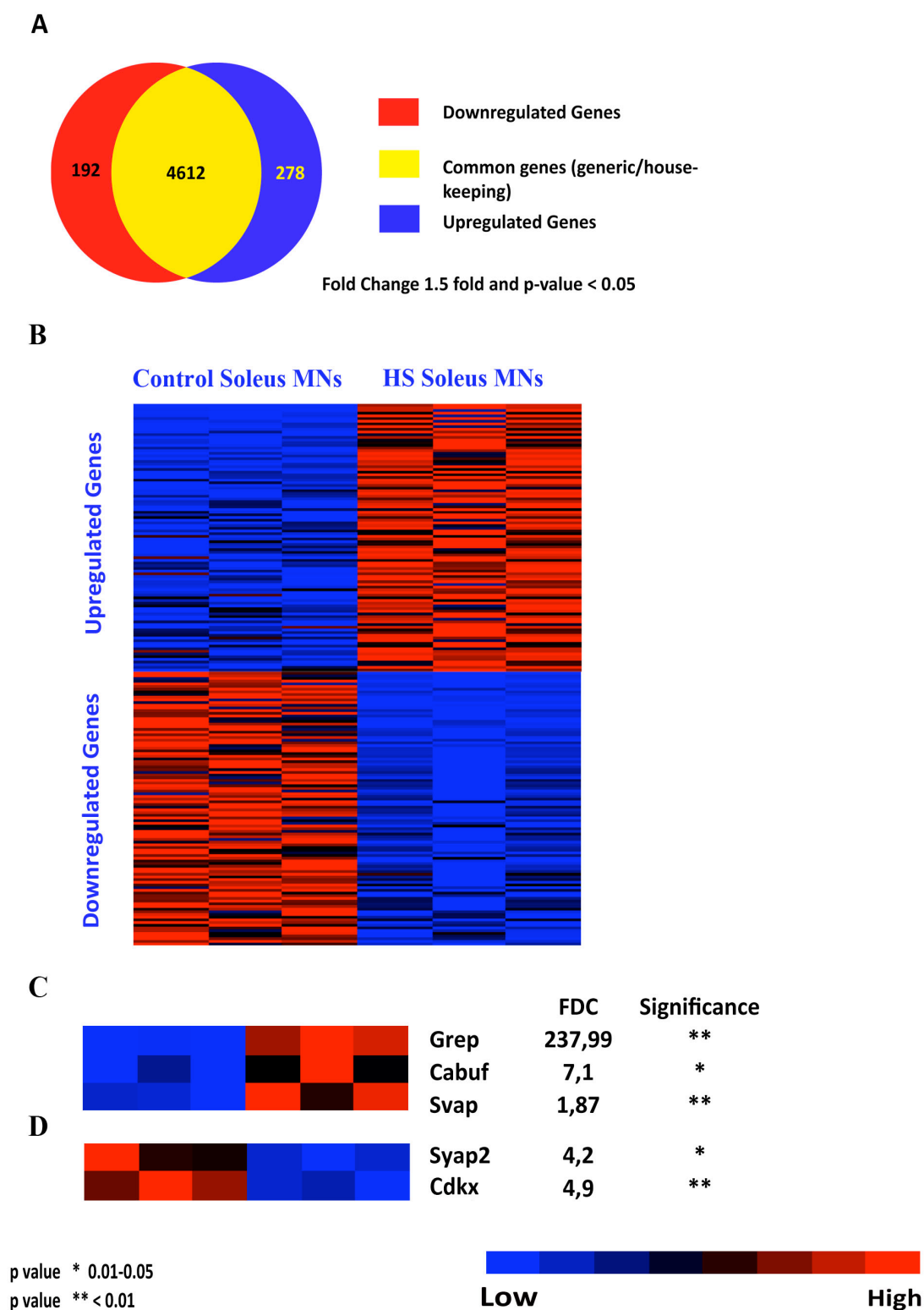
Figure 36: Expression analysis of control versus hindlimb suspended soleus motor neurons. Venn diagram representing gene expression changes in hindlimb suspended soleus MNs (versus controls) (A). Heatmaps of selected genes that are significantly up or downregulated post HS in mouse soleus MNs (B). Heatmaps of selected candidates with fold change (FDC) and significance values (upregulated, C; downregulated, D).The threshold level for gene expression was set to 100 relative units to avoid false positive results. Red represents high level of expression and blue represents low level of expression. p-value criteria are shown in the bottom left-hand side of the image.
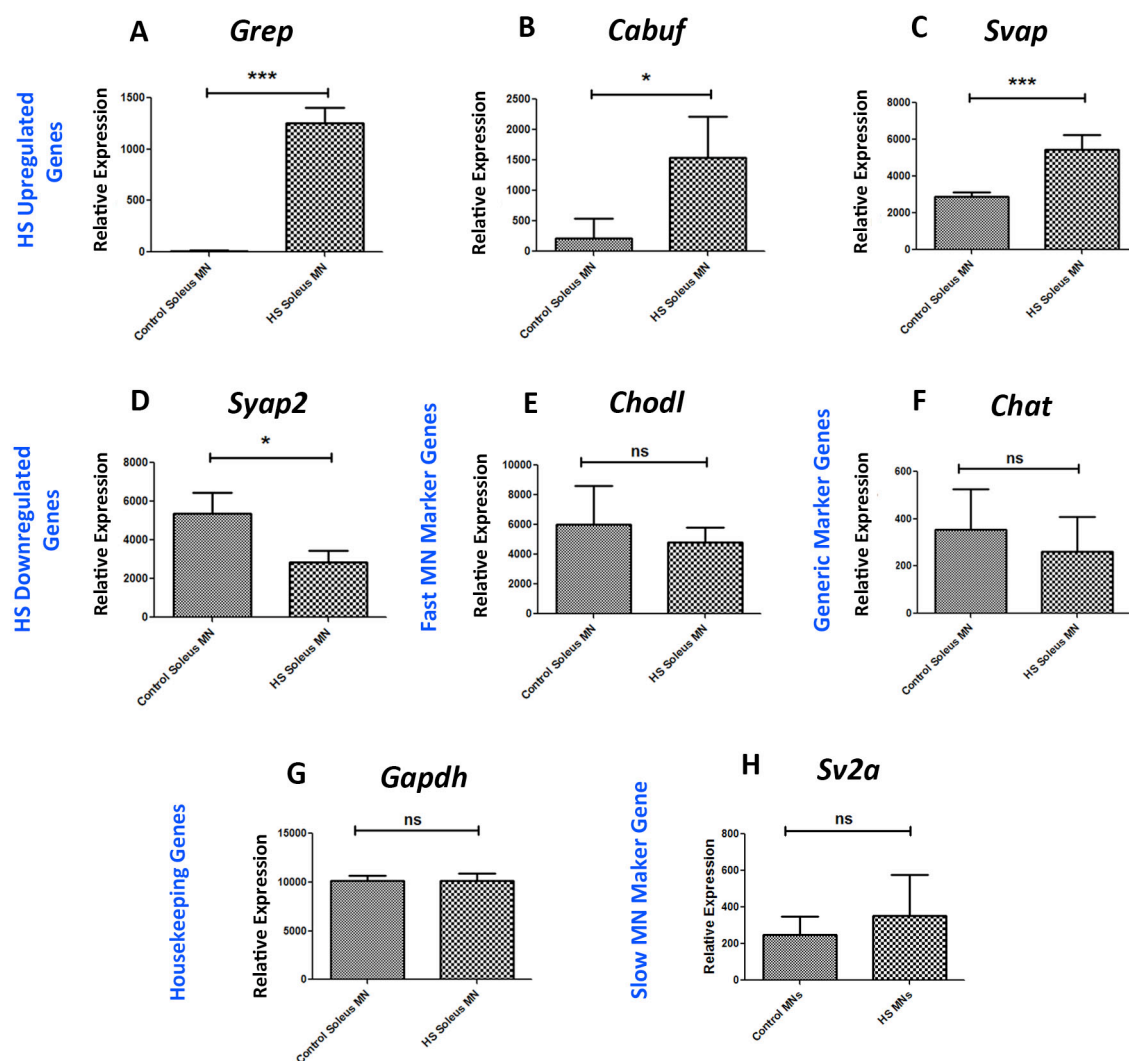
Figure 37: Comparison of expression levels of selected genes from hindlimb suspended soleus motor neurons (versus control soleus motor neurons). Comparison of expression levels of HS altered soleus MN genes. Upregulated genes (A, B and C). Downregulated genes (D). Fast MN marker gene (E). Generic MN marker gene (F). Housekeeping genes (G). Slow MN marker gene (H). Significance is calculated using student's t-test (* p-value <0.05, *** p-value <0.001, ns-no significance).

Panther Analysis of Genes Upregulated in MNs (HS)

A **Molecular Function**

B **Biological Process**

Total genes 241; Total function hits 250

Total genes 241; Total process hits 452

C

Sr. No	Biological Process	No. of Genes	Percentage 1	Percentage 2		
1	ion channel activity (GO:0005216)	4	1.7%	1.6%		antioxidant activity (GO:0016209)
2	transporter activity (GO:0005215)	13	5.4%	5.2%		binding (GO:0005488)
3	translation regulator activity (GO:0045182)	2	0.8%	0.8%		catalytic activity (GO:0003824)
4	transcription regulator activity (GO:0030528)	16	6.6%	6.4%		enzyme regulator activity (GO:0030234)
5	enzyme regulator activity (GO:0030234)	11	4.6%	4.4%		Ion channel activity (GO:0005216)
6	catalytic activity (GO:0003824)	89	36.9%	35.6%		motor activity (GO:0003774)
7	motor activity (GO:0003774)	3	1.2%	1.2%		receptor activity (GO:0004872)
8	receptor activity (GO:0004872)	10	4.1%	4.0%		structural molecule activity (GO:0005198)
9	antioxidant activity (GO:0016209)	1	0.4%	0.4%		transcription regulator activity (GO:0030528)
10	structural molecule activity (GO:0005198)	21	8.7%	8.4%		translation regulator activity (GO:0045182)
11	binding (GO:0005488)	80	33.2%	32.0%		transporter activity (GO:0005215)

D

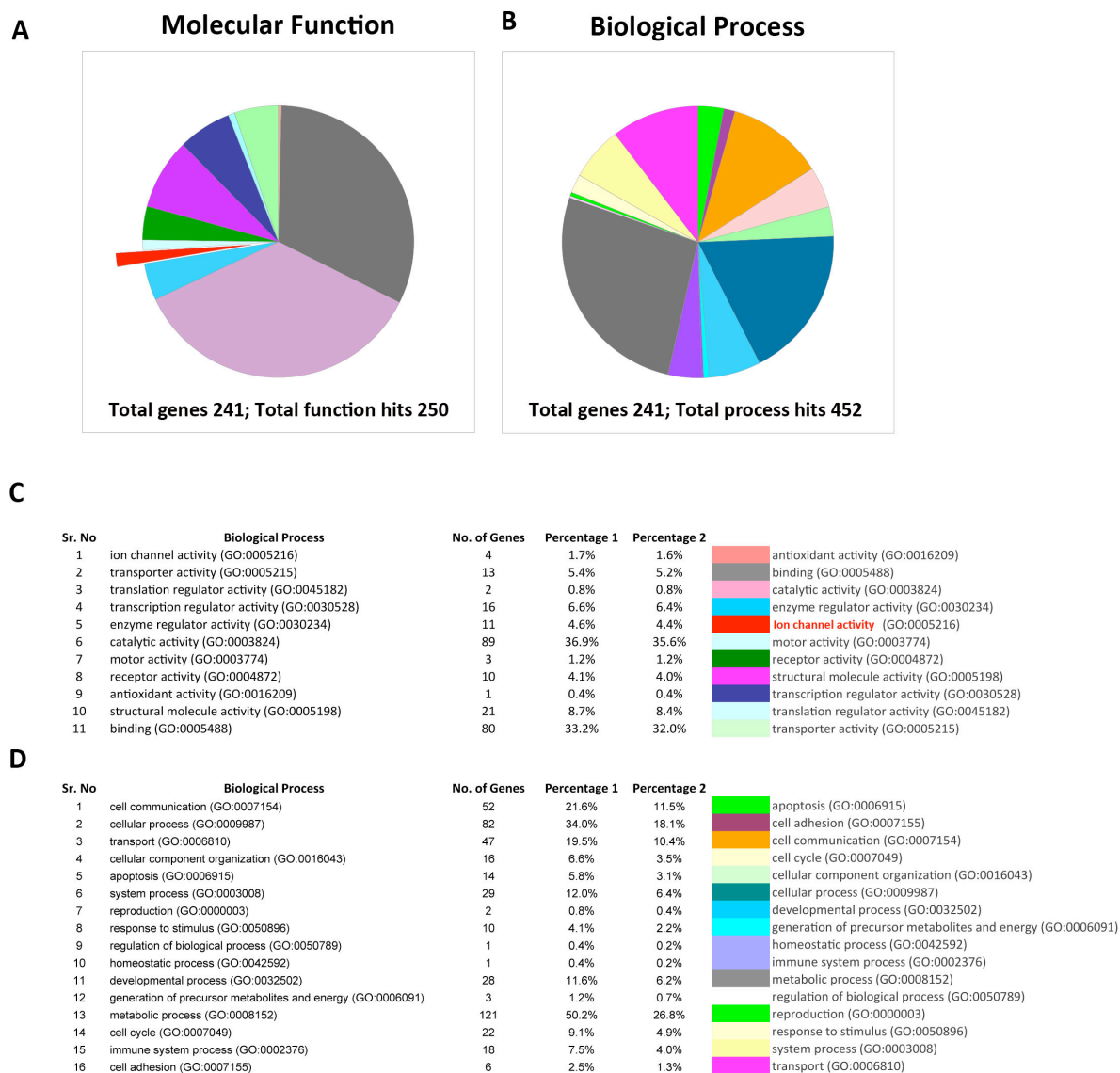| Sr. No	Biological Process	No. of Genes	Percentage 1	Percentage 2		
1	cell communication (GO:0007154)	52	21.6%	11.5%		apoptosis (GO:0006915)
2	cellular process (GO:0009987)	82	34.0%	18.1%		cell adhesion (GO:0007155)
3	transport (GO:0006810)	47	19.5%	10.4%		cell communication (GO:0007154)
4	cellular component organization (GO:0016043)	16	6.6%	3.5%		cell cycle (GO:0007049)
5	apoptosis (GO:0006915)	14	5.8%	3.1%		cellular component organization (GO:0016043)
6	system process (GO:0003008)	29	12.0%	6.4%		cellular process (GO:0009987)
7	reproduction (GO:0000003)	2	0.8%	0.4%		developmental process (GO:0032502)
8	response to stimulus (GO:0050896)	10	4.1%	2.2%		generation of precursor metabolites and energy (GO:0006091)
9	regulation of biological process (GO:0050789)	1	0.4%	0.2%		homeostatic process (GO:0042592)
10	homeostatic process (GO:0042592)	1	0.4%	0.2%		immune system process (GO:0002376)
11	developmental process (GO:0032502)	28	11.6%	6.2%		metabolic process (GO:0008152)
12	generation of precursor metabolites and energy (GO:0006091)	3	1.2%	0.7%		regulation of biological process (GO:0050789)
13	metabolic process (GO:0008152)	121	50.2%	26.8%		reproduction (GO:0000003)
14	cell cycle (GO:0007049)	22	9.1%	4.9%		response to stimulus (GO:0050896)
15	immune system process (GO:0002376)	18	7.5%	4.0%		system process (GO:0003008)
16	cell adhesion (GO:0007155)	6	2.5%	1.3%		transport (GO:0006810)

Figure 38: Panther analysis of gene expression profiles. Classification of genes 'upregulated' after hindlimb suspension in mouse soleus MNs (A-B). Guides (legends) to follow the pie charts represented in A, B (C is the legend for A and D is the legend for B). Ion channel percentage is highlighted in red (A and C). Percentage 1 indicates percent of gene hit against total genes and percentage 2 indicates percent of gene hit against total process hits.

Panther Analysis of Genes Downregulatedregulated in MNs (HS)

A **Molecular Function**

B **Biological Process**

C

Sr. No	Molecular Functions	No. of Genes	Percentage 1	Percentage 2	
1	transporter activity (GO:0005215)	10	6.3%	6.9%	▮ antioxidant activity (GO:0016209)
2	translation regulator activity (GO:0045182)	1	0.6%	0.7%	▮ binding (GO:0005488)
3	transcription regulator activity (GO:0030528)	15	9.4%	10.3%	▮ catalytic activity (GO:0003824)
4	enzyme regulator activity (GO:0030234)	5	3.1%	3.4%	▮ enzyme regulator activity (GO:0030234)
5	catalytic activity (GO:0003824)	49	30.8%	33.8%	▮ receptor activity (GO:0004872)
6	receptor activity (GO:0004872)	6	3.8%	4.1%	▮ structural molecule activity (GO:0005198)
7	antioxidant activity (GO:0016209)	1	0.6%	0.7%	▮ transcription regulator activity (GO:0030528)
8	structural molecule activity (GO:0005198)	6	3.8%	4.1%	▮ translation regulator activity (GO:0045182)
9	binding (GO:0005488)	52	32.7%	35.9%	▮ transporter activity (GO:0005215)

D

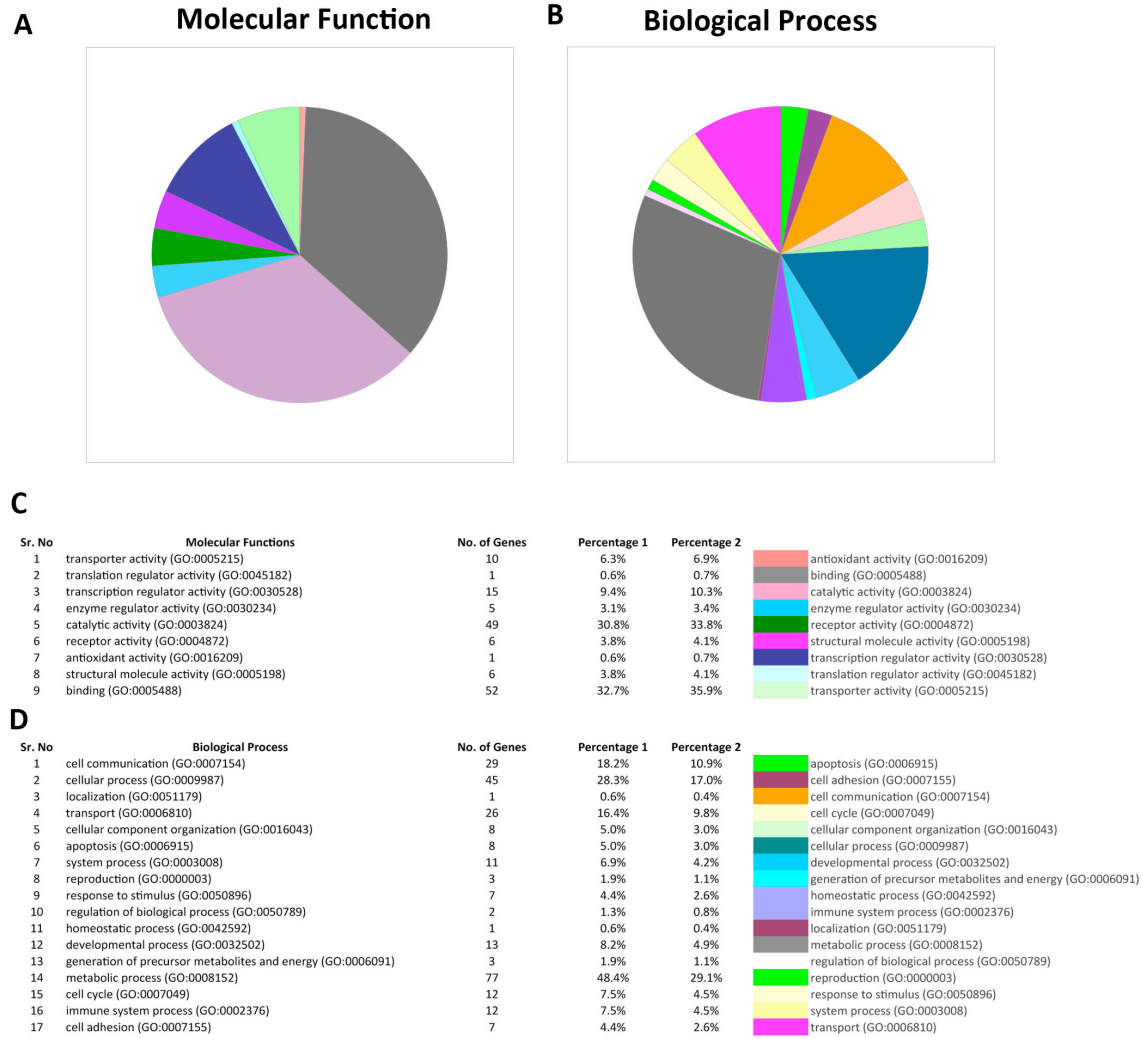| Sr. No	Biological Process	No. of Genes	Percentage 1	Percentage 2	
1	cell communication (GO:0007154)	29	18.2%	10.9%	▮ apoptosis (GO:0006915)
2	cellular process (GO:0009987)	45	28.3%	17.0%	▮ cell adhesion (GO:0007155)
3	localization (GO:0051179)	1	0.6%	0.4%	▮ cell communication (GO:0007154)
4	transport (GO:0006810)	26	16.4%	9.8%	▮ cell cycle (GO:0007049)
5	cellular component organization (GO:0016043)	8	5.0%	3.0%	▮ cellular component organization (GO:0016043)
6	apoptosis (GO:0006915)	8	5.0%	3.0%	▮ cellular process (GO:0009987)
7	system process (GO:0003008)	11	6.9%	4.2%	▮ developmental process (GO:0032502)
8	reproduction (GO:0000003)	3	1.9%	1.1%	▮ generation of precursor metabolites and energy (GO:0006091)
9	response to stimulus (GO:0050896)	7	4.4%	2.6%	▮ homeostatic process (GO:0042592)
10	regulation of biological process (GO:0050789)	2	1.3%	0.8%	▮ immune system process (GO:0002376)
11	homeostatic process (GO:0042592)	1	0.6%	0.4%	▮ localization (GO:0051179)
12	developmental process (GO:0032502)	13	8.2%	4.9%	▮ metabolic process (GO:0008152)
13	generation of precursor metabolites and energy (GO:0006091)	3	1.9%	1.1%	▮ regulation of biological process (GO:0050789)
14	metabolic process (GO:0008152)	77	48.4%	29.1%	▮ reproduction (GO:0000003)
15	cell cycle (GO:0007049)	12	7.5%	4.5%	▮ response to stimulus (GO:0050896)
16	immune system process (GO:0002376)	12	7.5%	4.5%	▮ system process (GO:0003008)
17	cell adhesion (GO:0007155)	7	4.4%	2.6%	▮ transport (GO:0006810)

.

Figure 39: Panther analysis of gene expression profiles. Classification of genes 'downregulated' after hindlimb suspension in mouse soleus MNs (A-B). Guides (legends) to follow the pie charts represented in A, B (C is the legend for A and D is the legend for B). Percentage 1 indicates percent of gene hit against total genes and percentage 2 indicates percent of gene hit against total process hits.

V Discussion

The execution of body movements and maintenance of body posture depends on the structured development and maintenance of the neuromuscular system. Spinal motor neurons (MNs) that control the contraction of innervated skeletal muscle fibers are a part of the final common pathway for execution of body movements (Sherrington, 1904). Spinal MNs are heterogeneous; they can be classified as alpha, beta and gamma-MNs, with alpha-MNs being further subdivided into several functional motor neuron subtypes (FMNTs) namely αFF, αFI, αFR and αS. This diversity, together with the heterogeneity of the innervated muscle fibers, is the basis of the flexibility that allows neuromuscular system to perform a multitude of tasks ranging from breathing to running. The FMNTs can be readily distinguished by electrophysiological techniques (Kernell 2006) and spinal MN physiology indeed provided many key insights into the functioning of nervous system in general. Slow and fast MNs can be distinguished by their different electrophysiological profiles, with slow MNs displaying low rheobase, high input resistance and a long afterhyperpolarization (AHP) half-decay time (Bakels and Kernell, 1993; Gardiner, 1993), and fast MNs displaying high rheobase, low input resistance and a shorter AHP half-decay time (Gardiner, 1993; Zengel et al., 1985). Moreover, the properties of MNs covary with the properties of the innervated muscle fibers (Kernell, 2006). Thus, based on the physiological signature of a given MN, the properties of the motor unit it forms (i.e.: all the muscle fibers it innervate) can be predicted with high accuracy (Gardiner, 1993; Zengel et al., 1985). The initial steps of spinal MN development have been well characterized. Over the past several years, molecular pathways leading to the specification of MN columnar and pool identities that assemble within discrete clusters in the spinal cord and innervate specific muscle groups or individual muscle have been well characterized (Alaynick et al., 2011; Dasen et al., 2003; Sharma and Izpisua Belmonte, 2001; Shirasaki and Pfaff, 2002; Tripodi et al., 2011).

However, how MNs throughout the spinal cord acquire distinctive alpha, beta and gamma or FMNT identities remains elusive. Moreover, knowledge regarding markers and gene signatures of different FMNT populations is rather scarce, apart from a few recent studies which have proposed markers (Err3, Gfra1, 5ht1d) for distinguishing alpha and gamma-MNs and for distinguishing fast (Calca, Chodl) and

slow MNs (Sv2a) (Ashrafi et al., 2012; Chakkalakal et al., 2010; Enjin et al., 2012; Enjin et al., 2010; Friese et al., 2009). However, apart from Sv2a, other recently proposed markers have not yet been studied in correlation with the muscle fibers, and their association with bona fide FMNTs remains to be confirmed. This acute scarcity of stringently established markers currently limits our understanding of FMNT biology. Understanding these molecular profiles, apart from giving insights into functional and/or physiological significance, are important in the context of MN plasticity and diseases like ALS. FMNTs show differential susceptibility towards neurodegeneration in neuromuscular diseases, including ALS, injury or ageing wherein slow MNs are relatively resistant towards degeneration as opposed to the highly susceptible fast MNs (Hegedus et al., 2008; Saxena et al., 2009).

Studies from various model systems have provided evidence that MNs and muscles display adaptive plasticity to elevated neuromuscular activity or lack thereof (Beaumont and Gardiner, 2002; Beaumont and Gardiner, 2003; Cormery et al., 2005). Skeletal muscle is a plastic tissue and displays fiber type transformations depending on the type of neuromuscular perturbation. In general, endurance training (regular usage) promotes fast to slow conversions and hindlimb suspension (HS) promotes slow to fast fiber conversions (Pette, 1998; Pette, 2002; Pette and Staron, 2001; Thayer et al., 2000). However, it should be kept in mind, that the range of these modifications is limited by the intrinsic differences between muscle fiber types (Schiaffino et al., 2007; Talmadge et al., 2004). As the properties of MNs covary with muscle fibers, it may be assumed that when the muscle fiber properties change, the properties of the innervating MNs would also change in a similar fashion to meet the new properties achieved by the muscle. Indeed, electrophysiological studies from various model systems have shown that MNs do change upon altered neuromuscular activity levels. Elegant studies from endurance trained or hindlimb suspended rats have shown that MNs display general and type-specific (FMNT specific- fast or slow specific) adaptations (Gardiner et al., 2005; Gardiner et al., 2006; Gardiner, 2006). For instance, MNs of endurance-trained animals display altered voltage-thresholds for action potential generation indicating their altered excitability. However, not all MNs might be equally affected upon neuromuscular activity alteration (Gardiner, 2006). This emphasizes the importance of studying type-specific MN molecular profiles in addition to generic MN molecular profiles. Additionally, studies aiming to

study generic MN profiles might dilute certain expression differences (depending on muscle alteration paradigm used) owing to the differential responses of FMNTs towards different paradigms. Thus, studying type-specific molecular profiles will yield important insights into the adaptive plasticity displayed by MNs. Studying fast-type specific adaptations and then comparing them to native slow MN profiles would reveal candidates that show a fast-to-slow transition. This has important clinical applications as endurance training was found to be beneficial in mouse models of ALS in terms of motor function and lifespan extension (Carreras et al., 2010; Deforges et al., 2009). Understanding these fast type specific adaptations after exercise might reveal candidates with neuroprotective activities, which could have important implications for therapeutic or rehabilitative measures. To enable all these comparisons, it is important to elucidate native fast/slow profiles as relatively little is known at the molecular level about fast/ slow MN differences. Therefore, I have developed a screen to study native fast/slow profiles and then proceeded with neuromuscular conditioning to study "fast type" specific adaptations with the aim of comparing fast to native slow profiles to identify potential candidates conferring neuroprotection/plasticity.

5.1 Adult FMNT Screen

Despite the wealth of electrophysiological knowledge, little is known about the molecular profiles of FMNTs. One of the reasons for this gap in literature about markers and gene signatures of FMNTs is due to the relative difficulty in labelling and isolating them for gene expression studies, which can be attributed to their scattered organization in a heterogeneous tissue, intermingled with other neuronal and glial cell types. Different types of MNs co-exist in motor pools distributed in the spinal cord and their specific isolation thus proves to be tedious. However, by retrogradely tracing MNs innervating muscles enriched in either fast or slow muscle fibers and combining this with laser capture microdissection and downstream transcriptome analysis, I achieved identification of gene signatures and markers for different FMNTs, including a marker which I could positively identify as a bona fide marker for fast MNs.

The strength and fidelity of the screen are illustrated by the fact that previously proposed markers for slow and fast MNs (Sv2a, Calca and Chodl - identified by alternative approaches) show high enrichment in their respective MNs. Calca and Chodl (Fig. 6C and Fig. 7F, G) are enriched in TA (fast MNs) and Sv2a is enriched in soleus (slow/ αFR) MNs (Fig. 6D and Fig. 7H). Calca and Chodl transcripts are also present at relatively high levels in slow/FR MNs (Fig. 7F and G), which is explained by the presence of fast αFR MNs in soleus motor pool. However, the reliability of Calca as an exclusive fast MN marker has to be thoroughly examined as inconsistencies were reported in assigning it as a bona fide fast MN marker (Kernell et al., 1999; Piehl et al., 1993).

Among the potential slow MN markers I have identified, Cart has been implicated in neuroprotection, e.g. in ischemic brain injury (Chang et al., 2011; Mao et al., 2007). Thus, it is possible that its enrichment in slow MNs could contribute to their relative resistance towards degeneration in ALS. The other potential slow MN marker Nplx has previously been reported to be present in spinal MNs, including presence of Nplx-like immunoreactivity at the neuromuscular junction (Dubessy et al., 2008). With Nplx being implicated in accelerating spontaneous release of acetylcholine at frog NMJ (Brailoiu et al., 2003; Dubessy et al., 2008) suggests a role for Nplx in neuromuscular physiology and its enrichment in putative slow MNs (innervating postural muscles) might be important from the functional aspect, as their synapses are active for long durations. Calchas1 (calcium channel alpha subunit 1) is enriched in slow MNs (2.21 fold and highly significant, discussed later in plasticity section) and may account for easier excitability of these neurons (Cain and Snutch, 2010). *Prkcx* encodes an isoform belonging to the PKC (protein kinase C) family. PKC family plays an important role in neuronal function and plasticity. Ten isoforms of PKCs have been identified so far and several studies have indicated differential tissue expression of these isoforms and for instance, cPKCα is a differentially expressed in the retina and is a marker for rod bipolar neurons (Greferath et al., 1990; Tanaka and Nishizuka, 1994). Thus, enrichment of Prkcx in putative fast MNs (124 fold enriched) suggests its potential to be a marker for fast MNs. However, further studies like the one summarized in Fig. 9 are required to establish it as a bona fide fast MN marker. This screen also identifies Tamnec1 as a putative fast MN marker. Initial screen for its expression pattern in Allen mouse spinal cord atlas hinted at the possibility of it

being a bona fide fast MN marker owing to its scattered expression in ventral horn neurons. Further, it has been reported that the expression of Tamnec1-related members of the matrix metalloproteinase (MMP) family are elevated in spinal cords of the G93A SOD1 ALS mouse model, and that their absence could confer neuroprotection (Kiaei et al., 2007; Soon et al., 2010). This prompted me to examine Tamnec1 expression in greater detail.

5.2 Tamnec1 as a bona fide marker for fast motor neurons

MMPs, including Tamnec1 have been implicated in several pathologies, including neurodegeneration (Rosenberg, 2009). They regulate the extracellular matrix remodelling, and have been proposed to play a role in neuronal plasticity (Kaczmarek et al., 2002). In FMNT screen, Tamnec1 was found to be highly (9. 58 fold) enriched in TA MNs as opposed to soleus MNs. I further confirmed the association of Tamnec1 with bona fide fast MNs by its fulfilment of a defined set of criteria (Fig. 9), including expression at all spinal cord levels (cervical, thoracic, lumbar and sacral), scattered expression by subset of MNs (identified by vAChT immunostaining), absence of association with motor columns or discrete motor pools, its association with large-diameter alpha-MNs (as opposed to small gamma-MNs), and it being highly enriched in fast motor pools (TA and RF MNs) and absent in most soleus MNs (Fig. 11). Interestingly, very few Tamnec1 expressing cells also express very high levels of the gamma-MN marker Err3 (Fig. 14 F, blue arrow). It is therefore, tempting to speculate that these few cells correspond to the rare population of beta-MNs that innervate both, extra and intrafusal muscle fibers, and which can exhibit both, fast or slow-MN properties (Manuel and Zytnicki, 2011). Moreover, using triple immunodetection it is possible to identify (for the first time) 3 classes of MNs in a single spinal cord section: fast MNs (Tamnec1, vAChT and NeuN positive), putative slow MNs (vAChT, NeuN positive, and Tamnec1 negative) and gamma MNs (VAChT positive, Tamnec1 and NeuN negative) (Figure 13). Electrophysiological experiments in adult rats and cats have established that AHP half-decay time is the best predictor of MN type status (Gardiner, 1993; Zengel et al., 1985). However, whether this is a good predictor of adult mouse MN type status is unclear. Analyzing physiological properties of Tamnec1 expressing cells will thus be important in establishing it as a

novel fast MN marker. Proven positive, genetic labelling of Tamnec1 expressing MNs would enable one to study fast MN properties in great detail.
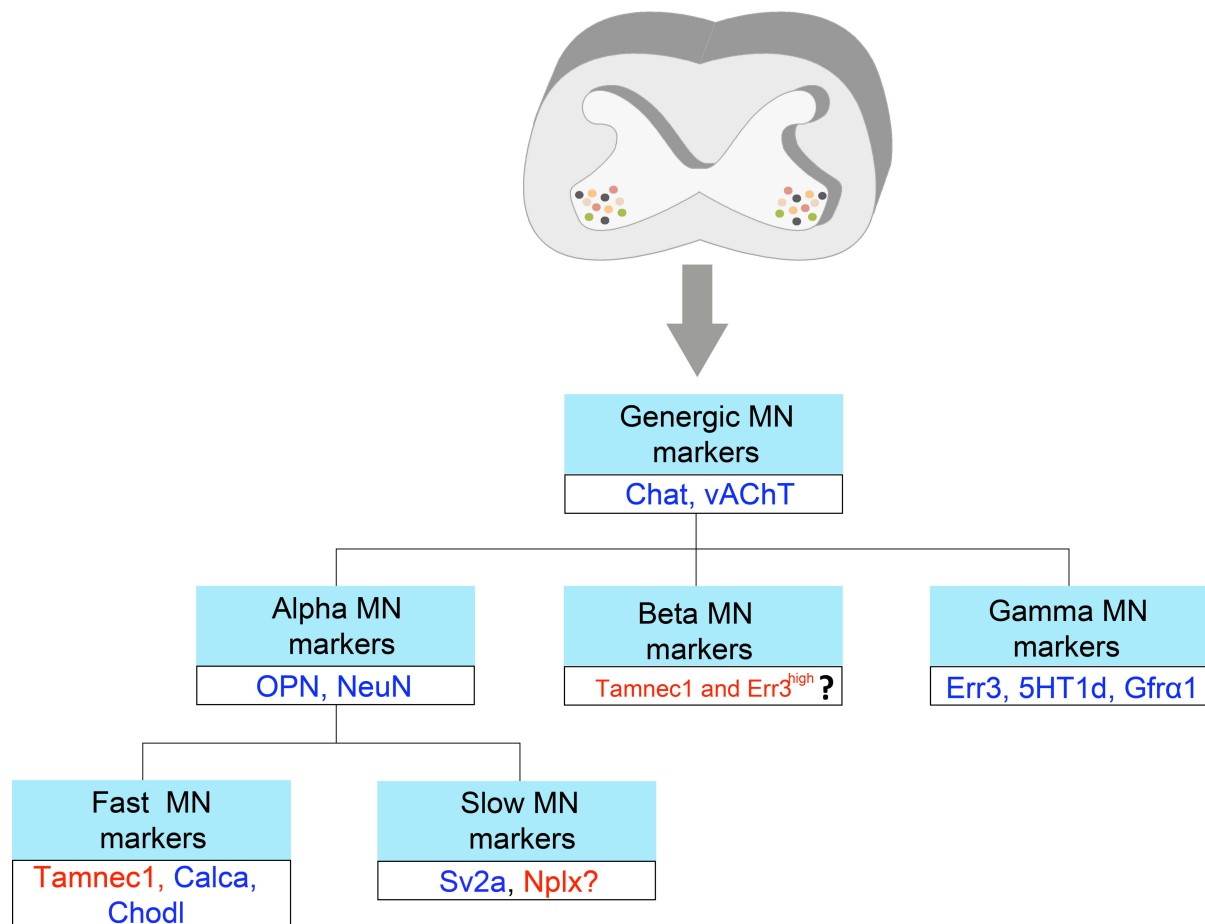

Fig. 40: Summary of motor neuronal markers. Known marker candidates are highlighted in dark blue. Tamnec1 is identified as a novel fast MN marker. Tamnec1 positive and Err3 high MNs may be beta MNs. Nplx is a putative slow MN marker. The candidates identified in this study are highlighted in red.

More specifically, my results hint that Tamnec1 could be type αFF fast MN marker that excludes fast-fatigue resistant (αFR) MNs, since it is absent from a majority of MNs innervating the soleus muscle which is devoid of type IIb fibers, but which contains a high proportion of type IIa fibers. The same interpretation can be derived from the strong association of Tamnec1 expression with MNs innervating the TA and RF muscles, which are highly enriched in type IIb fibers, but contains relatively fewer, type IIa fibers.

However, this interpretation (of being a αFF marker) will have to be experimentally verified with direct fiber type correlation using immunohistochemistry.

Most importantly, the functions normally served by Tamnec1 in fast MNs remain to be elucidated. As mentioned earlier, Tamnec1-related MMPs have been implicated in ALS and my findings that its expression is associated with fast MNs that degenerate early in ALS could indicate a sub-type specific role in disease pathology (Kiaei et al., 2007; Rosenberg, 2009; Saxena et al., 2009; Soon et al., 2010). To understand its possible role in neurodegeneration, however, it will be critical to understand the functions served by Tamnec1 in normal fast MNs. One interesting functional aspect could be its ability to regulate dendritic remodelling as Tamnec1-related MMPs have been shown to be important for dendritic spine morphology and neuronal plasticity (!!! INVALID CITATION !!!; Michaluk et al., 2011). Fast MNs have more dendritic branches as compared to slow MNs and Tamnec1, by facilitating extracellular matrix remodelling may aid in achieving this complexity. Further, MMPs are known to regulate signalling through cleavage of several molecules (receptors, etc) and thus Tamnec1 might influence functional properties of fast MNs in a similar fashion. However, these ideas should be verified experimentally in mouse genetic models. Alternatively, by stable transgenic expression or knock-down of Tamnec1 in chick MNs, coupled with electrophysiological measurements and intraneuronal dye injections will further elucidate the functional role of Tamnec1 in fast MNs.

5.3 Molecular correlates of plasticity in fast motor neurons

The ultimate aim of my thesis research was to identify molecular and functional correlates of MN adaptive plasticity in response to chronically altered physical activity patterns. Because it is established that endurance training promotes a fast-to-slow shift in the properties of both MNs (to a less degree) and muscle (to a high degree), I focused on changes in predominantly fast MNs innervating the TA muscle. I further studied TA muscle transcript profiles along with its MN transcript profile, since downstream comparative analysis would enable understanding of functional matching between components of the neuromuscular circuit. During the course of the work, I was able to develop a strategy to study type-specific MN and muscle adaptations and to validate the candidates obtained from such a screen. The long-term goal will be to genetically alter the verified candidates in mouse models in order to address their respective roles in adjusting neuromuscular output in response to

altered activity levels. *Angptl4*, which I found to be upregulated in TA muscle upon 6 weeks of endurance training, is known to be induced by PPAR and plays a role in lipid metabolism (Hato et al., 2008) . Since exercise is known to improve oxidative metabolism and angiogenesis in the muscle (Gustafsson and Kraus, 2001; Kiens, 2006), upregulation of Angptl4 as an early response towards exercise may be involved in these processes. *Lp1*, which I found to be upregulated in muscle following endurance training, belongs to the family of low density lipoprotein receptor related proteins. A related Lrp appears to function as a co-receptor of agrin during formation of AchR (acetylcholine receptor) clusters during neuromuscular synaptogenesis, including presynaptic differentiation (Wu et al., 2012). This could indicate a role for "Lp1" in adjusting NMJ efficacy in response to endurance training.

My data indicated that 6 week training was not sufficient to induce a wholesale fiber type shift in the muscle. However, a deregulation in levels of Rcan1 might indirectly indicate that muscle fibers are at a stage of fiber remodelling (Oh et al., 2005) owing to its known role in calcineurin signalling pathway. It is therefore an intriguing finding that TA MNs, which were recruited early in the training process as indicated by upregulation of c-Fos, show much more extensive changes in their transcriptional profiles than TA muscle after the same period of endurance training. This suggests that the MNs are highly plastic, possibly reflecting their increased recruitment and activity levels by premotor activity during endurance exercise. Notably, *Prkcx*, which I could identify as a putative fast MN marker, is upregulated by 2.4 fold in fast MNs upon endurance training. Activation of PKCs was shown to induce morphological plasticity in dendrites (Pilpel and Segal, 2004). Further, PKC family members are known to modulate of ion channel activity (Shearman et al., 1989) and an upregulation of Prkcx after endurance training could indicate a similar role of PKCs, for it in shaping fast MN plasticity. Since, I identified *Prkcx* as a putative fast MN marker, an upregulation of it in fast MNs clearly indicates a role for it in subtype specific plasticity (and a functional role in fast MNs) and emphasizes the importance of studying subtype specific plasticity.

Endurance training triggered upregulation of several ion channel transcripts in MNs, suggesting their contribution to altered MN firing, which is seen as an adaptive response towards increased activity (Beaumont and Gardiner, 2003). *Sodchas1* (a

sodium channel alpha- subunit 1), *Potch1* (a potassium channel subunit), *Calchs1* and *Calchas1* (calcium channel subunits) were upregulated following endurance training. All of these channel subunits were reported to contribute to neuronal excitability and firing in other neuron types (Bean, 2007; Cain and Snutch, 2010; Halter et al., 1995). Further, these channel subunits are also implicated MN action potential (Fig. 41) (Brownstone and Stuart, 2011). Modelling data from rats, proposed upregulation of sodium conductance at the AIS, to account for altered electrophysiological profiles seen with endurance training, which could suggest that the observed upregulation of *Sodchas1* could account for these adaptive changes in MN properties (Gardiner et al., 2006). Another channel subunit, Potch1, belongs to the family of calcium-activated potassium channels which contribute to post spike-AHP and are important regulators of neuronal firing (Bean, 2007; Faber and Sah, 2007). Interestingly, MN AHP amplitude was found to be increased in rats post-training (Gardiner, 2006). *Potch1* upregulation in MNs may thus contribute to enhanced motor neuronal firing pattern (i.e. sustained frequency) by modulating AHP, such as the one required to continuously sustain muscle contractions occurring during an endurance training session. Calchas1 belongs to the family of low voltage-activated calcium channels, which were reported to contribute to neuronal excitability and firing (Huguenard, 1996). Further, the expression of related calcium channel currents was reported in early postnatal MNs (Anderson et al., 2012). *Calchas1* is one example of the candidates that show a fast-to-slow shift upon endurance training. It is enriched in slow MNs and post endurance training it is upregulated in fast MNs and this emphasizes a possible important role for Calchas1 in regulating FMNT plasticity. Taken together, these channels may make a trained MN easily excitable (Sodchas1 and Calchas1) and supports it to sustain its firing for relatively long time (Potch1 by contributing to AHP). The above-mentioned channels are all known to be important in regulating spike threshold, depolarization and AHP in other neuronal types, and could thereby directly contribute to the alterations in MN properties induced by chronically altered activity.
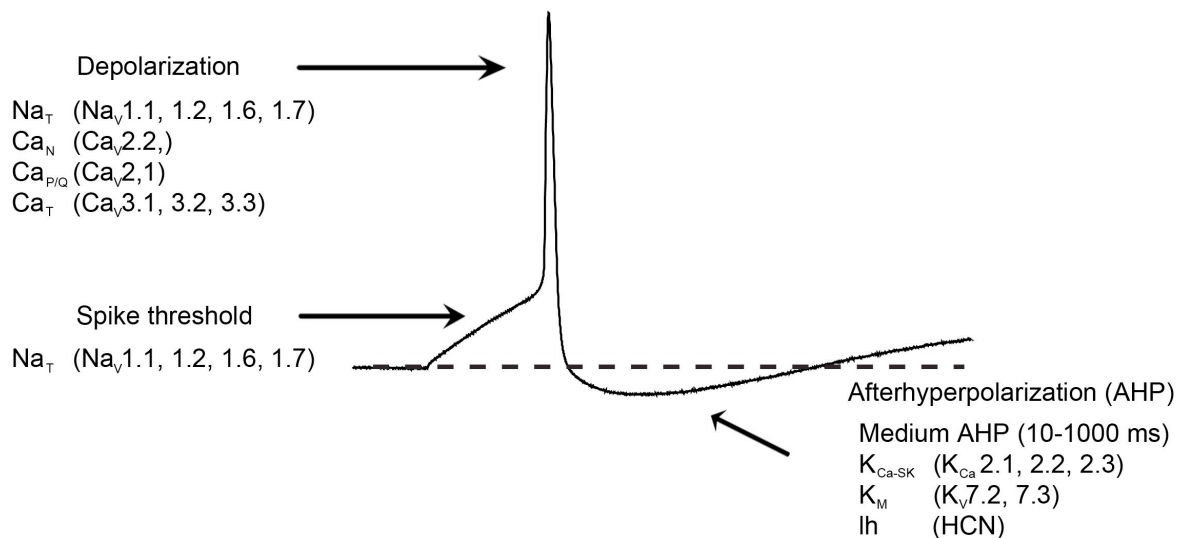
Depolarization

Na_T (Na_V1.1, 1.2, 1.6, 1.7)
Ca_N (Ca_V2.2,)
$Ca_{P/Q}$ (Ca_V2,1)
Ca_T (Ca_V3.1, 3.2, 3.3)

Spike threshold

Na_T (Na_V1.1, 1.2, 1.6, 1.7)

Afterhyperpolarization (AHP)

Medium AHP (10-1000 ms)
K_{Ca-SK} (K_{Ca}2.1, 2.2, 2.3)
K_M (K_V7.2, 7.3)
Ih   (HCN)

Fig. 41: Ion channels proposed to be contributing to the action potential of a generic adult vertebrate spinal motor neuron. Sodchas1 may be involved in regulating spike threshold and depolarization. Calchas1 may be involved in depolarization phase and Potch1 may be important in regulating AHP phase. Modified from, Brownstone RM and Stuart DG 2011.

However, all these interpretations have to be experimentally verified and in this context, the chick embryo system proves to be a good model for comparatively fast and straightforward verification of these channels contribution to motor output. These ion channels can be stably expressed in the embryonic chick MNs by using transposon-based approaches and their contribution to motor neuronal firing can be studied using patch clamp techniques. These functional results will give key insights into the contribution of these channels to neuronal firing. In the long term, generation of conditional mutant mice for these channels and studying their MN properties and neuromuscular performance may further shed light on their role in neuromuscular plasticity. It is noteworthy to mention here that these ion channel transcripts were not differentially regulated in either brain or liver tissue post endurance training. This suggests that these adaptive changes are motor neuron-specific and are not a systemic response towards altered activity.

Pathway analysis of differentially regulated transcripts using DAVID (Database for Annotation, Visualization and Integrated Discovery) revealed the involvement of upregulated transcripts in neurotrophin and MAPK signalling pathways. These observations are interesting in the context of the proposed role for these signalling pathways in regulating MN plasticity (Gardiner, 2006). MAPK and neurotrophin

signalling pathways have been shown to play important role in neuronal plasticity by regulating ion channel subunit expression (Lesser et al., 1997). The upregulation of above-mentioned ion channel transcripts thus may be downstream to these signalling pathways. It is interesting to mention here, that BDNF (brain-derived neurotrophic factor) can alter the excitability of spinal MNs and in the present study I found that its receptor TrkB and several other neurotrophin signalling pathway components are upregulated following endurance training in MNs (Gonzalez and Collins, 1997). However, after 6 weeks of training I haven't seen differential expression of BDNF mRNA in the muscle. However, intraspinal sources cannot be excluded and in fact, BDNF expression was reported to be increased in lumbar spinal cord after exercise (!!! INVALID CITATION !!!; Gomez-Pinilla et al., 2002). These interpretations remain to be verified experimentally. Apart from changes in ion channel transcripts, several transcripts involved in mitochondrial function, transport, etc. are upregulated following endurance exercise (data not shown). Transport related proteins are interesting in the context of the known findings which have shown that axonal transport is improved following endurance training (Jasmin et al., 1988). Taken together, to my knowledge this is the first report describing molecular profiles in fast MNs following chronic endurance training. One study has reported transcriptional profiles of all lumbar MNs following voluntary wheel running (Ferraiuolo et al., 2009). I see no significant overlap between our and their gene profiles and this might be attributed to the different training paradigms and difference in the duration of training (voluntary versus forced training; 3 versus 6 weeks).

5.4 Hindlimb suspension and motor neuronal plasticity

Hindlimb suspension drives fiber transitions in the direction of fast fibers (slow to fast transitions) and decreases the excitability of MNs (Cormery et al., 2005). The present study also shows atrophy and fiber type shift in soleus muscle following 4 weeks of HS and microarray profiling of soleus muscle upon HS revealed the downregulation of slow myosin and upregulation of fast myosin transcripts in accordance with the reported findings. Ingenuity and KEGG (Kyoto encyclopedia of genes and genomes) pathway analysis revealed a mapping of downregulated genes to fatty acid metabolism and PPAR pathways. PPAR signalling has been implicated

in promoting muscle endurance and together, these findings indicate a reduction in the oxidative potential of soleus muscle (which normally uses oxidative metabolism for energy generation) (Bassel-Duby and Olson, 2006; Thomason and Booth, 1990). All these results indicate that soleus muscle is undergoing dramatic changes in fiber type composition and metabolic profile. Similar changes were reported from animals subjected to chronic HS (Thomason and Booth, 1990). While the molecular correlates of plasticity in soleus muscle upon HS is well documented, the molecular correlates of plasticity in soleus MNs remain largely unknown. My screening results indicate that soleus MNs show extensive changes in transcriptional profile following HS. Notably, *Grep1* (growth response gene 1), which I found to be upregulated in MNs following HS is a member of the EGR (early growth response) family of transcriptional-regulatory proteins (O'Donovan et al., 1999). A related member was proposed to confer neuroprotection (Bakalash et al., 2011), and upregulation of Grep1 in MNs following HS might reflect a neuroprotective strategy (owing to the possible loss of trophic support from the atrophying muscle, decreased use). Calcium buffering proteins are known to play a role in neuronal survival and, *Cabuf* (transcript encoding calcium buffer protein) upregulation in MNs following HS might also indicate a survival strategy (Dekkers et al., 2004). Further, deregulation of several transcripts encoding proteins associated with synaptic vesicles (Fig. 37 C and data not shown) following HS indicates that MNs tend to modulate their neurotransmission which might be important in controlling (or a consequence of) muscle atrophy. Moreover, upregulation of transcripts encoding ion channels indicate their possible contribution to altered MN excitability following HS. MNs were shown to reduce their excitability following HS indicating a role for these ion channels in shaping MN excitability (Cormery et al., 2005). Notably, I found *Calchas1* to be significantly downregulated following HS in MNs (data not shown). As mentioned earlier, Calchas1 is enriched in native slow MNs and it was found to be upregulated in fast MNs following endurance training (upregulated after endurance; downregulated after HS). Thus, this downregulation in slow MNs following HS indicates a shift towards fast emphasizing a role for Calchas1 in MN plasticity and function. However, all these interpretations have to be experimentally verified to make a qualified statement. Functional analysis using chick system, introduced earlier offers a good platform to study the functional significance of the deregulated candidates and their contribution to neuromuscular output. To my knowledge, this study is the first to report MN molecular profiles

following HS (and in conditions of decreased neuromuscular use). Further, these findings are interesting in the context of chronically bedridden patients, displaying significant muscle wastage and atrophy and insights into MN plasticity following decreased neuromuscular use might be important to develop interventions counteracting muscle wastage and atrophy (LeBlanc et al., 1992).

All these results (FMNT, endurance training and HS MN screens) indicate that MNs show extensive changes in their transcriptional profiles following neuromuscular perturbation and this study opens the possibility to study FMNT biology (in terms of their native gene profiles, plasticity responses) in unprecedented detail which might in the long run contribute to a better understanding (and treatment) of devastating neurodegenerative disorders like ALS.

VI Outlook

In my thesis research, I could establish molecular correlates of MN functional specification and adaptive plasticity. This work therefore paves the way for studying MN biology and plasticity in great detail. Ongoing work is currently aimed at understanding the functional significance of Tamnec1 expression in the context of fast MNs (establishment of dendritic morphology, etc). I am planning to conduct experiments in chick embryo and gene targeted mice to validate this hypothesis. Characterizing performance of these mice on neuromuscular tasks and elucidating dendritic profiles of MNs will give insights into functional significance of Tamnec1 in fast MNs. Further, correlated electrophysiological characterization and subsequent immunohistochemical analysis (of recorded, dye-filled MNs) will be important for further establishing Tamnec1 as a bona fide fast MN marker. Regarding the novel molecular correlates of MN plasticity, I am currently in the process of characterizing MN output following stable ion channel over expression in chick embryo system. The representative traces from chick MNs are shown in Fig. 42.
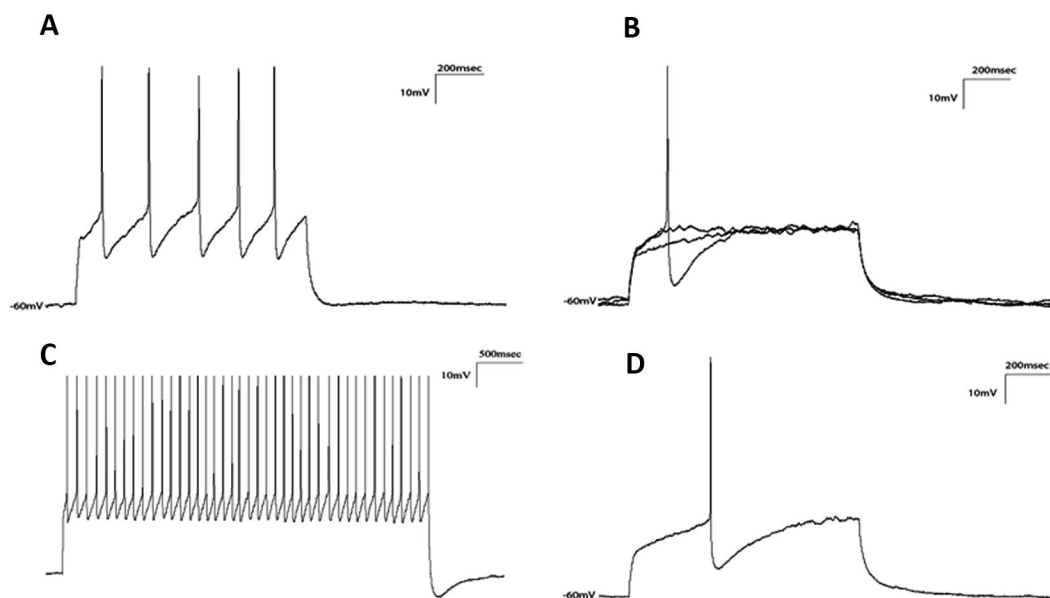
Figure 42: Representative traces from chick spinal motor neurons. Representative traces showing repetitive firing in chick spinal MNs (A and C). Representative traces of action potential at rheobase current injection (B and D).

I am further in the process of verifying ion channel expression at the protein level by using antibodies. Ultimately, mutant mice will be studied to investigate the impacts of reducing (in heterozygous null mutants) or inactivating (in homozygous null mutants) the respective ion channel subunits on MN function, adaptive plasticity and overall neuromuscular performance in endurance tasks. This will give insights at the molecular level into mechanisms mediating MN plasticity. Moreover, using newly available NanoString analysis for detailed study of gene expression, I am planning to characterize genes involved in MAPK, neurotrophin signalling pathways in the context of MN plasticity. Further, it will be interesting to correlate the transcript profiles of MNs with that of the muscles following endurance training to study anterograde/retrograde influences (using comparative pathway analysis). Moreover, it is also necessary to study transcriptional profile of MNs, after achieving fiber type transformations (end state plasticity) using either the extended endurance training paradigm or chronic low frequency stimulation paradigm, and compare it to the present screen (early plasticity). Further, it will be interesting to study the responses of gamma-MNs as well as proprioceptive sensory neurons to altered activity to gain insight into the responses of whole neuromuscular circuit. Upon completion, these studies will contribute to our understanding of MN and neuromuscular biology in great detail. In addition, these studies may ultimately yield insights into the molecular pathways that underlie neuroprotective effects of exercise.

VII Summary

By analyzing gene expression profiles in different FMNTs, identified by their muscle fiber type (TA and soleus), I have found Tamnec1 as a novel marker for fast motor neurons (MNs). Tamnec1 expression was studied at all spinal levels and in motor pools enriched in fast MNs. Tamnec1 expression was found to be relatively specific to motor neurons (a subset of motor neurons) and it showed no column or pool bias in its expression. Further, its expression was enriched in fast motor pools and was found to be absent from majority of motor neurons in the soleus pool indicating its potential to be a fast motor neuronal marker. Apart from this, I have also found gene signatures enriched in different FMNTs and potential markers for slow MNs. Moreover, in the present study it was possible to indirectly identify putative slow MNs based on triple immunodetection experiments. The putative slow motor neurons were vAChT positive, NeuN positive and Tamnec1 negative. This study is the first report of adult FMNT molecular profiles, and will be instrumental in advancing our understanding of FMNT biology.

In the second part of my work, I have screened for potential candidates mediating adaptive MN plasticity following neuromuscular conditioning. I have found several transcripts enriched in endurance trained tibialis anterior (fast) MNs, which may have an important role in conferring plasticity. Ion channels are interesting in the context of their role in regulating neuronal firing and I have found several important ion channel subunits (like Sodchas1 and Potch1) to be upregulated following endurance training. Attributing to their roles in neuronal excitability, this upregulation might be important, in context of neuromuscular plasticity. Further, pathway analysis revealed that the upregulated (in MNs following endurance training) genes participate in MAPK and neurotrophin signalling pathways. These pathways are well established in terms of their contribution to neuronal plasticity, and this study proposes a role for them in mediating MN plasticity following endurance training. I have also studied the transcriptional profile of MNs upon hindlimb suspension (HS), an intervention which is known to promote muscle fiber transitions in an opposite direction as compared to endurance training. These results of the screen indicate, that MNs might upregulate strategies (owing to muscle atrophy seen in HS) to cope with reduced neuromuscular

activity and a possible loss of trophic support from the muscle. The functional assays to validate these interpretations are yet to be undertaken. Moreover, my results also indicate a possible perturbation/deregulation of neurotransmission in HS MNs, which might play a role in counteracting (or is a consequence of) muscle atrophy. Further, I have also studied the muscle transcriptional profiles upon neuromuscular activity alteration with the aim of matching (functional correlation) MN and muscle expression profiles, which might be important in understanding neuromuscular plasticity.

This is the first report of 'type specific' MN responses (on transcriptional level) towards altered neuromuscular activity levels.

Thus, this thesis provides key insights into important aspects of adult FMNT biology (markers, gene signatures and plasticity correlates) which might be important in understanding (and treating) neurodegenerative disorders like amyotrophic lateral sclerosis (ALS).

VIII References

(!!! INVALID CITATION !!!).

Alaynick, W. A., Jessell, T. M. and Pfaff, S. L. (2011). SnapShot: spinal cord development. *Cell* **146**, 178-178 e1.

Alford, E. K., Roy, R. R., Hodgson, J. A. and Edgerton, V. R. (1987). Electromyography of rat soleus, medial gastrocnemius, and tibialis anterior during hind limb suspension. *Exp Neurol* **96**, 635-49.

Anderson, T. M., Abbinanti, M. D., Peck, J. H., Gilmour, M., Brownstone, R. M. and Masino, M. A. (2012). Low-threshold calcium currents contribute to locomotor-like activity in neonatal mice. *J Neurophysiol* **107**, 103-13.

Andonian, M. H. and Fahim, M. A. (1988). Endurance exercise alters the morphology of fast- and slow-twitch rat neuromuscular junctions. *Int J Sports Med* **9**, 218-23.

Arvidsson, U., Riedl, M., Elde, R. and Meister, B. (1997). Vesicular acetylcholine transporter (VAChT) protein: a novel and unique marker for cholinergic neurons in the central and peripheral nervous systems. *J Comp Neurol* **378**, 454-67.

Ashrafi, S., Lalancette-Hebert, M., Friese, A., Sigrist, M., Arber, S., Shneider, N. A. and Kaltschmidt, J. A. (2012). Wnt7A identifies embryonic gamma-motor neurons and reveals early postnatal dependence of gamma-motor neurons on a muscle spindle-derived signal. *J Neurosci* **32**, 8725-31.

Baar, K. (2009). The signaling underlying FITness. *Appl Physiol Nutr Metab* **34**, 411-9.

Bakalash, S., Pham, M., Koronyo, Y., Salumbides, B. C., Kramerov, A., Seidenberg, H., Berel, D., Black, K. L. and Koronyo-Hamaoui, M. (2011). Egr1 expression is induced following glatiramer acetate immunotherapy in rodent models of glaucoma and Alzheimer's disease. *Invest Ophthalmol Vis Sci* **52**, 9033-46.

Bakels, R. and Kernell, D. (1993). Matching between motoneurone and muscle unit properties in rat medial gastrocnemius. *J Physiol* **463**, 307-24.

Bassel-Duby, R. and Olson, E. N. (2006). Signaling pathways in skeletal muscle remodeling. *Annu Rev Biochem* **75**, 19-37.

Bean, B. P. (2007). The action potential in mammalian central neurons. *Nat Rev Neurosci* **8**, 451-65.

Beaumont, E. and Gardiner, P. (2002). Effects of daily spontaneous running on the electrophysiological properties of hindlimb motoneurones in rats. *J Physiol* **540**, 129-38.

Beaumont, E. and Gardiner, P. F. (2003). Endurance training alters the biophysical properties of hindlimb motoneurons in rats. *Muscle Nerve* **27**, 228-36.

Berchtold, M. W., Brinkmeier, H. and Muntener, M. (2000). Calcium ion in skeletal muscle: its crucial role for muscle function, plasticity, and disease. *Physiol Rev* **80**, 1215-65.

Bessou, P., Emonet-Denand, F. and Laporte, Y. (1962a). [Action of fusimotor fibers on the discharge of secondary endings of neuromuscular spindles, in the cat]. *J Physiol (Paris)* **54**, 292-3.

Bessou, P., Emonet-Denand, F. and Laporte, Y. (1962b). [Effects of the stimulation of slow gamma fusimotor fibers on the secondary endings of neuromuscular spindles]. *C R Seances Soc Biol Fil* **156**, 1154-8.

Bessou, P., Emonet-Denand, F. and Laporte, Y. (1965). Motor fibres innervating extrafusal and intrafusal muscle fibres in the cat. *J Physiol* **180**, 649-72.

Blewett, C. and Elder, G. C. (1993). Quantitative EMG analysis in soleus and plantaris during hindlimb suspension and recovery. *J Appl Physiol* **74**, 2057-66.

Bonanomi, D. and Pfaff, S. L. (2010). Motor axon pathfinding. *Cold Spring Harb Perspect Biol* **2**, a001735.

Booth, F. W. and Thomason, D. B. (1991). Molecular and cellular adaptation of muscle in response to exercise: perspectives of various models. *Physiol Rev* **71**, 541-85.

Bostrom, P., Mann, N., Wu, J., Quintero, P. A., Plovie, E. R., Panakova, D., Gupta, R. K., Xiao, C., MacRae, C. A., Rosenzweig, A. et al. (2010). C/EBPbeta controls exercise-induced cardiac growth and protects against pathological cardiac remodeling. *Cell* **143**, 1072-83.

Brailoiu, E., Brailoiu, G. C., Miyamoto, M. D. and Dun, N. J. (2003). The vasoactive peptide urotensin II stimulates spontaneous release from frog motor nerve terminals. *Br J Pharmacol* **138**, 1580-8.

Braun, T. and Gautel, M. (2011). Transcriptional mechanisms regulating skeletal muscle differentiation, growth and homeostasis. *Nat Rev Mol Cell Biol* **12**, 349-61.

Briscoe, J., Pierani, A., Jessell, T. M. and Ericson, J. (2000). A homeodomain protein code specifies progenitor cell identity and neuronal fate in the ventral neural tube. *Cell* **101**, 435-45.

Brock, L. G., Coombs, J. S. and Eccles, J. C. (1952). The recording of potentials from motoneurones with an intracellular electrode. *J Physiol* **117**, 431-60.

Brownstone, R. M. (2006). Beginning at the end: repetitive firing properties in the final common pathway. *Prog Neurobiol* **78**, 156-72.

Brownstone, R. M. and Stuart, D. G. (2011). Whither motoneurons? *Brain Res* **1409**, 93-103.

Buchthal, F. and Schmalbruch, H. (1980). Motor unit of mammalian muscle. *Physiol Rev* **60**, 90-142.

Buller, A. J., Eccles, J. C. and Eccles, R. M. (1960). Interactions between motoneurones and muscles in respect of the characteristic speeds of their responses. *J Physiol* **150**, 417-39.

Burke, R. E., Levine, D. N., Salcman, M. and Tsairis, P. (1974). Motor units in cat soleus muscle: physiological, histochemical and morphological characteristics. *J Physiol* **238**, 503-14.

Burke, R. E., Levine, D. N., Tsairis, P. and Zajac, F. E., 3rd. (1973). Physiological types and histochemical profiles in motor units of the cat gastrocnemius. *J Physiol* **234**, 723-48.

Burke, R. E., Levine, D. N. and Zajac, F. E., 3rd. (1971). Mammalian motor units: physiological-histochemical correlation in three types in cat gastrocnemius. *Science* **174**, 709-12.

Cain, S. M. and Snutch, T. P. (2010). Contributions of T-type calcium channel isoforms to neuronal firing. *Channels (Austin)* **4**, 475-82.

Campbell, W. G., Gordon, S. E., Carlson, C. J., Pattison, J. S., Hamilton, M. T. and Booth, F. W. (2001). Differential global gene expression in red and white skeletal muscle. *Am J Physiol Cell Physiol* **280**, C763-8.

Canepari, M., Cappelli, V., Pellegrino, M. A., Zanardi, M. C. and Reggiani, C. (1998). Thyroid hormone regulation of MHC isoform composition and myofibrillar ATPase activity in rat skeletal muscles. *Arch Physiol Biochem* **106**, 308-15.

Canu, M. H., Falempin, M. and Orsal, D. (2001). Fictive motor activity in rat after 14 days of hindlimb unloading. *Exp Brain Res* **139**, 30-8.

Carreras, I., Yuruker, S., Aytan, N., Hossain, L., Choi, J. K., Jenkins, B. G., Kowall, N. W. and Dedeoglu, A. (2010). Moderate exercise delays the motor performance decline in a transgenic model of ALS. *Brain Res* **1313**, 192-201.

Celio, M. R. and Heizmann, C. W. (1982). Calcium-binding protein parvalbumin is associated with fast contracting muscle fibres. *Nature* **297**, 504-6.

Chakkalakal, J. V., Nishimune, H., Ruas, J. L., Spiegelman, B. M. and Sanes, J. R. (2010). Retrograde influence of muscle fibers on their innervation revealed by a novel marker for slow motoneurons. *Development* **137**, 3489-99.

Chang, L., Chen, Y., Li, J., Liu, Z., Wang, Z., Chen, J., Cao, W. and Xu, Y. (2011). Cocaine-and amphetamine-regulated transcript modulates peripheral immunity and protects against brain injury in experimental stroke. *Brain Behav Immun* **25**, 260-9.

Chin, E. R. and Allen, D. G. (1996). The role of elevations in intracellular [Ca2+] in the development of low frequency fatigue in mouse single muscle fibres. *J Physiol* **491 (Pt 3)**, 813-24.

Cormery, B., Beaumont, E., Csukly, K. and Gardiner, P. (2005). Hindlimb unweighting for 2 weeks alters physiological properties of rat hindlimb motoneurones. *J Physiol* **568**, 841-50.

Cormery, B., Marini, J. F. and Gardiner, P. F. (2000). Changes in electrophysiological properties of tibial motoneurones in the rat following 4 weeks of tetrodotoxin-induced paralysis. *Neuroscience Letters* **287**, 21-4.

Cotel, F., Antri, M., Barthe, J. Y. and Orsal, D. (2009). Identified ankle extensor and flexor motoneurons display different firing profiles in the neonatal rat. *J Neurosci* **29**, 2748-53.

Cotman, C. W. and Berchtold, N. C. (2002). Exercise: a behavioral intervention to enhance brain health and plasticity. *Trends Neurosci* **25**, 295-301.

Cotman, C. W. and Engesser-Cesar, C. (2002). Exercise enhances and protects brain function. *Exerc Sport Sci Rev* **30**, 75-9.

Cros, N., Muller, J., Bouju, S., Pietu, G., Jacquet, C., Leger, J. J., Marini, J. F. and Dechesne, C. A. (1999). Upregulation of M-creatine kinase and glyceraldehyde3-phosphate dehydrogenase: two markers of muscle disuse. *Am J Physiol* **276**, R308-16.

Da Cruz, S., Parone, P. A., Lopes, V. S., Lillo, C., McAlonis-Downes, M., Lee, S. K., Vetto, A. P., Petrosyan, S., Marsala, M., Murphy, A. N. et al. (2012). Elevated PGC-1alpha activity sustains mitochondrial biogenesis and muscle function without extending survival in a mouse model of inherited ALS. *Cell Metab* **15**, 778-86.

Dasen, J. S., Liu, J. P. and Jessell, T. M. (2003). Motor neuron columnar fate imposed by sequential phases of Hox-c activity. *Nature* **425**, 926-33.

Deforges, S., Branchu, J., Biondi, O., Grondard, C., Pariset, C., Lecolle, S., Lopes, P., Vidal, P. P., Chanoine, C. and Charbonnier, F. (2009). Motoneuron survival is promoted by specific exercise in a mouse model of amyotrophic lateral sclerosis. *J Physiol* **587**, 3561-72.

Dekkers, J., Bayley, P., Dick, J. R., Schwaller, B., Berchtold, M. W. and Greensmith, L. (2004). Over-expression of parvalbumin in transgenic mice rescues motoneurons from injury-induced cell death. *Neuroscience* **123**, 459-66.

Delp, M. D. and Duan, C. (1996). Composition and size of type I, IIA, IID/X, and IIB fibers and citrate synthase activity of rat muscle. *J Appl Physiol* **80**, 261-70.

Desaphy, J. F., Pierno, S., Leoty, C., George, A. L., Jr., De Luca, A. and Camerino, D. C. (2001). Skeletal muscle disuse induces fibre type-dependent enhancement of Na(+) channel expression. *Brain* **124**, 1100-13.

Desaulniers, P., Lavoie, P. A. and Gardiner, P. F. (2001). Habitual exercise enhances neuromuscular transmission efficacy of rat soleus muscle in situ. *J Appl Physiol* **90**, 1041-8.

Deschenes, M. R., Maresh, C. M., Crivello, J. F., Armstrong, L. E., Kraemer, W. J. and Covault, J. (1993). The effects of exercise training of different intensities on neuromuscular junction morphology. *J Neurocytol* **22**, 603-15.

Deschenes, M. R., Tenny, K. A. and Wilson, M. H. (2006). Increased and decreased activity elicits specific morphological adaptations of the neuromuscular junction. *Neuroscience* **137**, 1277-83.

Desplanches, D., Kayar, S. R., Sempore, B., Flandrois, R. and Hoppeler, H. (1990). Rat soleus muscle ultrastructure after hindlimb suspension. *J Appl Physiol* **69**, 504-8.

Dorlochter, M., Irintchev, A., Brinkers, M. and Wernig, A. (1991). Effects of enhanced activity on synaptic transmission in mouse extensor digitorum longus muscle. *J Physiol* **436**, 283-92.

Dubessy, C., Cartier, D., Lectez, B., Bucharles, C., Chartrel, N., Montero-Hadjadje, M., Bizet, P., Chatenet, D., Tostivint, H., Scalbert, E. et al. (2008). Characterization of urotensin II, distribution of urotensin II, urotensin II-related peptide and UT receptor mRNAs in mouse: evidence of urotensin II at the neuromuscular junction. *J Neurochem* **107**, 361-74.

Edstrom, L. and Grimby, L. (1986). Effect of exercise on the motor unit. *Muscle Nerve* **9**, 104-26.

Edstrom, L. and Kugelberg, E. (1968). Histochemical composition, distribution of fibres and fatiguability of single motor units. Anterior tibial muscle of the rat. *J Neurol Neurosurg Psychiatry* **31**, 424-33.

Elder, G. C. and McComas, A. J. (1987). Development of rat muscle during short- and long-term hindlimb suspension. *J Appl Physiol* **62**, 1917-23.

Enjin, A., Leao, K. E., Mikulovic, S., Le Merre, P., Tourtellotte, W. G. and Kullander, K. (2012). Sensorimotor function is modulated by the serotonin receptor 1d, a novel marker for gamma motor neurons. *Mol Cell Neurosci* **49**, 322-32.

Enjin, A., Rabe, N., Nakanishi, S. T., Vallstedt, A., Gezelius, H., Memic, F., Lind, M., Hjalt, T., Tourtellotte, W. G., Bruder, C. et al. (2010). Identification of novel spinal cholinergic genetic subtypes disclose Chodl and Pitx2 as markers for fast motor neurons and partition cells. *J Comp Neurol* **518**, 2284-304.

Espina, V., Wulfkuhle, J. D., Calvert, V. S., VanMeter, A., Zhou, W., Coukos, G., Geho, D. H., Petricoin, E. F., 3rd and Liotta, L. A. (2006). Laser-capture microdissection. *Nat Protoc* **1**, 586-603.

Faber, E. S. and Sah, P. (2007). Functions of SK channels in central neurons. *Clin Exp Pharmacol Physiol* **34**, 1077-83.

Ferraiuolo, L., De Bono, J. P., Heath, P. R., Holden, H., Kasher, P., Channon, K. M., Kirby, J. and Shaw, P. J. (2009). Transcriptional response of the neuromuscular

system to exercise training and potential implications for ALS. *J Neurochem* **109**, 1714-24.

Fitts, R. H., Riley, D. R. and Widrick, J. J. (2001). Functional and structural adaptations of skeletal muscle to microgravity. *J Exp Biol* **204**, 3201-8.

Fitts, R. H., Winder, W. W., Brooke, M. H., Kaiser, K. K. and Holloszy, J. O. (1980). Contractile, biochemical, and histochemical properties of thyrotoxic rat soleus muscle. *Am J Physiol* **238**, C14-20.

Flavell, S. W. and Greenberg, M. E. (2008). Signaling mechanisms linking neuronal activity to gene expression and plasticity of the nervous system. *Annu Rev Neurosci* **31**, 563-90.

Fox, M. A., Sanes, J. R., Borza, D. B., Eswarakumar, V. P., Fassler, R., Hudson, B. G., John, S. W., Ninomiya, Y., Pedchenko, V., Pfaff, S. L. et al. (2007). Distinct target-derived signals organize formation, maturation, and maintenance of motor nerve terminals. *Cell* **129**, 179-93.

Friese, A., Kaltschmidt, J. A., Ladle, D. R., Sigrist, M., Jessell, T. M. and Arber, S. (2009). Gamma and alpha motor neurons distinguished by expression of transcription factor Err3. *Proc Natl Acad Sci U S A* **106**, 13588-93.

Fujioka, H., Dairyo, Y., Yasunaga, K. and Emoto, K. (2012). Neural functions of matrix metalloproteinases: plasticity, neurogenesis, and disease. *Biochem Res Int* **2012**, 789083.

Gardiner, P., Beaumont, E. and Cormery, B. (2005). Motoneurones "learn" and "forget" physical activity. *Can J Appl Physiol* **30**, 352-70.

Gardiner, P., Dai, Y. and Heckman, C. J. (2006). Effects of exercise training on alpha-motoneurons. *J Appl Physiol* **101**, 1228-36.

Gardiner, P. F. (1993). Physiological properties of motoneurons innervating different muscle unit types in rat gastrocnemius. *J Neurophysiol* **69**, 1160-70.

Gardiner, P. F. (2006). Changes in alpha-motoneuron properties with altered physical activity levels. *Exerc Sport Sci Rev* **34**, 54-8.

Gazula, V. R., Roberts, M., Luzzio, C., Jawad, A. F. and Kalb, R. G. (2004). Effects of limb exercise after spinal cord injury on motor neuron dendrite structure. *J Comp Neurol* **476**, 130-45.

Gharakhanlou, R., Chadan, S. and Gardiner, P. (1999). Increased activity in the form of endurance training increases calcitonin gene-related peptide content in lumbar motoneuron cell bodies and in sciatic nerve in the rat. *Neuroscience* **89**, 1229-39.

Gomes da Silva, S., Unsain, N., Masco, D. H., Toscano-Silva, M., de Amorim, H. A., Silva Araujo, B. H., Simoes, P. S., Naffah-Mazzacoratti Mda, G., Mortara, R. A., Scorza, F. A. et al. (2012). Early exercise promotes positive hippocampal

plasticity and improves spatial memory in the adult life of rats. *Hippocampus* **22**, 347-58.

Gomez-Pinilla, F., Ying, Z., Roy, R. R., Molteni, R. and Edgerton, V. R. (2002). Voluntary exercise induces a BDNF-mediated mechanism that promotes neuroplasticity. *J Neurophysiol* **88**, 2187-95.

Gonzalez, M. and Collins, W. F., 3rd. (1997). Modulation of motoneuron excitability by brain-derived neurotrophic factor. *J Neurophysiol* **77**, 502-6.

Gordon, T., Tyreman, N., Rafuse, V. F. and Munson, J. B. (1997). Fast-to-slow conversion following chronic low-frequency activation of medial gastrocnemius muscle in cats. I. Muscle and motor unit properties. *J Neurophysiol* **77**, 2585-604.

Goulding, M. (2009). Circuits controlling vertebrate locomotion: moving in a new direction. *Nat Rev Neurosci* **10**, 507-18.

Gramsbergen, A., Ijkema-Paassen, J., Westerga, J. and Geisler, H. C. (1996). Dendrite bundles in motoneuronal pools of trunk and extremity muscles in the rat. *Exp Neurol* **137**, 34-42.

Greferath, U., Grunert, U. and Wassle, H. (1990). Rod bipolar cells in the mammalian retina show protein kinase C-like immunoreactivity. *J Comp Neurol* **301**, 433-42.

Grondard, C., Biondi, O., Pariset, C., Lopes, P., Deforges, S., Lecolle, S., Gaspera, B. D., Gallien, C. L., Chanoine, C. and Charbonnier, F. (2008). Exercise-induced modulation of calcineurin activity parallels the time course of myofibre transitions. *J Cell Physiol* **214**, 126-35.

Gupta, R. C., Misulis, K. E. and Dettbarn, W. D. (1985). Changes in the cholinergic system of rat sciatic nerve and skeletal muscle following suspension-induced disuse. *Exp Neurol* **89**, 622-33.

Gustafsson, T. and Kraus, W. E. (2001). Exercise-induced angiogenesis-related growth and transcription factors in skeletal muscle, and their modification in muscle pathology. *Front Biosci* **6**, D75-89.

Haddad, F., Qin, A. X., Zeng, M., McCue, S. A. and Baldwin, K. M. (1998). Interaction of hyperthyroidism and hindlimb suspension on skeletal myosin heavy chain expression. *J Appl Physiol* **85**, 2227-36.

Halter, J. A., Carp, J. S. and Wolpaw, J. R. (1995). Operantly conditioned motoneuron plasticity: possible role of sodium channels. *J Neurophysiol* **73**, 867-71.

Han, P., Nakanishi, S. T., Tran, M. A. and Whelan, P. J. (2007). Dopaminergic modulation of spinal neuronal excitability. *J Neurosci* **27**, 13192-204.

Hashimoto, K., Hayashi, Y., Inuzuka, T. and Hozumi, I. (2009). Exercise induces metallothioneins in mouse spinal cord. *Neuroscience* **163**, 244-51.

Hato, T., Tabata, M. and Oike, Y. (2008). The role of angiopoietin-like proteins in angiogenesis and metabolism. *Trends Cardiovasc Med* **18**, 6-14.

Heckman, C. J., Mottram, C., Quinlan, K., Theiss, R. and Schuster, J. (2009). Motoneuron excitability: the importance of neuromodulatory inputs. *Clin Neurophysiol* **120**, 2040-54.

Hegedus, J., Putman, C. T., Tyreman, N. and Gordon, T. (2008). Preferential motor unit loss in the SOD1 G93A transgenic mouse model of amyotrophic lateral sclerosis. *J Physiol* **586**, 3337-51.

Huang da, W., Sherman, B. T. and Lempicki, R. A. (2009a). Bioinformatics enrichment tools: paths toward the comprehensive functional analysis of large gene lists. *Nucleic Acids Res* **37**, 1-13.

Huang da, W., Sherman, B. T. and Lempicki, R. A. (2009b). Systematic and integrative analysis of large gene lists using DAVID bioinformatics resources. *Nat Protoc* **4**, 44-57.

Huguenard, J. R. (1996). Low-threshold calcium currents in central nervous system neurons. *Annu Rev Physiol* **58**, 329-48.

Hultborn, H. and Kiehn, O. (1992). Neuromodulation of vertebrate motor neuron membrane properties. *Curr Opin Neurobiol* **2**, 770-5.

Inglis, F. M., Zuckerman, K. E. and Kalb, R. G. (2000). Experience-dependent development of spinal motor neurons. *Neuron* **26**, 299-305.

Ishihara, A., Naitoh, H., Araki, H. and Nishihira, Y. (1988). Soma size and oxidative enzyme activity of motoneurones supplying the fast twitch and slow twitch muscles in the rat. *Brain Res* **446**, 195-8.

Jasmin, B. J., Lavoie, P. A. and Gardiner, P. F. (1987). Fast axonal transport of acetylcholinesterase in rat sciatic motoneurons is enhanced following prolonged daily running, but not following swimming. *Neuroscience Letters* **78**, 156-60.

Jasmin, B. J., Lavoie, P. A. and Gardiner, P. F. (1988). Fast axonal transport of labeled proteins in motoneurons of exercise-trained rats. *Am J Physiol* **255**, C731-6.
Jessell, T. M. (2000). Neuronal specification in the spinal cord: inductive signals and transcriptional codes. *Nat Rev Genet* **1**, 20-9.

Jurata, L. W., Thomas, J. B. and Pfaff, S. L. (2000). Transcriptional mechanisms in the development of motor control. *Curr Opin Neurobiol* **10**, 72-9.

Kaczmarek, L., Lapinska-Dzwonek, J. and Szymczak, S. (2002). Matrix metalloproteinases in the adult brain physiology: a link between c-Fos, AP-1 and remodeling of neuronal connections? *EMBO J* **21**, 6643-8.

Kanehisa, M. and Goto, S. (2000). KEGG: kyoto encyclopedia of genes and genomes. *Nucleic Acids Res* **28**, 27-30.

Kang, C. M., Lavoie, P. A. and Gardiner, P. F. (1995). Chronic exercise increases SNAP-25 abundance in fast-transported proteins of rat motoneurones. *Neuroreport* **6**, 549-53.

Kanning, K. C., Kaplan, A. and Henderson, C. E. (2010). Motor neuron diversity in development and disease. *Annu Rev Neurosci* **33**, 409-40.

Kernell, D. (2003). Principles of force gradation in skeletal muscles. *Neural Plast* **10**, 69-76.

Kernell, D., Bakels, R. and Copray, J. C. (1999). Discharge properties of motoneurones: how are they matched to the properties and use of their muscle units? *J Physiol Paris* **93**, 87-96.

Kernell, D. and Monster, A. W. (1982). Motoneurone properties and motor fatigue. An intracellular study of gastrocnemius motoneurones of the cat. *Exp Brain Res* **46**, 197-204.

Kiaei, M., Kipiani, K., Calingasan, N. Y., Wille, E., Chen, J., Heissig, B., Rafii, S., Lorenzl, S. and Beal, M. F. (2007). Matrix metalloproteinase-9 regulates TNF-alpha and FasL expression in neuronal, glial cells and its absence extends life in a transgenic mouse model of amyotrophic lateral sclerosis. *Exp Neurol* **205**, 74-81.

Kiens, B. (2006). Skeletal muscle lipid metabolism in exercise and insulin resistance. *Physiol Rev* **86**, 205-43.

Kuffler, S. W. and Hunt, C. C. (1952). The mammalian small-nerve fibers: a system for efferent nervous regulation of muscle spindle discharge. *Res Publ Assoc Res Nerv Ment Dis* **30**, 24-47.

Kugelberg, E. (1976). Adaptive transformation of rat soleus motor units during growth. *J Neurol Sci* **27**, 269-89.

LeBlanc, A. D., Schneider, V. S., Evans, H. J., Pientok, C., Rowe, R. and Spector, E. (1992). Regional changes in muscle mass following 17 weeks of bed rest. *J Appl Physiol* **73**, 2172-8.

Lee, R. H. and Heckman, C. J. (1998a). Bistability in spinal motoneurons in vivo: systematic variations in persistent inward currents. *J Neurophysiol* **80**, 583-93.

Lee, R. H. and Heckman, C. J. (1998b). Bistability in spinal motoneurons in vivo: systematic variations in rhythmic firing patterns. *J Neurophysiol* **80**, 572-82.

Lee, S. K. and Pfaff, S. L. (2001). Transcriptional networks regulating neuronal identity in the developing spinal cord. *Nat Neurosci* **4 Suppl**, 1183-91.

Lesser, S. S., Sherwood, N. T. and Lo, D. C. (1997). Neurotrophins differentially regulate voltage-gated ion channels. *Mol Cell Neurosci* **10**, 173-83.

Leuner, B. and Gould, E. (2010). Structural plasticity and hippocampal function. *Annu Rev Psychol* **61**, 111-40, C1-3.

MacDonell, C. W., Button, D. C., Beaumont, E., Cormery, B. and Gardiner, P. F. (2012). Plasticity of rat motoneuron rhythmic firing properties with varying levels of afferent and descending inputs. *J Neurophysiol* **107**, 265-72.

Manuel, M. and Zytnicki, D. (2011). Alpha, beta and gamma motoneurons: functional diversity in the motor system's final pathway. *J Integr Neurosci* **10**, 243-76.

Mao, P., Ardeshiri, A., Jacks, R., Yang, S., Hurn, P. D. and Alkayed, N. J. (2007). Mitochondrial mechanism of neuroprotection by CART. *Eur J Neurosci* **26**, 624-32.

McComas, A. J. and Thomas, H. C. (1968). Fast and slow twitch muscles in man. *J Neurol Sci* **7**, 301-7.

McDonagh, J. C., Binder, M. D., Reinking, R. M. and Stuart, D. G. (1980). Tetrapartite classification of motor units of cat tibialis posterior. *J Neurophysiol* **44**, 696-712.

McHanwell, S. and Biscoe, T. J. (1981). The localization of motoneurons supplying the hindlimb muscles of the mouse. *Philos Trans R Soc Lond B Biol Sci* **293**, 477-508.

Michaluk, P., Wawrzyniak, M., Alot, P., Szczot, M., Wyrembek, P., Mercik, K., Medvedev, N., Wilczek, E., De Roo, M., Zuschratter, W. et al. (2011). Influence of matrix metalloproteinase MMP-9 on dendritic spine morphology. *J Cell Sci* **124**, 3369-80.

Misawa, H., Hara, M., Tanabe, S., Niikura, M., Moriwaki, Y. and Okuda, T. (2012). Osteopontin is an alpha motor neuron marker in the mouse spinal cord. *J Neurosci Res* **90**, 732-42.

Molkentin, J. D. and Olson, E. N. (1996). Defining the regulatory networks for muscle development. *Curr Opin Genet Dev* **6**, 445-53.

Morey-Holton, E. R. and Globus, R. K. (2002). Hindlimb unloading rodent model: technical aspects. *J Appl Physiol* **92**, 1367-77.

Munson, J. B., Foehring, R. C., Mendell, L. M. and Gordon, T. (1997). Fast-to-slow conversion following chronic low-frequency activation of medial gastrocnemius muscle in cats. II. Motoneuron properties. *J Neurophysiol* **77**, 2605-15.

Muramoto, T., Mendelson, B., Phelan, K. D., Garcia-Rill, E., Skinner, R. D. and Puskarich-May, C. (1996). Developmental changes in the effects of serotonin and N-methyl-D-aspartate on intrinsic membrane properties of embryonic chick motoneurons. *Neuroscience* **75**, 607-18.

Narkar, V. A., Downes, M., Yu, R. T., Embler, E., Wang, Y. X., Banayo, E., Mihaylova, M. M., Nelson, M. C., Zou, Y., Juguilon, H. et al. (2008). AMPK and PPARdelta agonists are exercise mimetics. *Cell* **134**, 405-15.

Narkar, V. A., Fan, W., Downes, M., Yu, R. T., Jonker, J. W., Alaynick, W. A., Banayo, E., Karunasiri, M. S., Lorca, S. and Evans, R. M. (2011). Exercise and

PGC-1alpha-independent synchronization of type I muscle metabolism and vasculature by ERRgamma. *Cell Metab* **13**, 283-93.

O'Donovan, K. J., Tourtellotte, W. G., Millbrandt, J. and Baraban, J. M. (1999). The EGR family of transcription-regulatory factors: progress at the interface of molecular and systems neuroscience. *Trends Neurosci* **22**, 167-73.

Ogborn, D. I. and Gardiner, P. F. (2010). Effects of exercise and muscle type on BDNF, NT-4/5, and TrKB expression in skeletal muscle. *Muscle Nerve* **41**, 385-91.

Oh, M., Rybkin, II, Copeland, V., Czubryt, M. P., Shelton, J. M., van Rooij, E., Richardson, J. A., Hill, J. A., De Windt, L. J., Bassel-Duby, R. et al. (2005). Calcineurin is necessary for the maintenance but not embryonic development of slow muscle fibers. *Mol Cell Biol* **25**, 6629-38.

Parnow, A., Gharakhanlou, R., Gorginkaraji, Z., Rajabi, S., Eslami, R., Hedayati, M. and Mahdian, R. (2012). Effects of endurance and resistance training on calcitonin gene-related Peptide and acetylcholine receptor at slow and fast twitch skeletal muscles and sciatic nerve in male wistar rats. *Int J Pept* **2012**, 962651.

Pedersen, B. K. and Febbraio, M. A. (2008). Muscle as an endocrine organ: focus on muscle-derived interleukin-6. *Physiol Rev* **88**, 1379-406.

Pette, D. (1985). Metabolic heterogeneity of muscle fibres. *J Exp Biol* **115**, 179-89.
Pette, D. (1998). Training effects on the contractile apparatus. *Acta Physiol Scand* **162**, 367-76.

Pette, D. (2001). Historical Perspectives: plasticity of mammalian skeletal muscle. *J Appl Physiol* **90**, 1119-24.

Pette, D. (2002). The adaptive potential of skeletal muscle fibers. *Can J Appl Physiol* **27**, 423-48.

Pette, D. and Spamer, C. (1986). Metabolic properties of muscle fibers. *Fed Proc* **45**, 2910-4.

Pette, D. and Staron, R. S. (1990). Cellular and molecular diversities of mammalian skeletal muscle fibers. *Rev Physiol Biochem Pharmacol* **116**, 1-76.

Pette, D. and Staron, R. S. (1997). Mammalian skeletal muscle fiber type transitions. *Int Rev Cytol* **170**, 143-223.

Pette, D. and Staron, R. S. (2001). Transitions of muscle fiber phenotypic profiles. *Histochem Cell Biol* **115**, 359-72.

Piehl, F., Arvidsson, U., Hokfelt, T. and Cullheim, S. (1993). Calcitonin gene-related peptide-like immunoreactivity in motoneuron pools innervating different hind limb muscles in the rat. *Exp Brain Res* **96**, 291-303.

Pilpel, Y. and Segal, M. (2004). Activation of PKC induces rapid morphological plasticity in dendrites of hippocampal neurons via Rac and Rho-dependent mechanisms. *Eur J Neurosci* **19**, 3151-64.

Pogozelski, A. R., Geng, T., Li, P., Yin, X., Lira, V. A., Zhang, M., Chi, J. T. and Yan, Z. (2009). p38gamma mitogen-activated protein kinase is a key regulator in skeletal muscle metabolic adaptation in mice. *PLoS One* **4**, e7934.

Pun, S., Santos, A. F., Saxena, S., Xu, L. and Caroni, P. (2006). Selective vulnerability and pruning of phasic motoneuron axons in motoneuron disease alleviated by CNTF. *Nat Neurosci* **9**, 408-19.

Quiat, D., Voelker, K. A., Pei, J., Grishin, N. V., Grange, R. W., Bassel-Duby, R. and Olson, E. N. (2011). Concerted regulation of myofiber-specific gene expression and muscle performance by the transcriptional repressor Sox6. *Proc Natl Acad Sci U S A* **108**, 10196-201.

Rafuse, V. F., Milner, L. D. and Landmesser, L. T. (1996). Selective innervation of fast and slow muscle regions during early chick neuromuscular development. *J Neurosci* **16**, 6864-77.

Rattner, B. A., Michael, S. D. and Altland, P. D. (1980). Plasma concentrations of hypophyseal hormones and corticosterone in male mice acutely exposed to simulated high altitude. *Proc Soc Exp Biol Med* **163**, 367-71.

Reid, B., Slater, C. R. and Bewick, G. S. (1999). Synaptic vesicle dynamics in rat fast and slow motor nerve terminals. *J Neurosci* **19**, 2511-21.

Ren, J. C., Fan, X. L., Song, X. A., Zhao, X. H., Chen, M. X. and Shi, L. (2012). Prolonged hindlimb unloading leads to changes in electrophysiological properties of L5 dorsal root ganglion neurons in rats after 14 days. *Muscle Nerve* **45**, 65-9.

Rexed, B. (1952). The cytoarchitectonic organization of the spinal cord in the cat. *J Comp Neurol* **96**, 414-95.

Rosenberg, G. A. (2009). Matrix metalloproteinases and their multiple roles in neurodegenerative diseases. *Lancet Neurol* **8**, 205-16.

Rossi, A. C., Mammucari, C., Argentini, C., Reggiani, C. and Schiaffino, S. (2010). Two novel/ancient myosins in mammalian skeletal muscles: MYH14/7b and MYH15 are expressed in extraocular muscles and muscle spindles. *J Physiol* **588**, 353-64.

Roy, R. R., Gilliam, T. B., Taylor, J. F. and Heusner, W. W. (1983). Activity-induced morphologic changes in rat soleus nerve. *Exp Neurol* **80**, 622-32.

Safdar, A., Abadi, A., Akhtar, M., Hettinga, B. P. and Tarnopolsky, M. A. (2009). miRNA in the regulation of skeletal muscle adaptation to acute endurance exercise in C57Bl/6J male mice. *PLoS One* **4**, e5610.

Saxena, S., Cabuy, E. and Caroni, P. (2009). A role for motoneuron subtype-selective ER stress in disease manifestations of FALS mice. *Nat Neurosci* **12**, 627-36.

Saxena, S. and Caroni, P. (2011). Selective neuronal vulnerability in neurodegenerative diseases: from stressor thresholds to degeneration. *Neuron* **71**, 35-48.

Schiaffino, S. and Reggiani, C. (1994). Myosin isoforms in mammalian skeletal muscle. *J Appl Physiol* **77**, 493-501.

Schiaffino, S. and Reggiani, C. (1996). Molecular diversity of myofibrillar proteins: gene regulation and functional significance. *Physiol Rev* **76**, 371-423.

Schiaffino, S. and Reggiani, C. (2011). Fiber types in mammalian skeletal muscles. *Physiol Rev* **91**, 1447-531.

Schiaffino, S. and Salviati, G. (1997). Molecular diversity of myofibrillar proteins: isoforms analysis at the protein and mRNA level. *Methods Cell Biol* **52**, 349-69.

Schiaffino, S., Sandri, M. and Murgia, M. (2007). Activity-dependent signaling pathways controlling muscle diversity and plasticity. *Physiology (Bethesda)* **22**, 269-78.

Scott, W., Stevens, J. and Binder-Macleod, S. A. (2001). Human skeletal muscle fiber type classifications. *Phys Ther* **81**, 1810-6.

Serratrice, G., Pellissier, J. F., Vignon, C. and Baret, J. (1976). The histochemical profile of the human masseter. An autopsy and biopsy study. *J Neurol Sci* **30**, 189-200.

Sharma, K. and Izpisua Belmonte, J. C. (2001). Development of the limb neuromuscular system. *Curr Opin Cell Biol* **13**, 204-10.

Shearman, M. S., Sekiguchi, K. and Nishizuka, Y. (1989). Modulation of ion channel activity: a key function of the protein kinase C enzyme family. *Pharmacol Rev* **41**, 211-37.

Shenkman, B. S. and Nemirovskaya, T. L. (2008). Calcium-dependent signaling mechanisms and soleus fiber remodeling under gravitational unloading. *J Muscle Res Cell Motil* **29**, 221-30.

Sherrington, C.S. (1904). Correlation of reflexes and the principle of the common path. *Nature* 70 (No. 1819), 460-473

Shirasaki, R. and Pfaff, S. L. (2002). Transcriptional codes and the control of neuronal identity. *Annu Rev Neurosci* **25**, 251-81.

Shneider, N. A., Brown, M. N., Smith, C. A., Pickel, J. and Alvarez, F. J. (2009). Gamma motor neurons express distinct genetic markers at birth and require muscle spindle-derived GDNF for postnatal survival. *Neural Dev* **4**, 42.

Soon, C. P., Crouch, P. J., Turner, B. J., McLean, C. A., Laughton, K. M., Atkin, J. D., Masters, C. L., White, A. R. and Li, Q. X. (2010). Serum matrix metalloproteinase-9 activity is dysregulated with disease progression in the mutant SOD1 transgenic mice. *Neuromuscul Disord* **20**, 260-6.

Staron, R. S. and Pette, D. (1993). The continuum of pure and hybrid myosin heavy chain-based fibre types in rat skeletal muscle. *Histochemistry* **100**, 149-53.

Talmadge, R. J., Otis, J. S., Rittler, M. R., Garcia, N. D., Spencer, S. R., Lees, S. J. and Naya, F. J. (2004). Calcineurin activation influences muscle phenotype in a muscle-specific fashion. *BMC Cell Biol* **5**, 28.

Tanaka, C. and Nishizuka, Y. (1994). The protein kinase C family for neuronal signaling. *Annu Rev Neurosci* **17**, 551-67.

Thayer, R., Collins, J., Noble, E. G. and Taylor, A. W. (2000). A decade of aerobic endurance training: histological evidence for fibre type transformation. *J Sports Med Phys Fitness* **40**, 284-9.

Thomas, P. D., Kejariwal, A., Campbell, M. J., Mi, H., Diemer, K., Guo, N., Ladunga, I., Ulitsky-Lazareva, B., Muruganujan, A., Rabkin, S. et al. (2003). PANTHER: a browsable database of gene products organized by biological function, using curated protein family and subfamily classification. *Nucleic Acids Res* **31**, 334-41.

Thomason, D. B. and Booth, F. W. (1990). Atrophy of the soleus muscle by hindlimb unweighting. *J Appl Physiol* **68**, 1-12.

Totsuka, Y., Nagao, Y., Horii, T., Yonekawa, H., Imai, H., Hatta, H., Izaike, Y., Tokunaga, T. and Atomi, Y. (2003). Physical performance and soleus muscle fiber composition in wild-derived and laboratory inbred mouse strains. *J Appl Physiol* **95**, 720-7.

Tripodi, M., Stepien, A. E. and Arber, S. (2011). Motor antagonism exposed by spatial segregation and timing of neurogenesis. *Nature* **479**, 61-6.

Vinay, L., Brocard, F. and Clarac, F. (2000). Differential maturation of motoneurons innervating ankle flexor and extensor muscles in the neonatal rat. *Eur J Neurosci* **12**, 4562-6.

Wang, F. C., Bouquiaux, O., De Pasqua, V. and Delwaide, P. J. (2002). Changes in motor unit numbers in patients with ALS: a longitudinal study using the adapted multiple point stimulation method. *Amyotroph Lateral Scler Other Motor Neuron Disord* **3**, 31-8.

Wang, Y. X., Zhang, C. L., Yu, R. T., Cho, H. K., Nelson, M. C., Bayuga-Ocampo, C. R., Ham, J., Kang, H. and Evans, R. M. (2004). Regulation of muscle fiber type and running endurance by PPARdelta. *PLoS Biol* **2**, e294.

Westerblad, H. and Allen, D. G. (1991). Changes of myoplasmic calcium concentration during fatigue in single mouse muscle fibers. *J Gen Physiol* **98**, 615-35.

Westerga, J. and Gramsbergen, A. (1992). Structural changes of the soleus and the tibialis anterior motoneuron pool during development in the rat. *J Comp Neurol* **319**, 406-16.

Wittwer, M., Fluck, M., Hoppeler, H., Muller, S., Desplanches, D. and Billeter, R. (2002). Prolonged unloading of rat soleus muscle causes distinct adaptations of the gene profile. *FASEB J* **16**, 884-6.

Wood, S. J. and Slater, C. R. (2001). Safety factor at the neuromuscular junction. *Prog Neurobiol* **64**, 393-429.

Wu, H., Lu, Y., Shen, C., Patel, N., Gan, L., Xiong, W. C. and Mei, L. (2012). Distinct Roles of Muscle and Motoneuron LRP4 in Neuromuscular Junction Formation. *Neuron* **75**, 94-107.

Yan, Z. (2009). Exercise, PGC-1alpha, and metabolic adaptation in skeletal muscle. *Appl Physiol Nutr Metab* **34**, 424-7.

Yan, Z., Okutsu, M., Akhtar, Y. N. and Lira, V. A. (2011). Regulation of exercise-induced fiber type transformation, mitochondrial biogenesis, and angiogenesis in skeletal muscle. *J Appl Physiol* **110**, 264-74.

Zajac, F. E. and Faden, J. S. (1985). Relationship among recruitment order, axonal conduction velocity, and muscle-unit properties of type-identified motor units in cat plantaris muscle. *J Neurophysiol* **53**, 1303-22.

Zengel, J. E., Reid, S. A., Sypert, G. W. and Munson, J. B. (1985). Membrane electrical properties and prediction of motor-unit type of medial gastrocnemius motoneurons in the cat. *J Neurophysiol* **53**, 1323-44.

Zwaagstra, B. and Kernell, D. (1980). The Duration of after-Hyperpolarization in Hindlimb Alpha-Motoneurones of Different Sizes in the Cat. *Neuroscience Letters* **19**, 303-307.

Rhoades, A.R., Tanner, G.A. (2003). Medical Physiology, Chapter- Exercise Physiology.

Appendix 1

Lipid network

AHNAK2	AHNAK nucleoprotein 2
AKR1B1	Aldo-keto reductase family 1, member B1
ANGPTL4	Angiopoietin-like 4
CCRL2	Chemokine (C-C motif) receptor-like 2
CEBP	CCAAT/enhancer binding protein
CLEC10A	C-type lectin domain family 10, member A
CSRNP1	Cysteine-serine-rich nuclear protein 1
EPHX1	Epoxide hydrolase 1, microsomal
PHLDA1	Pleckstrin homology-like domain, family A, member 1
SLC25A25	solute carrier family 25 (mitochondrial carrier, phosphate carrier), member 25
SWT1	SWT1 RNA endoribonuclease homolog (S. cerevisiae)
TIMP4	Tissue inhibitor of metalloproteinase 4
TLE1	Transducin-like enhancer of split 1, homolog of Drosophila E(spl)
YRDC	YrdC domain containing (E.coli)
ZBTB22	Zinc finger and BTB domain containing 22

Appendix 2

MAPK signalling pathway

CACN	Calcium channel
Cdc42/Rac	p21 protein (Cdc42/Rac)-activated kinase 3
GCK	Glucokinase
IKK	Inhibitor of kappaB kinase
p38	Mitogen-activated protein kinase 14
PKA	Protein kinase A
PKC	Protein kinase C
TrkA/B	Neurotrophic tyrosine kinase, receptor, type 1/2

Appendix 3

PPAR signalling pathway

ACBP	Acyl-CoA binding protein
ACS	Acyl-CoA synthase
CPT1	Palmityltransferase 1
CPT2	Palmityltransferase 2
FABP	Fatty acid binding protein
FABP3	Fatty acid binding protein 3
FATP	Fatty Acid Transport Protein
LCAD	Long-chain acyl-CoA dehydrogenase
LPL	Lipoprotein lipase
MCAD	Medium-chain acyl-CoA dehydrogenase
PPAR	Peroxisome proliferator-activated receptor
SCP-X	Sterol carrier protein-x

Appendix 4

Fatty acid metabolism pathway

1.1.1.211	long-chain-3-hydroxyacyl-CoA dehydrogenase
1.1.1.35	3-Hydroxyacyl-CoA dehydrogenase
1.14.14.1	Aryl hydrocarbon hydroxylase
1.3.99.13	long-chain-acyl-CoA dehydrogenase
2.3.1.16	Acetyl-CoA C-acyltransferase
4.2.1.17	Enoyl-CoA hydratase
5.3.3.8	Dodecenoyl-CoA isomerase
6.2.1.3	Long-chain-fatty-acid-CoA ligase
ACAA2	Acetyl-Coenzyme A acyltransferase 2 (mitochondrial 3-oxoacyl-Coenzyme A thiolase)
ACAD8	Acyl-Coenzyme A dehydrogenase family, member 8
ACADL	Acyl-Coenzyme A dehydrogenase, long-chain
ACADM	Acyl-Coenzyme A dehydrogenase, medium chain
ACADVL	Acyl-Coenzyme A dehydrogenase, very long chain
ACSL1	Acyl-CoA synthetase long-chain family member 1

ACSL6	Acyl-CoA synthetase long-chain family member 6
CPT2	Carnitine palmitoyltransferase 2
CYP4B1	Cytochrome P450, family 4, subfamily b, polypeptide 1
ECH1	Enoyl-Coenzyme A hydratase 1, peroxisomal
ECI1	Enoyl-Coenzyme A delta isomerase 1
HADHB	hydroxyacyl-Coenzyme A dehydrogenase/3-ketoacyl-Coenzyme A thiolase/enoyl-Coenzyme A hydratase (trifunctional protein), beta subunit
HSD17B4	Hydroxysteroid (17-beta) dehydrogenase 4
SLC27A1	Solute carrier family 27 (fatty acid transporter), member 1

Curriculum Vitae

Personal Information

Name: Pitchaiah Cherukuri

Date of Birth: 4th April 1982

Nationality: Indian

Address: Developmental Neurobiology Laboratory, European Neuroscience Institute Göttingen (ENI-G), Grisebachstr. 5, 37077, Göttingen, Germany.

Email: pitchaiahc@gmail.com, pcheruk@gwdg.de

Educational Background

2008-Present Graduate student with Dr. Till Marquardt at European Neuroscience Institute (ENI-G) Göttingen.

2007-2008   Course work with the IMPRS Neuroscience Program, Göttingen, Germany.

2005-2007   MSc in Neuroscience, National Brain Research Centre (NBRC), India

2002-2005   BSc (Chemistry), Yashwantrao Mohite College, Bharati Vidyapeeth Deemed University, Pune, India (Faculty of Chemistry).

1997-1999   HSC (Pre University Course), Andhra Pradesh, India.

1996-1997   SSC, Don Bosco High School, Guntupalli, Andhra Pradesh, India.

Scholarships

2009-2012   GGNB Excellence Fellowship (GGNB -Göttingen Graduate School for Neurosciences and Molecular Biosciences).

2008-2009   Fund by IMPRS Neurosciences Program (Max Planck Society).

2007-2008   Stipend of the Excellence Foundation for the Promotion of the Max Planck Society.

2005-2007   Department of Biotechnology (DBT) (Govt. of India) fellowship through National Brain Research Centre (NBRC), India.

Publications

1. Nagar, S.*, Krishnamoorthy, V.*, **Cherukuri, P. *,** Jain, V., and Dhingra, N.K. (2009). Early remodeling in an inducible animal model of retinal degeneration. Neuroscience *160*, 517-529. **(* These authors contributed equally.)**

2. Krishnamoorthy, V., Jain, V., **Cherukuri, P.**, Baloni, S., and Dhingra, N.K. (2008). Intravitreal injection of fluorochrome-conjugated peanut agglutinin results in specific and reversible labeling of mammalian cones in vivo. Invest Ophthalmol Vis Sci *49*, 2643-2650.

Posters

1. **Cherukuri, P.**, Lee, T.I., Müller, D., Poh, C.H., Marquardt, T.; Molecular mechanisms underlying neuromuscular plasticity in mouse.; Motor Neuron Meeting 2010; Paris, France.

2. Dhingra, N.K., **Cherukuri P.,** Krishnamoorthy, V., Baloni, S., Jose, S.K.; Morphological and behavioural characterization of N-methyl N-nitrosourea induced mouse model of retinal degeneration; Society for neuroscience (SFN) general meeting 2007; San Diego, USA.

3. Krishnamoorthy, V., **Cherukuri P.**, Baloni, S., Dhingra, N.K.; In vivo labelling of mammalian cone photoreceptors by intravitreal injection of fluorescently tagged peanut agglutinin – A potential tool for assessing photoreceptor degeneration in humans; Optical Society of America (OSA) Fall Vision Meeting 2007; Berkeley, USA.

Workshops attended (scientific)

1. Electrophysiology School of Strasbourg, Institut de Physiologie et de Chimie Biologique, Strasbourg, France, 2010.

2. Virus-based technologies for investigating function and pathology of the Nervous System, European Brain Research Institute (ENI-Rome) in Rome, Italy, 2009.

3. Behavioural studies in drug discovery, University of Tartu, Estonia, 2008.